In compliance with the
Canadian Privacy Legislation
some supporting forms
may have been removed from
this dissertation.

While these forms may be included
in the document page count,
their removal does not represent
any loss of content from the dissertation.

University of Alberta

Structural Consequences of Mutation on the BRCA1 BRCT Domain: Molecular Basis of Tumour Suppressor Inactivation

by

R. Scott Williams ©

A thesis submitted to the Faculty of Graduate Studies and Research in partial fulfillment of the requirements for the degree of Doctor of Philosophy

Department of Biochemistry

Edmonton, Alberta
Fall 2003

Your file Votre référence
ISBN: 0-612-88065-6
Our file Notre référence
ISBN: 0-612-88065-6

University of Alberta

Library Release Form

Name of Author: Robert Scott Williams

Title of Thesis: Structural Consequences of Mutation on the BRCA1 BRCT Domain: Molecular Basis of Tumour Suppressor Inactivation

Degree: Doctor of Philosophy

Year this Degree Granted: 2003

April 23, 2003
Date Submitted

University of Alberta

Faculty of Graduate Studies and Research

The undersigned certify that they have read, and recommend to the Faculty of Graduate Studies and Research for acceptance, a thesis entitled **Structural Consequences of Mutation on the BRCA1 BRCT Domain: Molecular Basis of Tumour Suppressor Inactivation** submitted by Robert Scott Williams in partial fulfillment of the requirements for the degree of *Doctor of Philosophy*

J.N. Mark Glover
(supervisor)

Michael N.G. James

Mike Schultz

Michael Weinfeld

Tom Ellenberger
(external)

April 23, 2003

Date of Approval

For my parents ...

Abstract:

The C-terminal, BRCT repeat region is essential to the DNA repair, transcriptional regulation and tumour suppressor functions of BRCA1. To gain structural insights into the function of this conserved domain, we determined the crystal structure of the tandem BRCT domain of human BRCA1 at 2.5 Å resolution. The domain contains two BRCT repeats that adopt similar structures and are packed together in a head-to-tail arrangement. The manner by which the two BRCT repeats interact in BRCA1 may represent a general mode of interaction between homologous domains within proteins that interact to regulate the cellular response to DNA damage.

We further employed CD spectroscopy, proteolysis, and crystallographic methods to assess the structural response of the BRCT to the well-characterized, cancer-associated single amino acid substitution, Met1775 → Arg1775. The structure of BRCT-M1775R reveals that the mutated side chain is extruded from the protein hydrophobic core, thereby altering the protein surface. Charge-charge repulsion, rearrangement of the hydrophobic core, and disruption of the native hydrogen bonding network at the interface between the two BRCT repeats contribute to the conformational instability of BRCT-M1775R. Destabilization and global unfolding of this mutated BRCT domain at physiological temperatures explains the pleiotropic molecular and genetic defects associated with the BRCA1- M1775R protein.

Using a protease-based assay developed here, we directly assessed the sensitivity of the folding of the BRCT domain to an extensive set of truncation and single amino acid substitutions derived from breast cancer screening programs. The protein can tolerate truncations of up to 8 amino acids but further deletion resulted in drastic BRCT folding defects. This molecular phenotype can be correlated with an increased susceptibility to disease. 20/25 missense mutations tested showed enhanced sensitivity to proteolytic digestion, suggesting that the large majority of BRCT missense mutations contribute to BRCA1 loss of function and disease through protein destabilizing effects. The use of simple proteolytic methods to detect mutant BRCA1 conformations at the protein level will augment the efficacy of current BRCA1 screening protocols, especially in the absence of clinical data that can discriminate deleterious BRCT missense mutations from benign polymorphisms.

Acknowledgements:

i would like to thank mark glover and my supervisory committee for their invaluable guidance and support. special thanks to the many people that have contributed to the brct project through the years ... these include david and ben and ruth and the many other members of the glover laboratory and the department of biochemistry at the u of a ... the past 6+ formative years that i've spent in edmonton have included some of the most enjoyable & difficult times of my life... thanks to: amir, brian and adi, the donx, the roo, the hippo, the badger, butt-la, arma-d/double-d/lil-scoopa, the sheep, bubbles, jopa and jane, the genius, the bikes and the squash and the skiing. without my family and my (soon to be!) wife jess, i surely would have gone mad ... thank you ... you are my sanity, my heart and my soul. i'm most certainly older, it's my hope that somehow I've become wiser ...

TABLE OF CONTENTS

List of Figures

List of Tables:

List of Abbreviations

Å	Angstroms (10^{-10} meters)
aa	amino acid
APS	Advanced Photon Source
ATM	Ataxia telangiectasia mutated protein
βME	β-mercaptoethanol
CD	Circular Dichroism
BARD1	BRCA1 associated RING domain protein 1
BACH1	BRCA1 associated helicase protein 1
BRCA1	Breast cancer associated protein 1
BRCT	BRCA1 carboxyl terminal domain
CtIP	CtBP associated transcriptional co-repressor
DNA	deoxyribonucleic acid
DNL3	DNA Ligase 3
DNL4	DNA Ligase 4
DSB	double strand break
DTT	dithiothreitol
EDTA	(ethylenedinitrilo)-tetraacetic acid
|F|	diffracted X-ray structure factor amplitude
GST	Glutathione-S-transferase
kDa	kiloDalton
HR	Homologous recombination
IPTG	Isopropyl β–D-thiogalactopyranoside
λ	Wavelength
LB	Luria Bertani
MAD	Multiwavelength Anomolous Dispersion
MES	(2-[N-morpholino]ethanesulfonic acid)
NMR	Nuclear Magnetic Resonance
PAGE	Polyacrylamide gel electrophoresis
PCR	Polymerase Chain reaction

PEG	polyethylene glycol
PMSF	phenylmethyl sulfonyl fluoride
RING	Really interesting new gene domain
SDS	Sodium dodecylsulfate
SKT11	Serine-threonine kinase 11
Tris	tris(hydroxymethyl)aminomethane
XRCC1	X-ray Repair cross complementation protein 1

Chapter 1:

Introduction

BRCA1

Familial breast cancer and the links to BRCA1

Breast cancer is a leading cause of cancer death among women, and it is estimated that 1/8 women in North America will be afflicted with some form of the disease over the course of their lives (Table 1.1). Second only to lung cancer, breast cancer was estimated to be responsible for greater than 5400 cancer deaths in Canada in the year 2002 (Fig. 1.1). Familial breast and ovarian cancer predisposition syndromes have long been recognized. Statistical modelling provided early evidence for dominant breast cancer susceptibility genes (Williams & Anderson 1984) and the subsequent cloning of two major disease susceptibility genes, *BRCA1* and *BRCA2,* has helped clarify the genetic bases of these diseases (Hall et al. 1990, Miki et al. 1994, Wooster et al. 1994, Wooster et al. 1995). It is estimated that germline mutations in these two tumour suppressor genes are responsible for 15-20% of inherited breast cancers, and fewer than 5% of all breast cancers. Mutations in p53 (Malkin et al. 1990), the serine-threonine kinase STK11/LKB1 (Boardman et al. 1998), and the PTEN tumour suppressor (Li et al. 1997, Liaw et al. 1997) account for an additional small fraction of inherited risk (Fig. 1.2). The genetic basis of the remaining breast cancer specific risk is likely to be described by a complicated, polygenic model, and extensive efforts to identify additional high penetrance breast cancer susceptibility genes have failed (Weber & Nathanson 2000, reviewed in Nathanson et al. 2001). Notably, *BRCA1* mutations are found in greater than 60% of families with inherited breast *and* ovarian cancer (Couch et al. 1997, Peto et al. 1999).

Expression of *BRCA1* is ubiquitous, however, and the reason for such tissue specific cancer predisposition remains unclear.

Characteristic for alleles of tumour-suppressor genes, inheritance of *BRCA1* within affected families exhibits an autosomal-dominant mode of transmission (Smith et al. 1992). Loss of heterozygosity at the locus is observed in familial tumours, with retention of the disease predisposing allele (Neuhausen & Marshall 1994). 60-80% of female *BRCA1* mutation carriers will suffer from breast cancer at some point in their lifetime (Easton et al. 1993, Struewing et al. 1996). The early identification of individuals at risk through breast cancer screening programs is now possible, and cancer management programs are being continually developed to prevent and monitor tumourigenesis in such high-risk patients. Indeed, the use of preventative surgery such as prophylactic mastectomy for women with germline *BRCA1* mutations appears to reduce breast cancer risk by as much as 60% (Rebbeck et al. 1999, Eisen & Weber 2001). Thus, study of the molecular details of BRCA1 protein function and how these functions are compromised by mutation offers important insights into the basic molecular biology of cancer, and will potentially lead to individualized risk assessment and ultimately, the reduction of disease incidence.

The Nuclear Functions of BRCA1

BRCA1 encodes a predominantly nuclear phosphoprotein of 1863 amino acids. With the exception of the N-terminal Ring finger domain, and two BRCT domains at the C-terminus, BRCA1 displays no marked similarity to other known

Table 1.1. Lifetime Probability estimates for Breast Cancer

Age of Breast cancer onset	Proportion of women affected
by age 30	1 out of 2000
by age 40	1 out of 233
by age 50	1 out of 53
by age 60	1 out of 22
by age 70	1 out of 13
by age 80	1 out of 9
Ever	1 out of 8

Source: http://cis.nci.nih.gov/
Estimates are for the US population, and based on incidence rates in 1999.

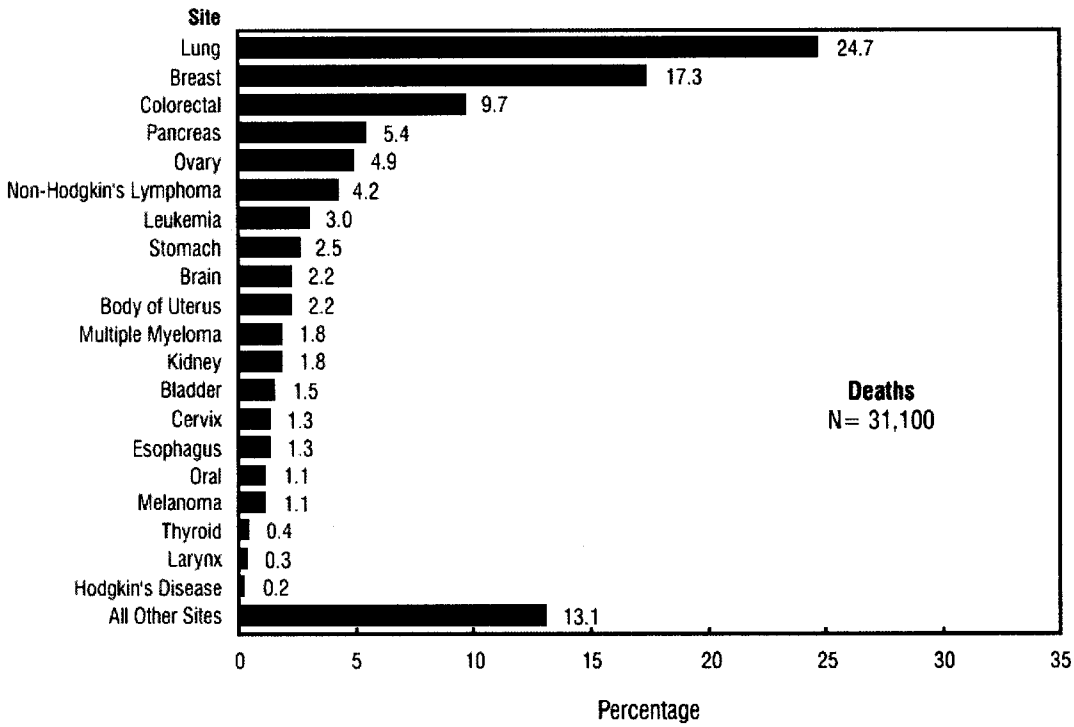

Figure 1.1. Cancer deaths for Canadian women for the year 2002, sorted by tissue specificity. Breast cancer is the second leading cause of cancer related mortalities, accounting for > 5400 deaths. *Source: www.ncic.cancer.ca.*

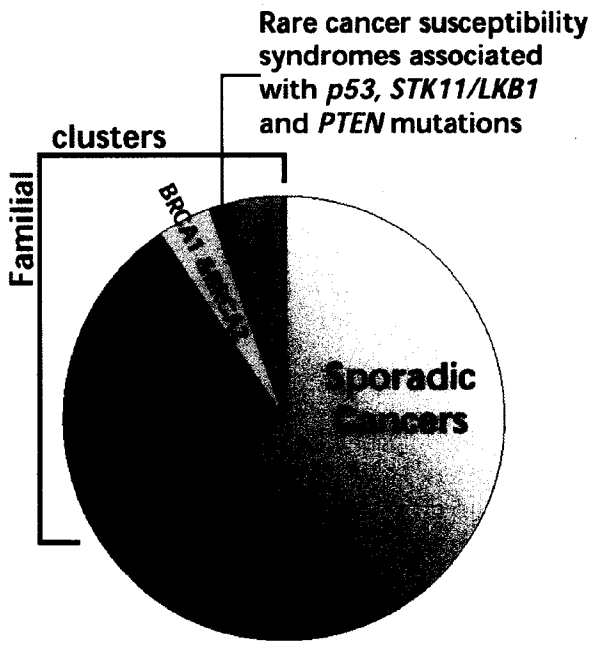

Figure 1.2. Distribution of breast cancers. Cases of breast cancer can be classified as those that are inherited (familial clusters) or sporadic (without specific genetic predisposition to disease). Germline mutations in *BRCA1* and *BRCA2* account for approximately 5% of all breast cancers. *BRCAX* represents a third high risk breast cancer susceptibility gene that has yet to be identified. A small fraction of breast cancers are caused by mutations in p53, STK11/LIK1 and the PTEN tumour suppressor. The large proportion of inherited breast cancers have unknown genetic causes. Adapted from Nathanson *et.al.* 2001.

proteins (Fig. 1.3) (Miki et al. 1994, Koonin et al. 1996). Although the precise function of BRCA1 remains obscure, evidence supports a role for BRCA1 in DNA repair, cell cycle regulation, and transcriptional activation (Fig. 1.4).

BRCA1 participates in DNA repair pathways

Early studies probing the function of BRCA1 revealed that it is found in complex with Rad51, a protein with a known role in homologous recombination (Scully et al. 1997). BRCA1 and Rad51 are coexpressed in developing mouse embryos and are colocalized in S-phase nuclear foci in somatic cells. Gene targeting experiments disrupting the genes encoding these proteins yielded a similar lethal phenotype (Gowen et al. 1996, Hakem et al. 1996, Lim & Hasty 1996). A specific role for this complex in DNA repair was implied by the rapid relocalization of BRCA1 and associated proteins to sites of DNA synthesis after exposure of cells to DNA-damaging agents in S phase (Scully et al. 1997). These sites are populated with the phosphorylated histone species, H2A-X, which can be ubiquitinated by the BRCA1/BARD1 heterodimeric ubiquitin E3 ligase *in vitro* (Mallery et al. 2002). BRCA1 may therefore directly regulate chromatin structure in response to DNA damage through its ubiquitin ligase activity, but the role of this histone-specific enzymatic activity remains unclear. Furthermore, a direct link of BRCA1 to the cellular response to double stranded DNA breaks was suggested by its interaction with the Rad50/MRE11/NBS1 complex (Fig. 1.4) (Zhong et al. 1999). *In vitro*, BRCA1 can bind to damaged DNA structures and prevent the nuclease activity of this complex, implicating BRCA1 as a possible regulator of DSB resection (Paull et al. 2001). The initial

activation of BRCA1 in response to DNA damage is likely achieved by CHK2 and ATM-related kinases, which play a quantitative role in the phosphorylation of BRCA1 following γ-irradiation (Cortez et al. 1999, Lee et al. 2000).

BRCA1 as a transcriptional regulator

The C-terminal domain of BRCA1 can activate transcription (Chapman & Verma 1996, Monteiro et al. 1996, Scully et al. 1997), and potential targets of this regulation include the p53 responsive genes encoding p21 as well as GADD45, (Somasundaram et al. 1997, Harkin et al. 1999) suggesting that BRCA1 has a role in regulating DNA repair and checkpoint controls. BRCA1 can also form complexes with various transcription factors and chromatin remodelling proteins including SWI-SNF related proteins (Bochar et al. 2000), histone deacetylases (Yarden & Brody 1999), the DNA helicase BACH1 (Cantor et al. 2001), p300/CBP (Pao et al. 2000) and the RNA polymerase holoenzyme (Scully, et al. 1997). These interactions could serve to regulate DNA structure at the site of lesions, or act directly in BRCA1 mediated transcription of checkpoint genes.

The observation that BRCA1 is required for transcription coupled DNA repair of oxidative DNA damage highlights one possible activity of BRCA1 that may bridge the transcription and DNA repair functions of the protein (Gowen et al. 1998). In this process, DNA adducts found in the transcribed strand of genes that are being actively expressed are preferentially repaired. This role is supported by the known association of BRCA1 with the RNA polymerase holoenzyme (Scully et al. 1997), and two mismatch repair proteins, MSH2 and

MSH6, that are known to mediate transcription-coupled DNA repair (Wang et al. 2000).

Tumourigenesis in BRCA1 compromised individuals

Functional studies of cells derived from BRCA1 (-/-) mutated mice confirmed the function of BRCA1 in maintenance of genomic integrity. BRCA1 (-/-) cells showed sensitivity to ionizing radiation and harboured chromosomal breaks, indicating deficiencies in recombination and/or DNA repair (Shen et al. 1998). A BRCA1 mutated cancer cell line is deficient in double strand break repair and this defect can be restored partially by the expression of wild type *BRCA1*, but not by clinically defined mutant *BRCA1* alleles (Scully et al. 1999). Specifically, *BRCA1* mutant cells are deficient in the repair of ionizing radiation induced double strand breaks via homology directed DNA repair (Fig. 1.5) (Moynahan et al. 1999). The mechanism of DSB repair in *BRCA1* (and *BRCA2*) mutant cells may be shunted away from error-free homology directed DNA repair, to a more error-prone pathway known as non-homologous end joining (NHEJ).

Indeed, genomic instability is characteristic of cancer cells, and it is possible that defective maintenance of genomic integrity, as found in BRCA-deficient cells, may greatly accelerate tumourigenesis by promoting gross chromosomal translocations or loss of heterozygosity events (Fig 1.5). The resulting accumulation of additional mutations in the genes encoding cellular checkpoint control regulators (e.g. p53) could then lead to the acceleration of tumour development (Scully & Livingston 2000, Venkitaraman 2002). In support

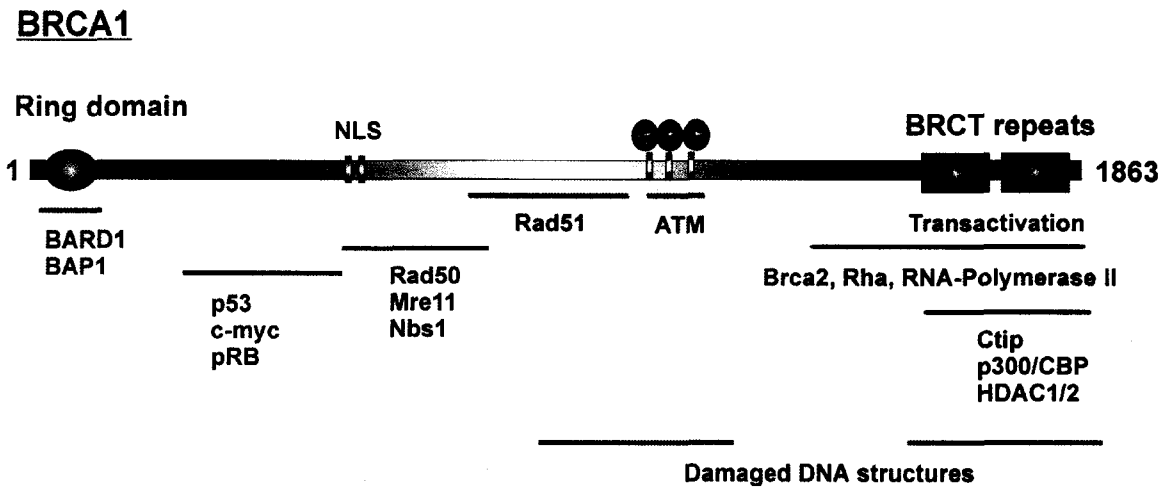

Figure 1.3. Primary structure of the BRCA1 polypeptide. The positioning of nuclear localization sequences and two regions with known homology to other proteins, the amino-terminal Ring finger domain and carboxyl terminal BRCT repeat domains, are marked. The approximate location of phosphorylation sites, and protein binding sites for a number of documented BRCA1 interacting proteins have been indicated. The BRCT domains interact with a variety of proteins and protein complexes with established roles in transcriptional regulation.

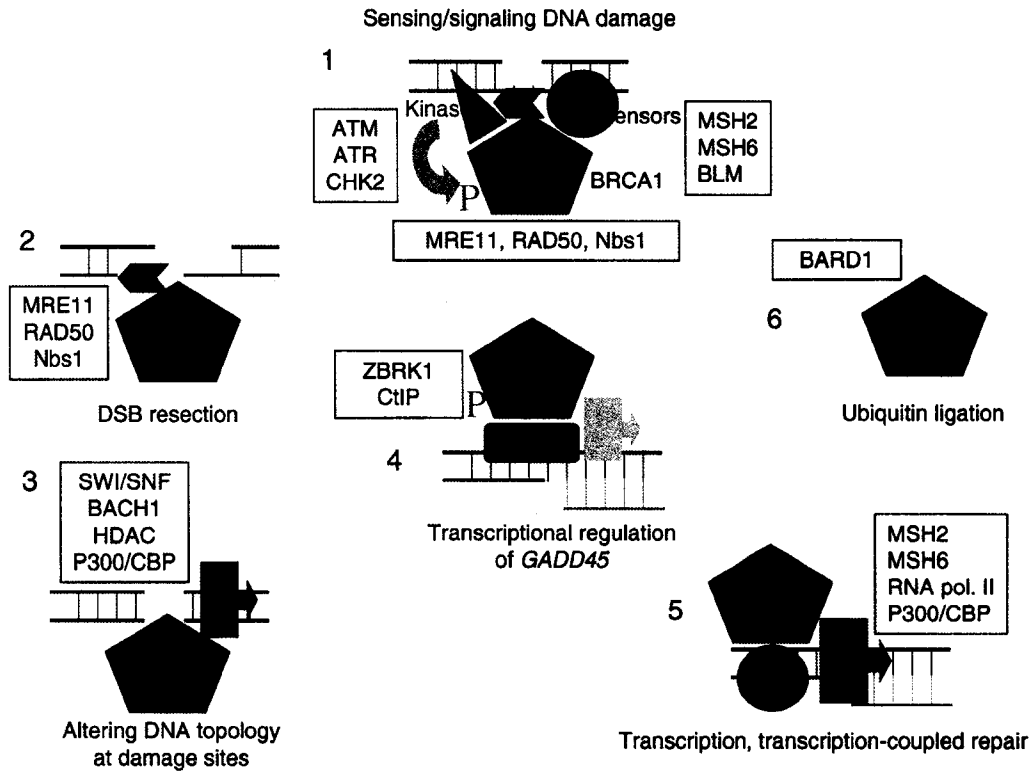

Figure 1.4. The diverse nuclear functions of the BRCA1 tumour suppressor. 1. BRCA1 is found in complex with proteins known to participate in DNA damage sensing and repair, and is phosphorylated by signaling proteins (ATM, ATR, CHK2) known to act in the cellular response to DNA damage. BRCA1 may act to transduce these signals to damage sensors. **2.** At the sites of a DNA lesion, the Mre11/Rad50/Nbs1 complex acts to recess double strand breaks via a nuclease activity and potentially mediates the annealing of complementary ssDNA ends to faciliate repair. BRCA1 can bind non-specifically to DNA and inhibits this activity, and may therefore regulate the double strand resection process. **3.** BRCA1 copurifies with proteins with established chromatin remodeling functions. These interactions may modulate the role for BRCA1 in transcription, or may serve to alter chromatin structure near DNA lesions. **4.** BRCA1 controls transcription activation of GADD45. The transcriptional corepressor CtIP may inhibit BRCA1 mediated transactivation of the GADD45 promoter. ATM phosphorylation of CtIP can liberate a CtIP/BRCA1 interaction in some cell lines. **5.** BRCA1 is essential for transcription coupled repair of DNA and copurifies with RNA polymerase II and other known mediators of this process. **6.** BRCA1 associates with BARD1 via its N-terminal Ring finger domain. This association potentiates a ubiquitin ligase activity of the BRCA1/BARD1 heterodimer that has apparent specificity for histones. Adapted from Venkitaraman, 2002.

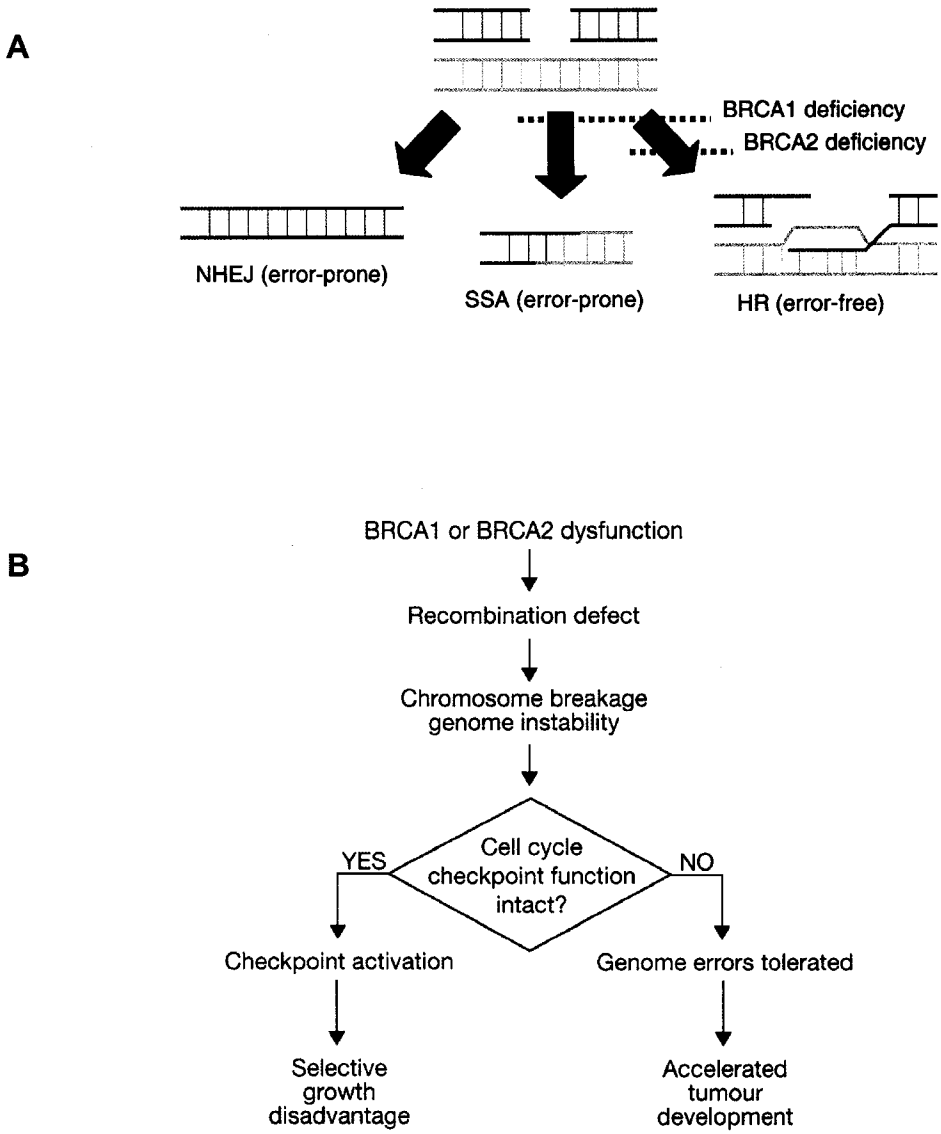

Figure 1.5 Generation of genomic instability in BRCA compromised cells. A. Mammalian cells repair double strand breaks by three alternative mechanisms. Non-homologous end-joining directly joins broken DNA ends and tolerates mutation at rejoining sites, and is therefore an error-prone repair process. Homology directed DNA repair (HR) is error-free and proceeds via the exchange between homologous chromosomes. Single strand annealing (SSA) utilizes short segments and is initiated by homologous pairing, but utilizes direct ligation rather than strand exchange – this process is also error prone. BRCA deficiency results in defects in HR and SSA mechanisms of DNA repair, potentially shunting repair to the error-prone NHEJ pathway. **B.** Defective DNA repair mechanisms and the resulting genomic instability lead to accumulation of mutations in BRCA deficient cells. In cells where relevant checkpoint functions are lost, the establishment of tumour cell lineages may occur. Adapted from Scully and Livingston 2001 and Venkitaraman, 2002.

of this hypothesis, p53 mutants identified from some BRCA1 compromised tumours have a unique mutation spectrum that is distinct from the traditionally classified mutation hotspots found in p53 mutated sporadic tumours (Greenblatt et al. 2001).

It is evident that inheritance of a single mutated *BRCA1* allele can predispose an individual to disease. The second *BRCA1* allele appears to be lost in a high percentage of familial breast carcinomas, (Neuhausen et al. 1994), but when this event occurs relative to the establishment of a tumour is unknown. At least one report suggests human cells heterozygous for a *BRCA1* mutation are impaired in double strand break repair mechanisms (Baldeyron et al. 2002). Mouse models of *BRCA1* deficiency, however, suggest *BRCA1* heterozygosity alone is not sufficient to confer cancer predisposition (Xu et al. 2001). Thus, more information regarding the chronology of accumulation of genetic abnormalities in human BRCA1 (+/-) heterozygous carriers, and the contributing role of the breast and ovarian tissue environments to disease progression, will be needed to fully understand the complex biology of *BRCA1* associated cancer risk.

The BRCA1 C-terminal Domain

The extreme C-terminal region of BRCA1 contains two ~90-100 amino acid sequence repeats called BRCT (**BR**CA1 **C**arboxyl-**t**erminal) repeats which are the prototypical members of a large protein fold superfamily. Two, tandem BRCT domains were originally identified as having weak sequence similarity to

the C-termini of *S. cerevisiae* RAD9 and the human p53 binding protein, 53BP1 (Koonin et al. 1996, Bork et al. 1997, Callebaut & Mornon 1997). Subsequent sequence analysis refined a conserved hydrophobic clustering signature for these domains and extended the family of BRCT containing proteins to include more than 50 unique proteins, many of which have established roles in cell cycle control and DNA repair pathways (Fig. 1.6) (Bork et al. 1997, Callebaut & Mornon 1997).

Molecular architecture of BRCT domains and BRCT containing proteins

The base excision repair protein XRCC1 (X-ray Repair Cross Complementation 1 protein) contains two BRCT domains separated by a 125-residue linker region. Seminal insights into the structure of BRCT domains came with the elucidation of the 3.2 Å crystal structure of the XRCC1 C-terminal BRCT repeat (Fig. 1.7) (Zhang et al. 1998). The fold is characterized by a central parallel 4 stranded β-sheet surrounded by 3 α-helicies. As predicted by Callebaut & Mornon (1997), the hydrophobic residues found at conserved BRCT positions contribute to the formation of the core of the XRCC1 BRCT. An amino acid sequence alignment of a subset of the BRCT family (Fig. 1.6) highlights that the majority of conserved hydrophobes are involved in β-sheet packing, helix α3, and the C-terminus of helix α1. There are few invariant residues amongst the BRCTs, and the sequences diverge greatly in regions that form α2 in XRCC1 and in two hypervariable insertion regions that are found at the β1-α1 and β2-β3 junctions.

BRCT domains are found in the context of a variety of protein architectures. They can exist as paired BRCT repeat domains (as in BRCA1, 53bp1 and Rad9), are found as autonomous BRCT domains (as in DNA-Ligase3 or RAP1), are present as fusions with other domains (e.g. the FHA-BRCT domain of Nbs1) and as many as eight BRCT repeats have been identified in a single protein (e.g. Topoisomerase binding protein-1) (Fig. 1.8). Evidence for the well-characterized BRCT proteins suggest these repeats function as multi-purpose protein-protein or protein-nucleic acid interaction modules. BRCT domains have been shown to bind to other BRCT repeats, or protein domains with apparently unrelated structures (Table 1.2, Fig. 1.9). For example, XRCC1 interacts with the BRCT domain of Poly(ADP-ribose)polymerase (PARP) via its N-terminal BRCT and with the BRCT region of DNA ligase III via its C-terminal BRCT (Kubota et al. 1996, Nash et al. 1997, Taylor et al. 1998). Conversely, the BRCT repeat linker region of DNA ligase IV binds to a non-BRCT coiled-coil of XRCC1 (Critchlow et al. 1997). Thus, a diverse array of protein-protein interaction sites formed by the highly variable surfaces and insertion regions of the BRCT superfamily members appear to have evolved upon the conserved BRCT core fold scaffolding. Altogether, there are at least four distinct modes of BRCT protein-ligand interactions (Table 1.2).

Functions of the BRCA1 Carboxyl terminal domain

The high concentration of acidic residues present in the BRCT repeats of BRCA1, and the potential role of the protein in transcriptional regulation, led investigators to test for a possible transactivation function of this domain. When

fused with a GAL4 DNA binding domain, the protein was found to stimulate transcription of a reporter gene (Chapman & Verma 1996, Monteiro et al. 1996) (Fig 1.10). This activation may result from the direct recruitment of the RNA polymerase holoenzyme (Scully et al. 1997), or alternatively may reflect an important function of the domain, such as chromatin remodeling, which has been reported for the BRCT (Ye et al. 2001, Hu et al. 1999).

A large body of evidence suggests that the BRCT region interacts with proteins involved in transcriptional control or DNA repair, including the transcriptional co-repressor CtIP (Yu et al. 1998, Yu et al. 1998, Li et al. 1999, histone deacetylases (Yarden & Brody 1999), p53, p300/CBP (Pao et al. 2000), the DNA damage-associated helicase BACH1 (Cantor et al. 2001), and the LIM-only transcriptional regulator LMO4 (Sum et al. 2002). These interactions may help modulate transcriptional activation/remodeling functions of the BRCT. For example, CtIP and LMO4 binding appears to attenuate BRCT transactivation function (Yu & Baer 2000, Sum et al. 2002,) whereas activation is enhanced by interactions with the transcriptional coactivator p300/CBP (Pao et al. 2000).

The multiple potential nuclear functions described for the isolated BRCT domain mirrors the apparent function diversity for the full length protein. *In vitro*, the BRCT can bind to damaged DNA structures, with specificity for nicks and double strand DNA breaks (Yamane & Tsuruo 1999). This function is conserved with another BRCT containing protein, Topoisomerase binding protein 1 (TopBP1), and suggests that some BRCTs may have a direct role in the

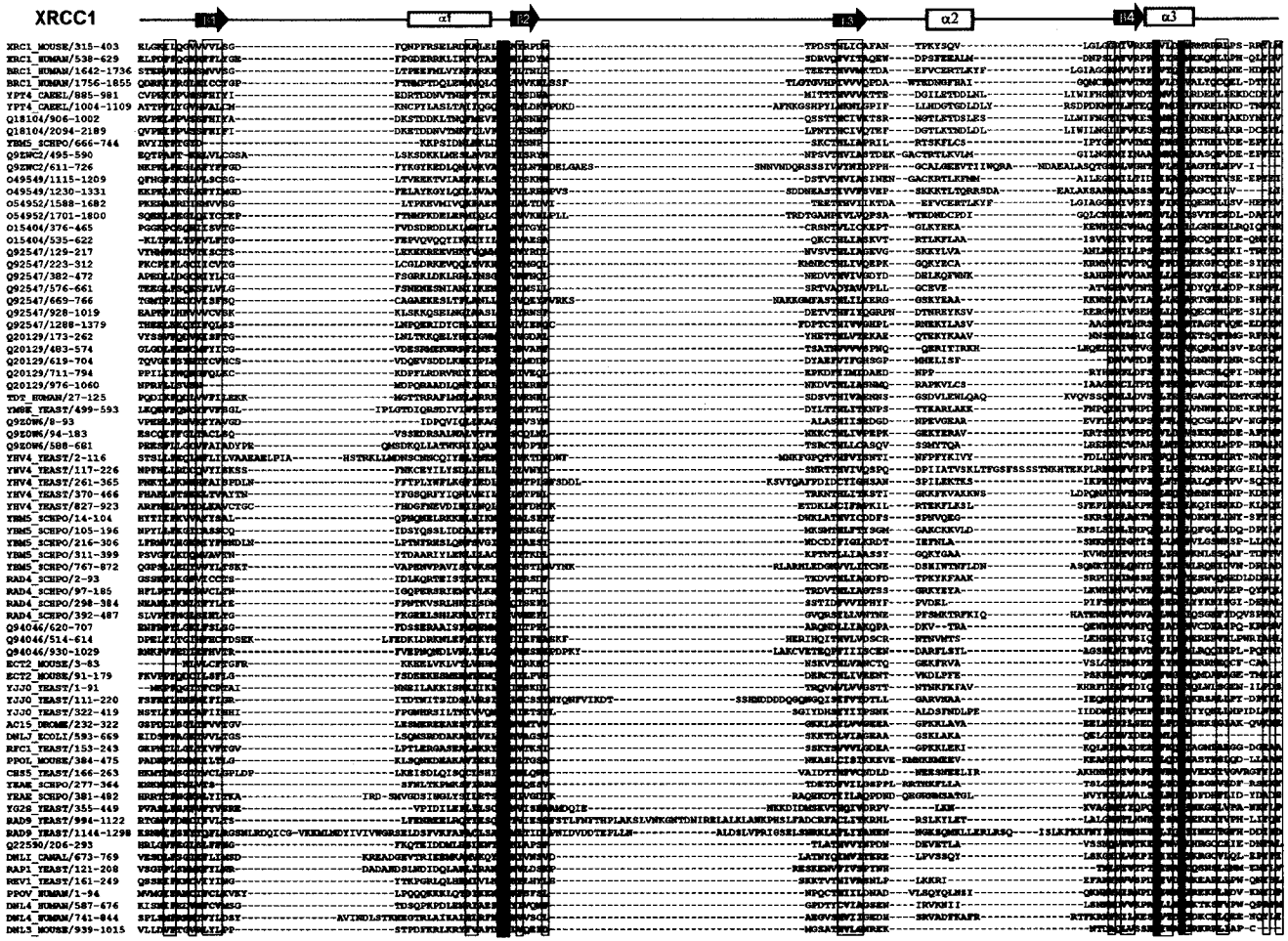

Figure 1.6. An amino acid sequence of BRCT domains found in the pFAM BRCT family. Secondary structure elements as determined from the XRCC1 C-terminal BRCT structure (Zhang et al. 1998) are indicated. Conserved BRCT hydrophobic residues are highlighted in yellow. Highly conserved residues (in red) include a nearly invariant "Gly-Gly" pair found at the α1-β2 junction and a W-h-h-x-C/S (h=hydrophobic residue,x= any residue) motif in helix α3.

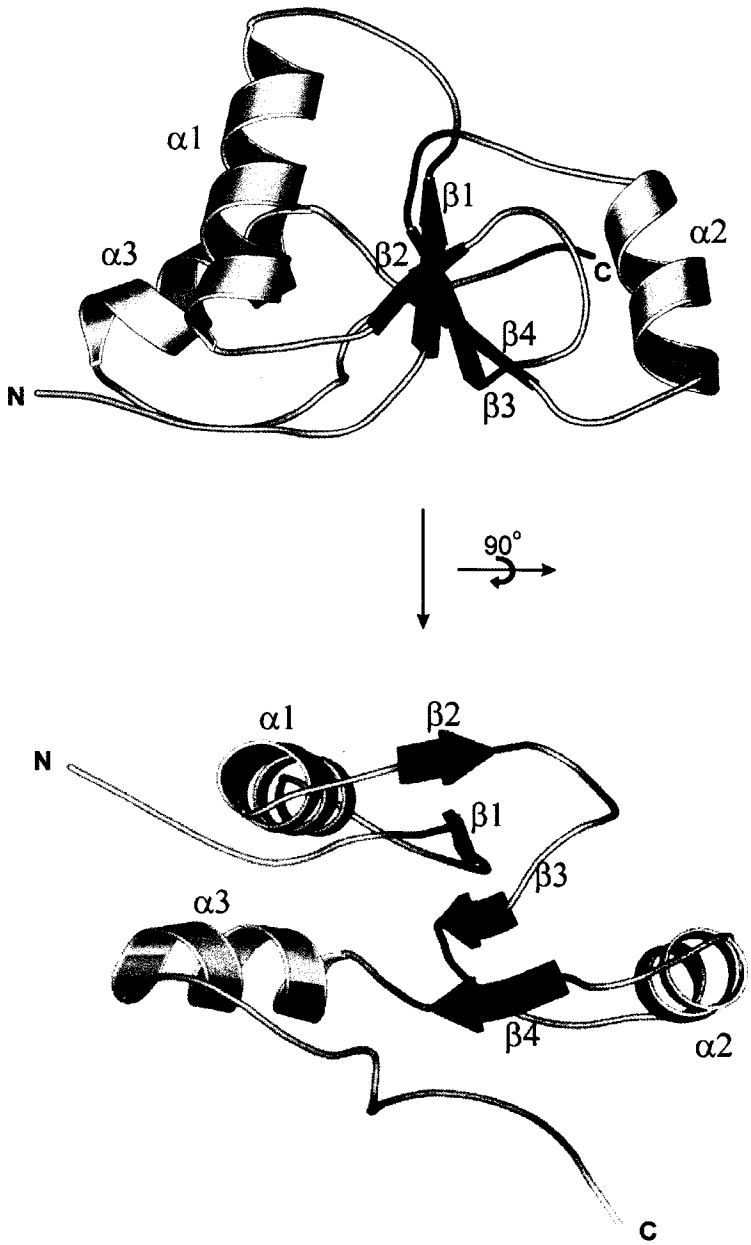

Figure 1.7. The X-ray crystal structure of the Xrcc1 C-terminal BRCT repeat (pdbID-1cdz, Zhang et.al. 1998). Orthogonal views of the structure are shown.

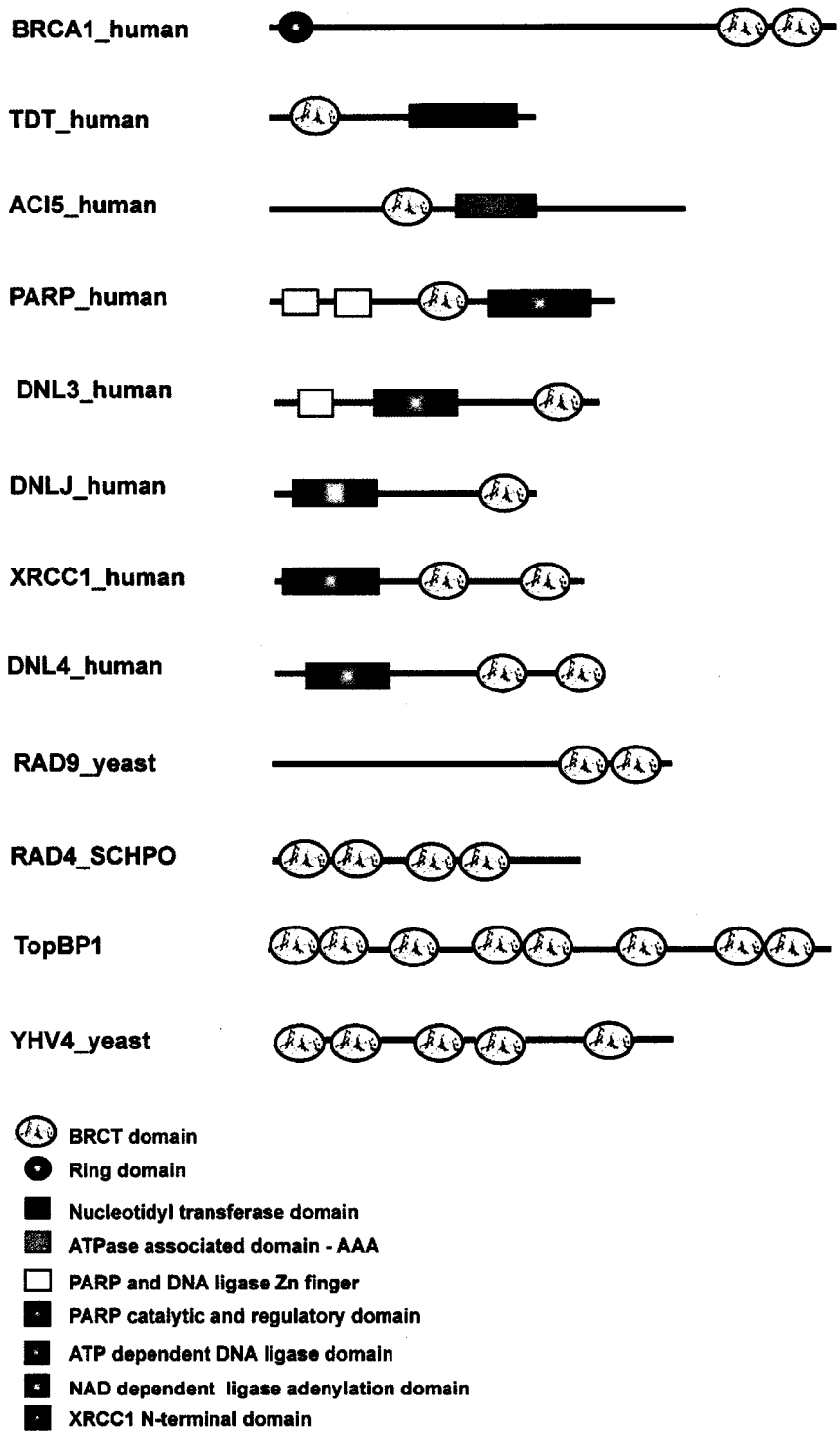

Figure 1.8. Domain structures for selected members of the superfamily of BRCT containing proteins.

Table 1.2. Modes of BRCT mediated interactions

Interaction type	Examples
Intramolecular BRCT-BRCT	**- tandem BRCT repeats of BRCA1, Rad9, 53BP1**
Intermolecular BRCT-BRCT	**- XRCC1(BRCTn):PARP, XRCC1(BRCTc):DNL3** **- Rad9 BRCT homodimerization**
Intramolecular BRCT-nonBRCT	**- FHA-BRCT fusion domain of NBS1**
Intermolecular BRCT-non-BRCT	**- DNL4 (BRCT linker): XRCC4** **- BRCA1 (BRCTnc)- CTIP** **- TopBP1 (BRCT)-DNA ends**

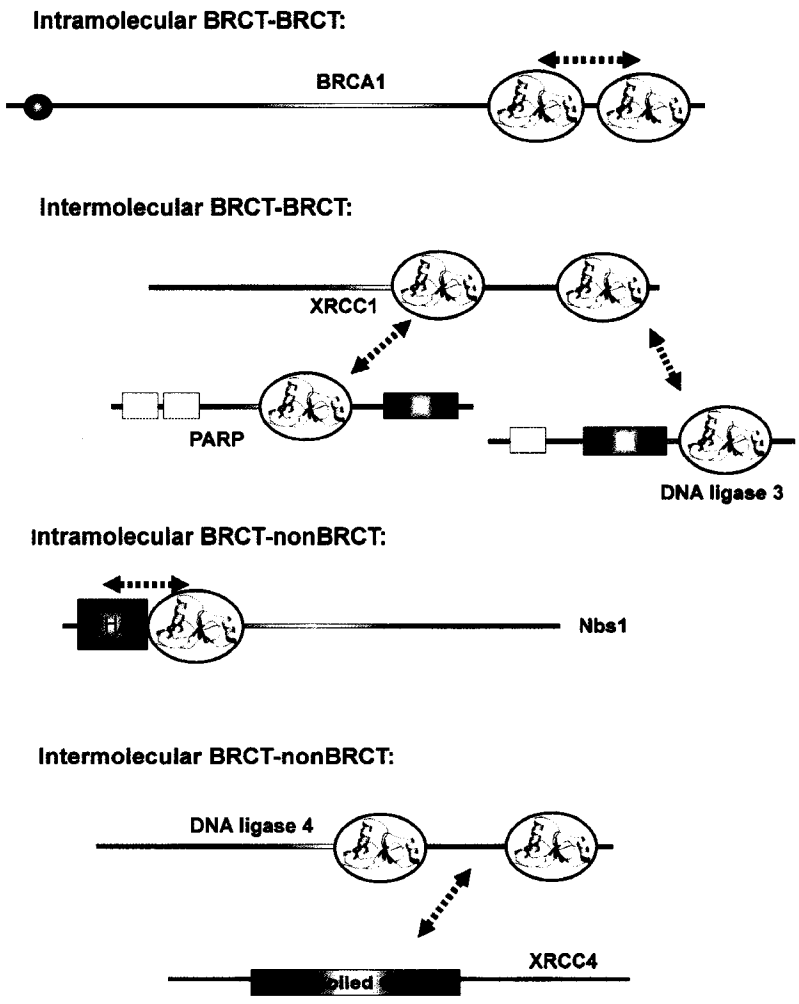

Figure 1.9. BRCT domains are protein-protein interaction modules. BRCT domains have evolved upon a conserved scaffold and have highly variable surfaces that mediate a variety of documented interactions.

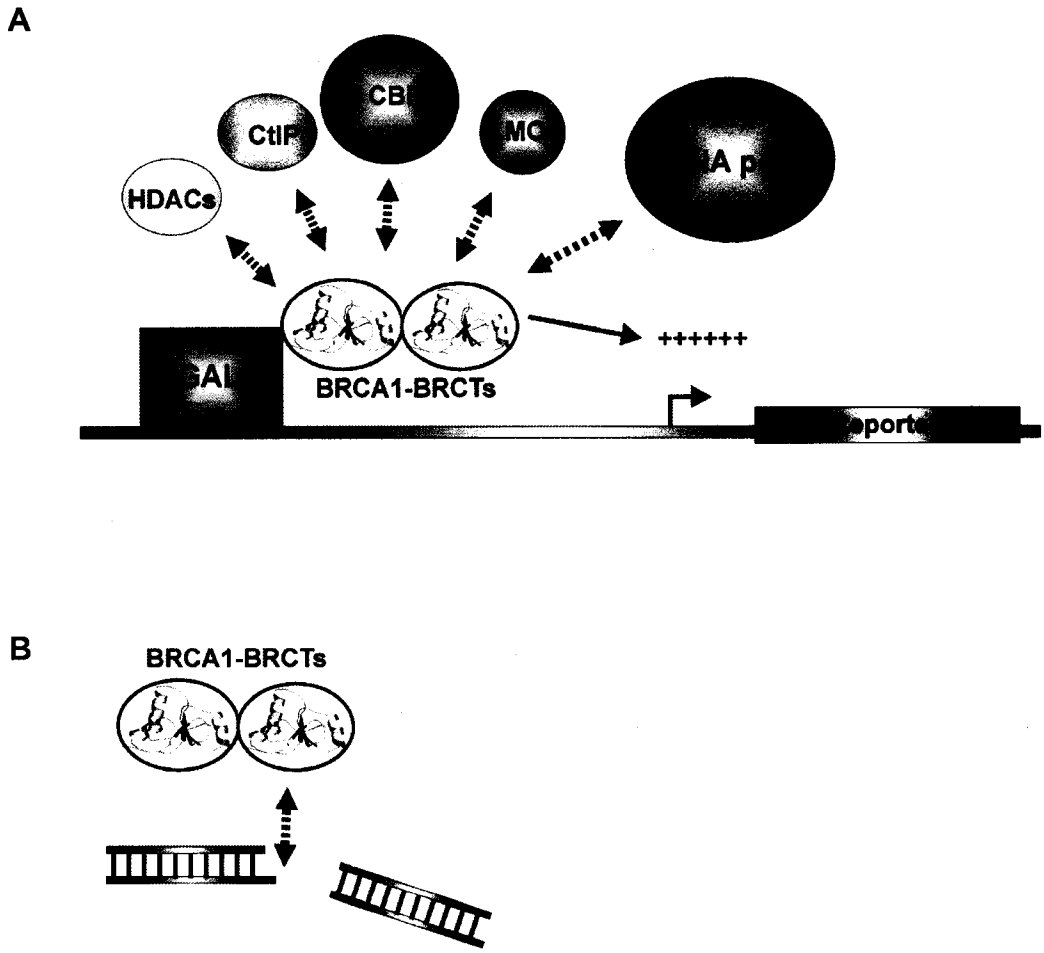

Figure 1.10. Functions of the carboxyl-terminal BRCT domain of BRCA1. A. When fused to a GAL4-DNA binding domain the BRCT can activate transcription. This activity is modulated by interaction with proteins involved in transcriptional activation and chromatin remodeling proteins. **B.** The BRCT can bind damaged DNA structures directly *in vitro*, and may have a direct role for DNA damage sensing.

detection of damaged DNA. BRCA1 is found associated with a number of proteins known to recognize and repair DNA damage (Wang et al. 2000). Such a role in damage recognition appears consistent with the early localization of BRCA1 to DNA damage foci (Scully et al. 1997). A central region of the protein (residues 452-1079) also binds to DNA with a preference for branched DNA structures, and this interaction confers DNA resistance to the nuclease activity of the Rad50-Mre11-Nbs1 complex (Paull et al. 2001). The *in vivo* relevance of these intriguing activities, however, has yet to be demonstrated.

BRCA1 mutations

The Breast cancer Information Core (BIC), was established to collate clinically derived information regarding mutations and polymorphisms in the breast cancer linked genes (Couch & Weber 1996, Shen & Vadgama 1999). Several methods have been employed in the routine screening of high-risk families for BRCA1 alterations. These include the direct sequencing of BRCA1 exon and intronic sequences, use of single strand conformation polymorphism assays and heteroduplex analysis (Shattuck-Eidens et al. 1995). The large majority of the mutations identified to date are frameshifts, single amino acid substitution (missense), and nonsense variants (Table 1.3).

Since the nonsense mutation Y1853ter, which causes the premature translational termination of the BRCA1 protein and removal of the 11 most C-terminal amino acids, is clearly cancer predisposing (Friedman et al. 1994), all frameshift or nonsense mutations that result in BRCA1 protein truncation are viewed as functionally deleterious. Although many BRCA1 missense variants

have been identified, physiological significance of the majority of these alterations has not been determined due to the lack of a simple, reliable functional assay for BRCA1. Thus, the functional role of the missense sequence variants constituting >27% of the BIC-BRCA1 database entries clearly merits further investigation.

The mutations occur throughout the BRCA1 coding sequence, but are clustered to exons encoding the N-terminal RING and C-terminal BRCT repeat regions (Fig 1.11), suggesting these domains have important roles in mediating BRCA1 tumour suppressor function. More than 50 unique missense variants have been recorded that alter the primary sequence of the tandem BRCT-repeats and of these, only seven are unequivocally linked to disease (Futreal et al. 1994, Miki et al. 1994, Couch & Weber 1996, Shen & Vadgama 1999, Gayther et al. 1995, Vallon-Christersson et al. 2001, Hayes et al. 2000). However, many of these amino acid substitutions that may be linked to cancer have been categorized as unclassified variants with respect to disease because the presence of the allele has not been tested in the general population, or the segregation of the allele with disease within a family is unclear.

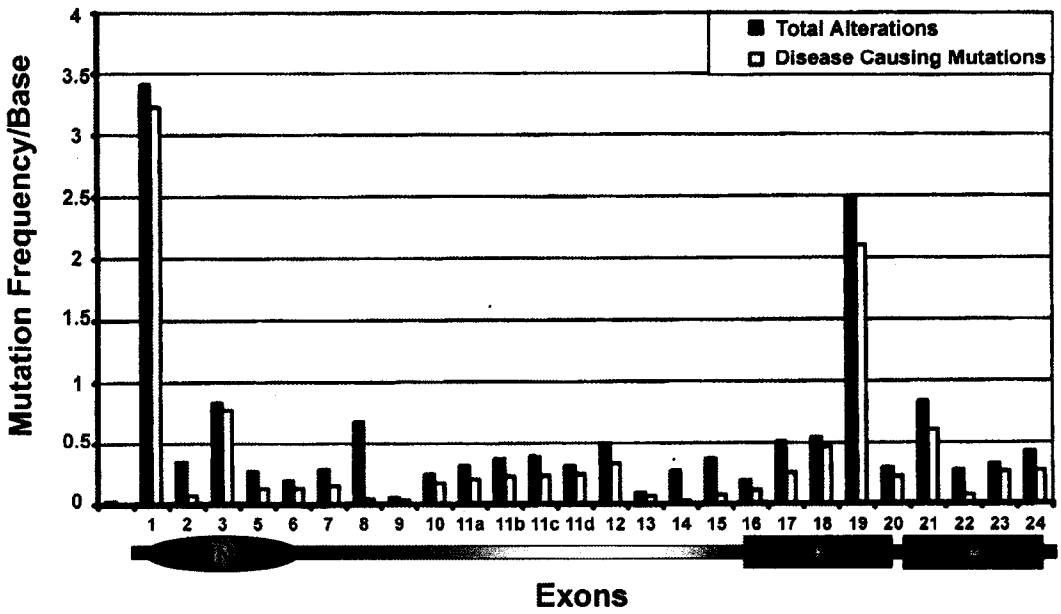

Figure 1.11. Distribution of BRCA1 mutations. The mutation frequency/base for recorded is plotted for BRCA1 exons. Exons 1-6 encode the N-terminal Ring finger domain, and exons 16-24 encode the BRCT repeat region. Mutations occur throughout the BRCA1 coding sequence, but cluster to the coding regions for the conserved Ring and BRCT domains. Adapted from Shen and Vadgama 1999.

Table 1.3. BRCA1 mutations

Mutation Type	Total Number of mutants recorded
Frameshift	3369
Missense	1837
Nonsense	739
Splice	369
Polymorphism	182
Unclassified	127
In Frame Deletion	31
Synonymous	3
In Frame Insertion	2
5'UTR	1

Source: http://research.nhgri.nih.gov/projects/bic (Jan. 2003)

Research Overview:

Despite the significant advances in BRCA1 research, the precise molecular mechanisms by which BRCA1 mediates its functions, and how these critical functions are abrogated by mutation remain largely unknown. Models of the BRCA1 BRCT region have been constructed based on the XRCC1 C-terminal BRCT, and used to predict the effects of BRCA1 mutations (Zhang et al 1998, Huyton et al. 2000). However, as sequence similarity amongst BRCT domains is typically very low (~14% pairwise mean sequence identity) these homology models are likely to be inaccurate in many respects, and inadequate to assess BRCA1 function and misfunction. In particular, several key questions remain: 1. What is the structural nature of dual and multiple repeat BRCT domains? 2. How do truncation and missense mutations affect the BRCA1 BRCT domains? 3. What are the molecular details of how the BRCA1-BRCT participates in protein-ligand interactions? This thesis describes my work towards acquisition of the crystal structure of the BRCT repeat region of the protein, and the molecular insights gained into the function of BRCA1 and how BRCT mutations result in the catastrophic inactivation of this highly conserved region of the BRCA1 tumour suppressor.

Chapter 2 outlines the biochemical dissection of a minimal, proteolytically resistant fragment of the extreme C-terminal region of human BRCA1 that proved amenable to crystallization studies. Further, I describe the determination of the crystal structure this BRCA1 fragment that has helped define the folding determinants of BRCT domains and highlights a conserved mode of

intramolecular BRCT-BRCT interaction. This work established a structural platform to understand, predict and measure the effects of mutations on this domain.

Building on the knowledge gained from the native BRCT structure, ***Chapter 3*** describes the response of the protein to a disease causing single amino acid substitution, M1775R, which has been used extensively to study misfunction of the *BRCA1* protein product. Data from proteolysis, circular dichroism and crystallographic experiments show that destabilization of the protein fold contributes to BRCA1 loss of function for this missense variant.

In ***Chapter 4,*** I present results of proteolysis experiments designed to assess structural defects associated with mutation of the BRCT. This section reveals that destabilization and misfolding of the BRCT is a common mechanism of BRCA1 inactivation. The work has provided a foundation for the interpretation of the effects of missense and truncation mutations on the structure and function of BRCA1 and it is our hope that these results will aid clinicians in assessing the risks associated with BRCT mutations.

In the final chapter (***Chapter 5***), I discuss the structure of the human BRCA1-BRCT repeats in the context of the growing number of BRCT containing protein nmr and crystal structures. These studies have unveiled the highly adaptable nature of BRCT domains that appear to serve as multipurpose protein-ligand interaction modules for a large number of proteins involved in cell-cycle control and DNA repair. I further speculate on the biological role of the BRCA1-BRCT repeat as a protein-protein and protein-DNA scaffolding domain and how

the inherent resistance of the BRCT to proteolytic degradation can be potentially exploited in the routine clinical assessment of risks associated with BRCT mutations.

References

Baldeyron, C., Jacquemin, E., Smith, J., Jacquemont, C., De Oliveira, I., Gad, S., Feunteun, J., Stoppa-Lyonnet, D., and Papadopoulo, D. A single mutated BRCA1 allele leads to impaired fidelity of double strand break end-joining. Oncogene, 21: 1401-10, 2002.

Boardman, L. A., Thibodeau, S. N., Schaid, D. J., Lindor, N. M., McDonnell, S. K., Burgart, L. J., Ahlquist, D. A., Podratz, K. C., Pittelkow, M., and Hartmann, L. C. Increased risk for cancer in patients with the Peutz-Jeghers syndrome. Ann Intern Med, 128: 896-9, 1998.

Bochar, D. A., Wang, L., Beniya, H., Kinev, A., Xue, Y., Lane, W. S., Wang, W., Kashanchi, F., and Shiekhattar, R. BRCA1 is associated with a human SWI/SNF-related complex: linking chromatin remodeling to breast cancer. Cell, 102: 257-65, 2000.

Bork, P., Hofmann, K., Bucher, P., Neuwald, A. F., Altschul, S. F., and Koonin, E. V. A superfamily of conserved domains in DNA damage-responsive cell cycle checkpoint proteins. FASEB J 11(1): 68-76. 1997.

Callebaut, I. and Mornon, J. P. From BRCA1 to RAP1: a widespread BRCT module closely associated with DNA repair. FEBS Lett 400(1): 25-30. 1997.

Cantor, S. B., Bell, D. W., Ganesan, S., Kass, E. M., Drapkin, R., Grossman, S., Wahrer, D. C., Sgroi, D. C., Lane, W. S., Haber, D. A., and Livingston, D. M. Bach1, a novel helicase-like protein, interacts directly with brca1 and contributes to its dna repair function. Cell 105(1): 149-60. 2001.

Chapman, M. S. and Verma, I. M. Transcriptional activation by BRCA1. Nature, 382: 678-9. 1996.

Cortez, D., Wang, Y., Qin, J., and Elledge, S. J. Requirement of ATM-dependent phosphorylation of brca1 in the DNA damage response to double-strand breaks. Science 286(5442): 1162-6. 1999.

Couch, F. J., DeShano, M. L., Blackwood, M. A., Calzone, K., Stopfer, J., Campeau, L., Ganguly, A., Rebbeck, T., and Weber, B. L. BRCA1 mutations in women attending clinics that evaluate the risk of breast cancer. N Engl J Med, 336: 1409-15. 1997.

Couch, F. J. and Weber, B. L. Mutations and polymorphisms in the familial early-onset breast cancer (BRCA1) gene. Breast Cancer Information Core. Hum Mutat , 8-18. 1996.

Critchlow, S. E., Bowater, R. P., and Jackson, S. P. Mammalian DNA double-strand break repair protein XRCC4 interacts with DNA ligase IV. Curr Biol, 7: 588-98, 1997.

Easton, D. F., Bishop, D. T., Ford, D., and Crockford, G. P. Genetic linkage analysis in familial breast and ovarian cancer: results from 214 families. The Breast Cancer Linkage Consortium. Am J Hum Genet, 52: 678-701, 1993.

Eisen, A. and Weber, B. L. Prophylactic mastectomy for women with BRCA1 and BRCA2 mutations--facts and controversy. N Engl J Med, 345: 207-8. 2001.

Friedman, L. S., Ostermeyer, E. A., Szabo, C. I., Dowd, P., Lynch, E. D., Rowell,

S. E., and King, M. C. Confirmation of BRCA1 by analysis of germline mutations linked to breast and ovarian cancer in ten families. Nat Genet, 8(4), 399-404. 1994.

Futreal, P. A., Liu, Q., Shattuck-Eidens, D., Cochran, C., Harshman, K., Tavtigian, S., Bennett, L. M., Haugen-Strano, A., Swensen, J., Miki, Y. and others. BRCA1 mutations in primary breast and ovarian carcinomas. Science, 266(5182): 120-2. 1994.

Gayther, S. A., Warren, W., Mazoyer, S., Russell, P. A., Harrington, P. A., Chiano, M., Seal, S., Hamoudi, R., van Rensburg, E. J., Dunning, A. M. and others. Germline mutations of the BRCA1 gene in breast and ovarian cancer families provide evidence for a genotype-phenotype correlation. Nat Genet, 11: 428-33. 1995.

Gowen, L. C., Avrutskaya, A. V., Latour, A. M., Koller, B. H., and Leadon, S. A. BRCA1 required for transcription-coupled repair of oxidative DNA damage. Science, 281(5379): 1009-12. 1998.

Gowen, L. C., Johnson, B. L., Latour, A. M., Sulik, K. K., and Koller, B. H. Brca1 deficiency results in early embryonic lethality characterized by neuroepithelial abnormalities. Nat Genet, 12: 191-4. 1996.

Greenblatt, M. S., Chappuis, P. O., Bond, J. P., Hamel, N., and Foulkes, W. D. TP53 mutations in breast cancer associated with BRCA1 or BRCA2 germ-line mutations: distinctive spectrum and structural distribution. Cancer Res, 61: 4092-7. 2001.

Grushcow, J. M., Holzen, T. M., Park, K. J., Weinert, T., Lichten, M., and Bishop,

D. K. Saccharomyces cerevisiae checkpoint genes MEC1, RAD17 and RAD24 are required for normal meiotic recombination partner choice. Genetics, 153(2): 607-20. 1999.

Hakem, R., de la Pompa, J. L., Sirard, C., Mo, R., Woo, M., Hakem, A., Wakeham, A., Potter, J., Reitmair, A., Billia, F., Firpo, E., Hui, C. C., Roberts, J., Rossant, J., and Mak, T. W. The tumor suppressor gene Brca1 is required for embryonic cellular proliferation in the mouse. Cell, 85(7): 1009-23. 1996.

Hall, J. M., Lee, M. K., Newman, B., Morrow, J. E., Anderson, L. A., Huey, B., and King, M. C. Linkage of early-onset familial breast cancer to chromosome 17q21. Science, 250: 1684-9. 1990.

Harkin, D. P., Bean, J. M., Miklos, D., Song, Y. H., Truong, V. B., Englert, C., Christians, F. C., Ellisen, L. W., Maheswaran, S., Oliner, J. D., and Haber, D. A. Induction of GADD45 and JNK/SAPK-dependent apoptosis following inducible expression of BRCA1. Cell, 97(5): 575-86. 1999.

Hayes, F., Cayanan, C., Barilla, D., and Monteiro, A. N. Functional assay for BRCA1: mutagenesis of the COOH-terminal region reveals critical residues for transcription activation. Cancer Res, 60: 2411-8. 2000.

Hu, Y. F., Hao, Z. L., and Li, R. Chromatin remodeling and activation of chromosomal DNA replication by an acidic transcriptional activation domain from BRCA1. Genes Dev, 13: 637-42. 1999.

Huyton, T., Bates, P. A., Zhang, X., Sternberg, M. J., and Freemont, P. S. The BRCA1 C-terminal domain: structure and function. Mutat Res, 460: 319-

332. 2000.

Koonin, E. V., Altschul, S. F., and Bork, P. BRCA1 protein products ... Functional motifs... Nature Genet, 13: 266-8. 1996.

Kubota, Y., Nash, R. A., Klungland, A., Schar, P., Barnes, D. E., and Lindahl, T. Reconstitution of DNA base excision-repair with purified human proteins: interaction between DNA polymerase beta and the XRCC1 protein. EMBO J, 15: 6662-70. 1996.

Li, J., Yen, C., Liaw, D., Podsypanina, K., Bose, S., Wang, S. I., Puc, J., Miliaresis, C., Rodgers, L., McCombie, R., Bigner, S. H., Giovanella, B. C., Ittmann, M., Tycko, B., Hibshoosh, H., Wigler, M. H., and Parsons, R. PTEN, a putative protein tyrosine phosphatase gene mutated in human brain, breast, and prostate cancer. Science, 275: 1943-7. 1997.

Li, S., Chen, P. L., Subramanian, T., Chinnadurai, G., Tomlinson, G., Osborne, C. K., Sharp, Z. D., and Lee, W. H. Binding of CtIP to the BRCT repeats of BRCA1 involved in the transcription regulation of p21 is disrupted upon DNA damage. J Biol Chem, 274(16): 11334-8. 1999.

Liaw, D., Marsh, D. J., Li, J., Dahia, P. L., Wang, S. I., Zheng, Z., Bose, S., Call, K. M., Tsou, H. C., Peacocke, M., Eng, C., and Parsons, R. Germline mutations of the PTEN gene in Cowden disease, an inherited breast and thyroid cancer syndrome. Nat Genet, 16: 64-7. 1997.

Lim, D. S. and Hasty, P. A mutation in mouse rad51 results in an early embryonic lethal that is suppressed by a mutation in p53. Mol Cell Biol, 16: 7133-43. 1996.

Malkin, D., Li, F. P., Strong, L. C., Fraumeni, J. F. Jr, Nelson, C. E., Kim, D. H., Kassel, J., Gryka, M. A., Bischoff, F. Z., Tainsky, M. A., and et, a. l. Germ line p53 mutations in a familial syndrome of breast cancer, sarcomas, and other neoplasms. Science, 250 : 1233-8, 1990.

Mallery, D. L., Vandenberg, C. J., and Hiom, K. Activation of the E3 ligase function of the BRCA1/BARD1 complex by polyubiquitin chains. EMBO J, 21: 6755-62. 2002.

Miki, Y., Swensen, J., Shattuck-Eidens, D., Futreal, P. A., Harshman, K., Tavtigian, S., Liu, Q., Cochran, C., Bennett, L. M., Ding, W. and others. A strong candidate for the breast and ovarian cancer susceptibility gene BRCA1. Science, 266(5182): 66-71. 1994.

Monteiro, A. N., August, A., and Hanafusa, H. Evidence for a transcriptional activation function of BRCA1 C-terminal region. Proc Natl Acad Sci U S A, 93: 13595-9, 1996.

Moynahan, M. E., Chiu, J. W., Koller, B. H., and Jasin, M. Brca1 controls homology-directed DNA repair. Mol Cell, 4(4): 511-8. 1999.

Nash, R. A., Caldecott, K. W., Barnes, D. E., and Lindahl, T. XRCC1 protein interacts with one of two distinct forms of DNA ligase III. Biochemistry, 36(17): 5207-11. 1997.

Nathanson, K. L., Wooster, R., Weber, B. L., and Nathanson, K. N. Breast cancer genetics: what we know and what we need. Nat Med, 7: 552-6, 2001.

Neuhausen, S. L. and Marshall, C. J. Loss of heterozygosity in familial tumors from three BRCA1-linked kindreds. Cancer Res, 54: 6069-72. 1994.

Pao, G. M., Janknecht, R., Ruffner, H., Hunter, T., and Verma, I. M. CBP/p300 interact with and function as transcriptional coactivators of BRCA1. Proc Natl Acad Sci U S A, 97 : 1020-5. 2000.

Paull, T. T., Cortez, D., Bowers, B., Elledge, S. J., and Gellert, M. Direct DNA binding by Brca1. Proc Natl Acad Sci U S A, 98: 6086-91, 2001.

Peto, J., Collins, N., Barfoot, R., Seal, S., Warren, W., Rahman, N., Easton, D. F., Evans, C., Deacon, J., and Stratton, M. R. Prevalence of BRCA1 and BRCA2 gene mutations in patients with early- onset breast cancer. J Natl Cancer Inst, 91: 943-9, 1999.

Rebbeck, T. R., Levin, A. M., Eisen, A., Snyder, C., Watson, P., Cannon-Albright, L., Isaacs, C., Olopade, O., Garber, J. E., Godwin, A. K., Daly, M. B., Narod, S. A., Neuhausen, S. L., Lynch, H. T., and Weber, B. L. Breast cancer risk after bilateral prophylactic oophorectomy in BRCA1 mutation carriers. J Natl Cancer Inst, 91: 1475-9. 1999.

Scully, R., Anderson, S. F., Chao, D. M., Wei, W., Ye, L., Young, R. A., Livingston, D. M., and Parvin, J. D. BRCA1 is a component of the RNA polymerase II holoenzyme. Proc Natl Acad Sci U S A, 94: 5605-10, 1997.

Scully, R., Chen, J., Ochs, R. L., Keegan, K., Hoekstra, M., Feunteun, J., and Livingston, D. M. Dynamic changes of BRCA1 subnuclear location and phosphorylation state are initiated by DNA damage. Cell, 90: 425-35, 1997.

Scully, R., Chen, J., Plug, A., Xiao, Y., Weaver, D., Feunteun, J., Ashley, T., and Livingston, D. M. Association of BRCA1 with Rad51 in mitotic and meiotic

cells. Cell, 88(2): 265-75. 1997.

Scully, R., Chen, J., Plug, A., Xiao, Y., Weaver, D., Feunteun, J., Ashley, T., and Livingston, D. M. Association of BRCA1 with Rad51 in mitotic and meiotic cells. Cell, 88: 265-75, 1997.

Scully, R., Ganesan, S., Vlasakova, K., Chen, J., Socolovsky, M., and Livingston, D. M. Genetic analysis of BRCA1 function in a defined tumor cell line. Mol Cell, 4: 1093-9. 1999.

Scully, R. and Livingston, D. M. In search of the tumour-suppressor functions of BRCA1 and BRCA2. Nature, 408: 429-32. 2000.

Shattuck-Eidens, D., McClure, M., Simard, J., Labrie, F., Narod, S., Couch, F., Hoskins, K., Weber, B., Castilla, L., Erdos, M. and others. A collaborative survey of 80 mutations in the BRCA1 breast and ovarian cancer susceptibility gene. Implications for presymptomatic testing and screening. JAMA, 273: 535-41. 1995.

Shen, D. and Vadgama, J. V. BRCA1 and BRCA2 gene mutation analysis: visit to the Breast Cancer Information Core (BIC). Oncol Res, 11: 63-9. 1999.

Shen, S. X., Weaver, Z., Xu, X., Li, C., Weinstein, M., Chen, L., Guan, X. Y., Ried, T., and Deng, C. X. A targeted disruption of the murine Brca1 gene causes gamma-irradiation hypersensitivity and genetic instability. Oncogene, 17(24): 3115-24. 1998.

Smith, S. A., Easton, D. F., Evans, D. G., and Ponder, B. A. Allele losses in the region 17q12-21 in familial breast and ovarian cancer involve the wild-type chromosome. Nat Genet, 2: 128-31, 1992.

Somasundaram, K., Zhang, H., Zeng, Y. X., Houvras, Y., Peng, Y., Zhang, H., Wu, G. S., Licht, J. D., Weber, B. L., and El-Deiry, W. S. Arrest of the cell cycle by the tumour-suppressor BRCA1 requires the CDK-inhibitor p21WAF1/CiP1. Nature, 389(6647): 187-90. 1997.

Struewing, J. P., Tarone, R. E., Brody, L. C., Li, F. P., and Boice, J. D. Jr BRCA1 mutations in young women with breast cancer. Lancet, 347:1493. 1996.

Sum, E. Y., Peng, B., Yu, X., Chen, J., Byrne, J., Lindeman, G. J., and Visvader, J. E. The LIM domain protein LMO4 interacts with the cofactor CtIP and the tumor suppressor BRCA1 and inhibits BRCA1 activity. J Biol Chem, 277: 7849-56, 2002.

Taylor, R. M., Wickstead, B., Cronin, S., and Caldecott, K. W. Role of a BRCT domain in the interaction of DNA ligase III-alpha with the DNA repair protein XRCC1. Curr Biol, 8: 877-80. 1998.

Vallon-Christersson, J., Cayanan, C., Haraldsson, K., Loman, N., Bergthorsson, J. T., Brondum-Nielsen, K., Gerdes, A. M., Moller, P., Kristoffersson, U., Olsson, H., Borg, A., and Monteiro, A. N. Functional analysis of BRCA1 C-terminal missense mutations identified in breast and ovarian cancer families. Hum Mol Genet, 10: 353-60. 2001.

Venkitaraman, A. R. Cancer susceptibility and the functions of BRCA1 and BRCA2. Cell, 108: 171-82, 2002.

Wang, Y., Cortez, D., Yazdi, P., Neff, N., Elledge, S. J., and Qin, J. BASC, a super complex of BRCA1-associated proteins involved in the recognition and repair of aberrant DNA structures. Genes Dev, 14: 927-39. 2000.

Weber, B. L. and Nathanson, K. L. Low penetrance genes associated with increased risk for breast cancer. Eur J Cancer, 36: 1193-9. 2000.

Williams, W. R. and Anderson, D. E. Genetic epidemiology of breast cancer: segregation analysis of 200 Danish pedigrees. Genet Epidemiol, 1: 7-20. 1984.

Wooster, R., Bignell, G., Lancaster, J., Swift, S., Seal, S., Mangion, J., Collins, N., Gregory, S., Gumbs, C., and Micklem, G. Identification of the breast cancer susceptibility gene BRCA2. Nature, 378: 789-92. 1995.

Wooster, R., Neuhausen, S. L., Mangion, J., Quirk, Y., Ford, D., Collins, N., Nguyen, K., Seal, S., Tran, T., Averill, D. and others. Localization of a breast cancer susceptibility gene, BRCA2, to chromosome 13q12-13. Science, 265(5181): 2088-90. 1994.

Xu, X., Qiao, W., Linke, S. P., Cao, L., Li, W. M., Furth, P. A., Harris, C. C., and Deng, C. X. Genetic interactions between tumor suppressors Brca1 and p53 in apoptosis, cell cycle and tumorigenesis. Nat Genet, 28: 266-71, 2001.

Yamane, K. and Tsuruo, T. Conserved BRCT regions of TopBP1 and of the tumor suppressor BRCA1 bind strand breaks and termini of DNA [In Process Citation]. Oncogene, 18(37): 5194-203. 1999.

Yarden, R. I. and Brody, L. C. BRCA1 interacts with components of the histone deacetylase complex. Proc Natl Acad Sci U S A, 96(9): 4983-8. 1999.

Ye, Q., Hu, Y. F., Zhong, H., Nye, A. C., Belmont, A. S., and Li, R. BRCA1-induced large-scale chromatin unfolding and allele-specific effects of

cancer-predisposing mutations. J Cell Biol, 155: 911-21. 2001.

Yu, X. and Baer, R. Nuclear localization and cell cycle-specific expression of CtIP, a protein that associates with the BRCA1 tumor suppressor. J Biol Chem, 275:18541-9. 2000.

Yu, X., Wu, L. C., Bowcock, A. M., Aronheim, A., and Baer, R. The C-terminal (BRCT) domains of BRCA1 interact in vivo with CtIP, a protein implicated in the CtBP pathway of transcriptional repression. J Biol Chem, 273: 25388-92. 1998.

Yu, X., Wu, L. C., Bowcock, A. M., Aronheim, A., and Baer, R. The C-terminal (BRCT) domains of BRCA1 interact in vivo with CtIP, a protein implicated in the CtBP pathway of transcriptional repression. J Biol Chem, 273: 25388-92. 1998.

Zhang, X., Morera, S., Bates, P. A., Whitehead, P. C., Coffer, A. I., Hainbucher, K., Nash, R. A., Sternberg, M. J., Lindahl, T., and Freemont, P. S. Structure of an XRCC1 BRCT domain: a new protein-protein interaction module. EMBO J, 17(21): 6404-11. 1998.

Zhong, Q., Chen, C. F., Li, S., Chen, Y., Wang, C. C., Xiao, J., Chen, P. L., Sharp, Z. D., and Lee, W. H. Association of BRCA1 with the hRad50-hMre11-p95 complex and the DNA damage response. Science, 285(5428): 747-50. 1999.

Chapter 2:

The crystal structure of the BRCT repeat region from the breast cancer-associated protein, BRCA1

SUMMARY

The C-terminal, BRCT repeat region is essential to the DNA repair, transcriptional regulation and tumor suppressor functions of BRCA1. Employing limited proteolysis and deletion mutagenesis, we defined a structurally ordered fragment of the BRCA1 C-terminus that is amenable to crystallization. This polypeptide includes the tandem BRCT repeats of BRCA1 joined by a proteolytically stable linker region. The crystal structure of the human BRCT domain has been determined at 2.5Å resolution using multiwavelength anomalous dispersion and a seleno-methionine protein derivative. The domain contains the two BRCT repeats that adopt similar structures and are packed together in a head-to-tail arrangement. Cancer-causing missense mutations occur at the interface between the two repeats, destabilize the structure, and increase its sensitivity to proteolytic degradation. The manner by which the two BRCT repeats interact in BRCA1 may represent a general mode of interaction between homologous domains within proteins that interact to regulate the cellular response to DNA damage. The structure provides a basis to predict the structural consequences of previously uncharacterized BRCT mutations.

INTRODUCTION:

The C-terminal region in BRCA1 is essential to its tumor suppressor activity because missense and truncation mutations within this region lead to early onset breast cancer (Friedman et al. 1994, Futreal et al. 1994, Miki et al. 1994, Gayther et al. 1995). This region contains two ~90-100 amino acid sequence repeats called BRCT (**BR**CA1 **C-t**erminal) repeats (Bork et al. 1997, Callebaut & Mornon 1997), which bear weak amino acid sequence similarity to other proteins involved in DNA repair, such as the yeast protein RAD9, the mammalian protein XRCC1, as well as the p53 binding protein, 53BP1. BRCT repeats are thought to serve as multi-purpose protein-protein interaction modules, binding to other BRCT repeats or other protein domains with apparently unrelated structures. A large body of evidence suggests that the BRCA1 BRCT region interacts with proteins involved in transcriptional control or DNA repair (for a review, see Deng & Brodie 2000), including the transcriptional co-repressor CtIP, histone deacetylases, p53, p300, and the DNA damage-associated helicase BACH1 (Cantor et al. 2001). We set out to determine the X-ray structure of the BRCT region of BRCA1 to gain structural insights into its function and to provide a basis to assess the cancer risks associated with specific BRCT mutations. The majority of this chapter was originally published in the journal *Nature Structural Biology* (Williams et al. 2001).

EXPERIMENTAL PROCEDURES:

Cloning and Vector Construction

Coding sequences for BRCT C-terminal truncations of human BRCA1 were amplified from the T7 promoter based expression vector for pGEX-6P1-BRCA1-(1528-1863) (plasmid kindly provided by Luc Gaudreau – University of Sherbrooke, Canada) using the following oligonucleotides: (fragment 1646-1859) FT7-5'-gga cga gaa ttc tta acc agg gag ctg att atg gtg aac aaa aga atg tcc atg-3', CD6-5'-gat ctg gga tcc tca ggg gat ctg ggg tat cag-3'; (fragment 1646-1858) FT7, CD7-5'-gat ctg gga tcc tca gat ctg ggg tat cag gta-3' ; (fragment 1646-1857) FT7, CD1-5'-gat ctg gga tcc tca ctg ggg tat cag gta ggt-3' ; (fragment 1646-1855) FT7, CD5-5'-gat ctg gga tcc tca tat cag gta ggt gtc cag-3' ; (fragment 1646-1853) FT7, CD4-5'- gat ctg gga tcc tca gta ggt gtc cag ctc ctg-3' ; (fragment 1646-1852) FT7, 1853Ystop-5'-gat ctg gga tcc tca ggt gtc cag ctc ctg gca-3' ; (fragment 1646-1851) FT7, CD3-5'-gat ctg gga tcc tca gtc cag ctc ctg gca ctg-3' ; (fragment 1646-1849) FT7, CD2-5'-gat ctg gga tcc tca ctc ctg gca ctg gta gag-3'. The 5' primer FT7 incorporates a ribosome binding site and an EcoRI site for cloning. 3' oligonucleotides include the relevant stop codons and a BamHI restriction site. Gel purified PCR products were digested with EcoRI and BamHI and cloned into BamHI-EcoRI digested pLM1 (Sodeoka 1993). The BRCT single amino acid substitutions were introduced into the BRCT-CD6 fragment (aa 1646-1859). For missense mutations A1708E and M1775R mutated BRCA1 coding sequences were used as templates for PCR amplification with the FT7 and CD6 primers (mutant templates kindly provided by Richard Baer – Columbia University, USA).

BRCT expression and purification

Human BRCA1(1528-1863), used in the initial domain mapping experiments, was expressed and purified as a GST-fusion protein by glutathione-affinity chromatography. BRCA1(1528-1863) was then cleaved from GST using Prescission protease (Amersham-Pharmacia) and the C-terminal BRCA1 polypeptide was purified from GST by gel filtration chromatography.

Native BRCT-CD6 (1646-1859) was expressed in BL21(DE3). Production of seleno-methionine substituted BRCT-CD6 was conducted essentially as described previously (Doublie 1997). All cell growth was carried out at 25 °C and cells were induced with 0.5 mM IPTG for 10-12 hours once the cultures had reached an OD_{600} of 1.0-1.2.

Recombinant native and selenomethionine-containing BRCT-CD6 were purified to >95 % purity using a combination of ammonium sulphate precipitation, hydrophobic interaction, gel filtration and anion exchange chromatography. Cells from 4 L of culture were resuspended on ice in 200 mL Lysis Buffer (50 mM Tris-HCl pH 7.5, 1 mM EDTA, 150 mM NaCl, 0.1% β–mercaptoethanol, 10 μg/mL PMSF) and disrupted by incubation for 30 minutes with 0.5 mg/mL HEW lysozyme and two 30 second sonication pulses with a Branson sonicator (75-80% power setting, 1 cm probe). Cell debris was removed by centrifugation at 12000 xg for 30 min. For solubility analysis of deletion mutants, samples before and after centrifugation at this stage of purification were electrophoresed on 15 % SDS-PAGE gels and visualized by Coomassie staining. Polyethylenimine (PEI) was added to the lysate to a final concentration of 0.3 %. After 20 minutes of

stirring, the lysate-PEI mix was centrifuged for 15 minutes at 12000 xg to remove precipitated nucleic acids. 32 g $(NH4)_2SO_4$ per 100 mL lysate was added to achieve an approximate ~50 % $(NH4)_2SO_4$ saturated protein lysate that was stirred at 4 °C for 20 minutes and then centrifuged for 20 minutes at 12000 xg to pellet the BRCT. The ammonium sulphate pellet was dissolved in 50 mL Low Salt Buffer (50 mM Tris-HCl pH 7.5, 0.1% β mercaptoethanol) and then adjusted to high salt with addition of 90 mL of Hic-High buffer (50 mM Tris-HCl pH 7.5, 1.5 M $(NH4)_2SO_4$, 0.1% β–ME) prior to loading of a Pharmacia C4-Butyl-sepharose column. Peak fractions from the 1.5 M to 0.0 M $(NH4)_2SO_4$ elution gradient were pooled, concentrated, and run on a Pharmacia Superdex-75 column in Gel Filtration Buffer (50 mM Tris-HCl pH 7.5, 150 mM NaCl, 0.1% β–ME). Pooled gel filtration fractions were then run on a Pharmacia SP-sepharose-FastFlow anion exchange column with an elution gradient from 0.0 M to 1.0 M NaCl in 50 mM Tris-HCl at pH 7.5. Pure fractions were concentrated and dialyzed into protein solution (see below) with a Millipore 10 KDa MW Cutoff ultrafiltration unit. Preparations typically yielded 5-10 mg/L *E. coli.*

Crystallization

Crystals were grown at 20-23 °C using the hanging drop vapor diffusion technique. Crystals of selenomethionine substituted BRCA1(1646-1859) were grown by mixing 3 μL of 20 mg mL^{-1} BRCT domain in protein solution (400 mM NaCl, 5 mM Tris-HCl pH 7.5) with 3 μL of well solution 1 (1.5 M $(NH4)_2SO_4$, 100 mM MES, pH 6.7, 10 mM $CoCl_2 x\ 6H_20$) (Table 1). Native crystals were grown by mixing 3 μL 18 mg mL^{-1} BRCA1 (1646-1859) in protein solution with 3 μL well

solution 2 (0.8 M Li_2SO_4, 100 mM Tris-HCl, pH 8.5, 2.5 mM $NiCl_2 \times 6H_20$, 5 mM $CaCl_2$).

Data collection and processing

For data collection at 100 K, crystals were flash frozen in liquid nitrogen after gradual transfer to a cryoprotectant solution comprised of the respective well solution supplemented with 26% glycerol. MAD and native data were obtained at beamlines 14BM-D and 14BM-C, respectively, at the Advanced Photon Source (APS, BioCARS). All data were scaled and reduced with the HKL package (Otwinowski & Minor 1997).

Phasing, model building and refinement

Eight of nine selenium positions were located and refined using SOLVE (Terwilliger & Berendzen 1999), and crystallographic phases were improved by solvent flattening and histogram matching implemented in DM (Cowtan 1994). The majority of the polypeptide chain was built with O (Jones et al. 1991) using the solvent-flattened, MAD-phased electron density map at 2.9 Å resolution. The initial model was first refined against the remote wavelength ($\lambda 3$) MAD dataset to 2.9 Å resolution in CNS (Brünger et al. 1998) using torsion angle molecular dynamics (MLHL target). Maximum likelihood targets, bulk solvent correction and overall anisotropic B-factor scaling were applied throughout the refinement process. Further refinement against the native data to 2.5 Å resolution involved iterative cycles of manual building and restrained refinement with TLS group anisotropic thermal parameter modeling as implemented in REFMAC (v5.0.32) (Collaborative Computational Project 1994, Winn et al. 2001). Anomalous

difference Fourier synthesis using the native data and phases calculated from the final model, confirmed the positions of 10/13 sulphur atoms. The three missing sulphur atoms correspond to somewhat poorly ordered methionines, Met 1650, Met 1728 and Met 1827, whose positions were determined from the MAD data. An additional 15σ peak was found in the anomalous difference map positioned between two histidine residues within a crystal contact. We have modeled a nickel atom at this position, however, Ca^{2+} is also present in the crystallization solution, and might also bind at this site. This accounts for the absolute requirement for divalent metals in the crystallization solution. Poor electron density was observed for much of the inter-repeat linker and the β3-α2 and β3'-α2' loops, suggesting that these regions are relatively flexible. As a result, linker residues 1743-1747 have been modeled as poly-alanine, while residue 1694 from the β3-α2 loop and residues 1817-1819 from the β3'-α2' loop have been omitted from the final model. Analysis of stereochemistry by PROCHECK (Laskowski et al. 1998) indicates that the model contains 82.8% of the residues in the most favorable regions of the Ramachandran plot, with no residues in the disallowed regions. Refinement statistics are provided in Table 1. Figures were created with BOBSCRIPT (Esnouf 1997, Esnouf 1999) and rendered with RASTER3D (Merritt & Bacon 1997) (Fig. 2.10*b,c*), or POVRAY (www.povray.org) (Fig. 2.7, 2.8, 2.9, 2.10*a*). The atomic coordinates and structure factors are available in the RCSB protein data bank (www.rcsb.org/pdb, *accession code* 1JNX).

Proteolytic mapping of the BRCT domain

Purified BRCA1(1528-1863) at 400 μg/mL was digested with either elastase (50 μg mL^{-1}) or trypsin (2 μg mL^{-1}) for the indicated times, the reactions were terminated with PMSF, and the reaction products were separated by SDS-PAGE and stained with Coomassie.

To assay the proteolytic sensitivity of BRCT domain mutants, wild type BRCA1 BRCT (1646-1859), as well as Ala 1708 → Glu, Met 1775 → Arg and Tyr 1853 → *stop* mutants were expressed by *in vitro* transcription/translation (TNTQuick, Promega) and labeled with ^{35}S-methionine. The transcription/translation reactions were centrifuged to remove insoluble material. Three μL of the supernatant from each reaction was then digested with either trypsin, elastase or chymotrypsin for 10 minutes at 25 °C in a final reaction volume of 15 μL. Reaction products were visualized by SDS-PAGE and autoradiography.

RESULTS AND DISCUSSION

Engineering the BRCT for Crystallization

Previous attempts to express the isolated BRCT domains of BRCA1 were unsuccessful, resulting in the production of insoluble or degraded protein products in *E. coli* (Zhang et al. 1998). A GST-fusion of a larger fragment of the human BRCA1 C-terminus, termed the SZ domain (aa 1528-1863) (Scully et al. 1997) could, however, be expressed and purified in an *E. coli.* system (Fig. 2.1, Experimental Procedures). We first used limited proteolytic mapping to locate a folded protein domain within this purified C-terminal fragment of BRCA1. As shown in Fig. 2.1, both trypsin and elastase rapidly digest BRCA1 (1528-1863) to a proteolytically stable fragment. Electrospray mass spectrometry and N-terminal sequencing of the products of the trypsin digestion indicated that the major species had a molecular weight of 25038 (+/- 5) Da and the N-terminal sequence "VNKR", corresponding to BRCA1 residues 1646-1863. This fragment contains both of the predicted BRCT repeats (Bork et al. 1997, Callebaut & Mornon 1997), which suggests that the two BRCT repeats and the associated linker together form a stable structural unit (Fig. 2.2). Although the trypsin fragment can be expressed and purified in milligram quantities, this protein aggregates in solution within days and extensive efforts to crystallize it failed. We produced a series of C-terminal deletions of this protein in a search for more soluble BRCT derivatives. As shown in Fig. 2.3 and summarized in Table 2.1, the protein tolerates removal of 8 residues from the C-terminus, but larger deletions

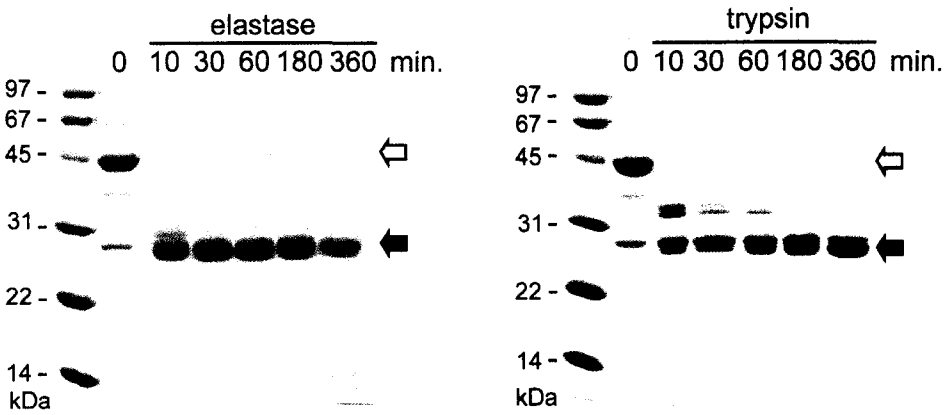

Figure. 2.1. The two BRCT repeats form a single protein domain – Defining the N-terminal boundary of the BRCT tandem repeat. Purified BRCA1 (1528-1863) was digested with either trypsin or elastase for the times indicated, and the products were analysed by SDS-PAGE. The open arrows indicate BRCA1(1528-1863), the closed arrows indicate the proteolytically resistant fragments.

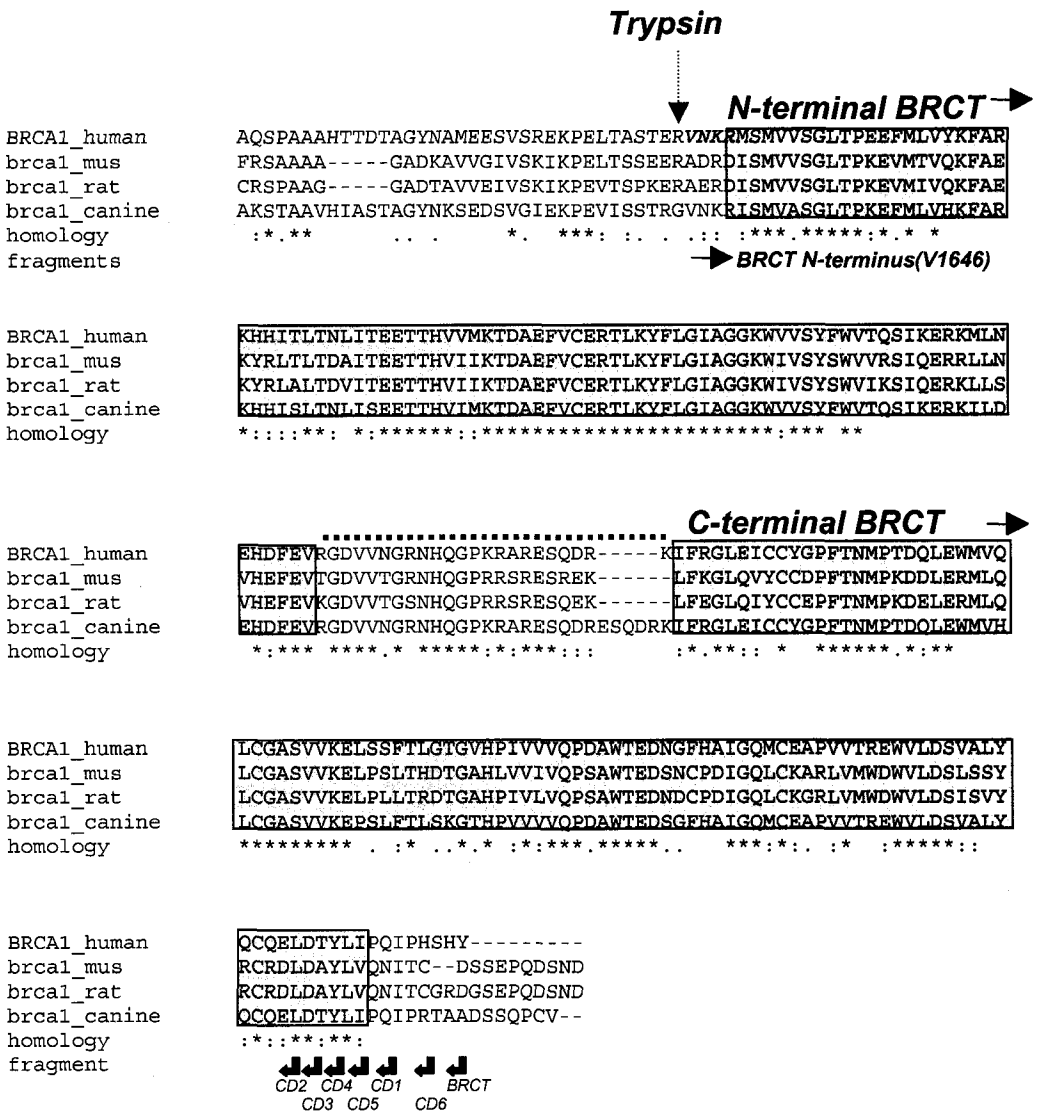

Figure 2.2. Defining the amino and carboxy terminal boundaries of the BRCT domain. Amino acid sequence alignment for the BRCT repeat region of mammalian BRCA1 homologues. Grey shading indicates the predicted BRCT domains. The N-terminal boundary of the BRCT dual repeat was determined by trypsinolysis. The dashed arrow indicates residue Arg-1645, which is an accessible trypsin cleavage site. Residues in bold italics were identified by N-terminal sequencing of the purified trypsin digestion product of BRCA1-SZ. The C-terminal boundaries of BRCT deletion fragments tested are indicated.

result in insoluble protein products. Crystallization analysis of proteins from the deletion series suggests that the CD6 truncation (aa 1646-1859), which removes the four most C-terminal residues of the protein that are not conserved among mammalian BRCA1 homologues (Fig. 2.2), produces the best crystals of a low salt – PEG orthorhombic crystal form (Table 2.1). The best of these crystals, however, diffract only to ~4.5 Å and are unsuitable for structural analysis (data not shown). Subsequent crystallization screens with the BRCT-CD6 fragment in higher salt conditions have yielded two additional crystal forms (Fig. 2.4). Two closely related hexagonal crystal forms diffract x-rays beyond 3.0 Å using synchrotron radiation (Figures 2.5 and 2.6). With these crystals we determined the structure of BRCA1 (1646-1859) at 2.5 Å resolution using the multiwavelength anomalous dispersion method (MAD) (Terwilliger & Berendzen 1999) and a seleno-methionine substituted BRCT derivative (see Experimental Procedures, Fig. 2.7, Table 2.2).

Overall structure

The dual-repeat, BRCT domain of BRCA1 adopts an elongated structure ~70 Å long and ~30-35 Å in diameter. Each of the two BRCT repeats adopts a structure similar to that previously observed in the isolated, C-terminal BRCT repeat from XRCC1 (Zhang et al. 1998), as well as the single BRCT repeat in an NAD^+-dependent DNA ligase (Lee et al. 2000). The BRCT fold is characterized by a central parallel four-stranded β-sheet with a pair of α-helices (α1 and α3) packed against one face and a single α-helix (α2) packed against the opposite

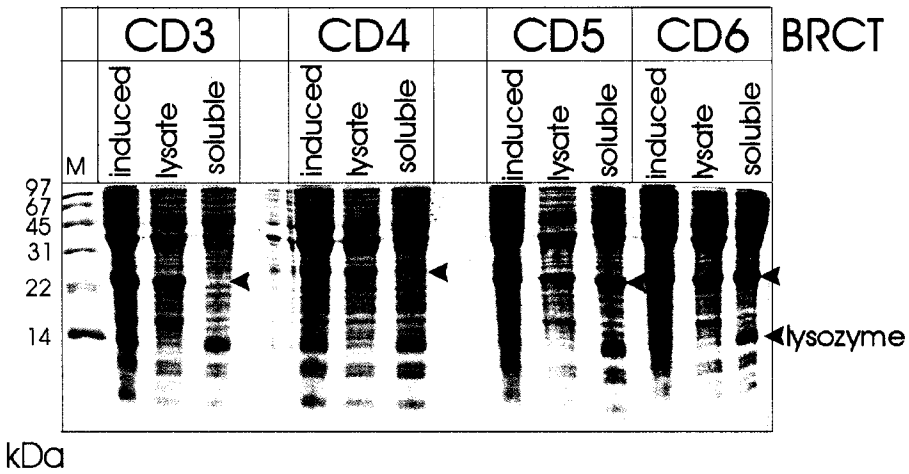

Figure 2.3. Defining the C-terminal boundary by deletion mutagenesis and solubility analysis. E. coli lysates harboring the indicated BRCA1-BRCT deletion mutants were analyzed by SDS-PAGE. Lysate and soluble fractions are the crude protein preparations before and after centrifugation (see Experimental Procedures). Arrows indicate the expressed ~25 kDa BRCT variants.

Table 2.1 Solubility and Crystallization analysis of BRCT Deletion fragments

C-terminal Sequence	Fragment	Solubility + soluble - insoluble	Crystallization (low salt PEG)
QCQELDTYLIPQIPHSHY-1863	BRCT	+	-
QCQELDTYLIPQIP-1859	CD6	+	++
QCQELDTYLIPQI-1858	CD7	+	+
QCQELDTYLIPQ-1857	CD1	+	+
QCQELDTYLI-1855	CD5	+	-
QCQELDTY-1853	CD4	-	-
QCQELDT-1852	Y1853ter	-	-
QCQELD-1851	CD3	-	-
QCQE-1849	CD2	-	-

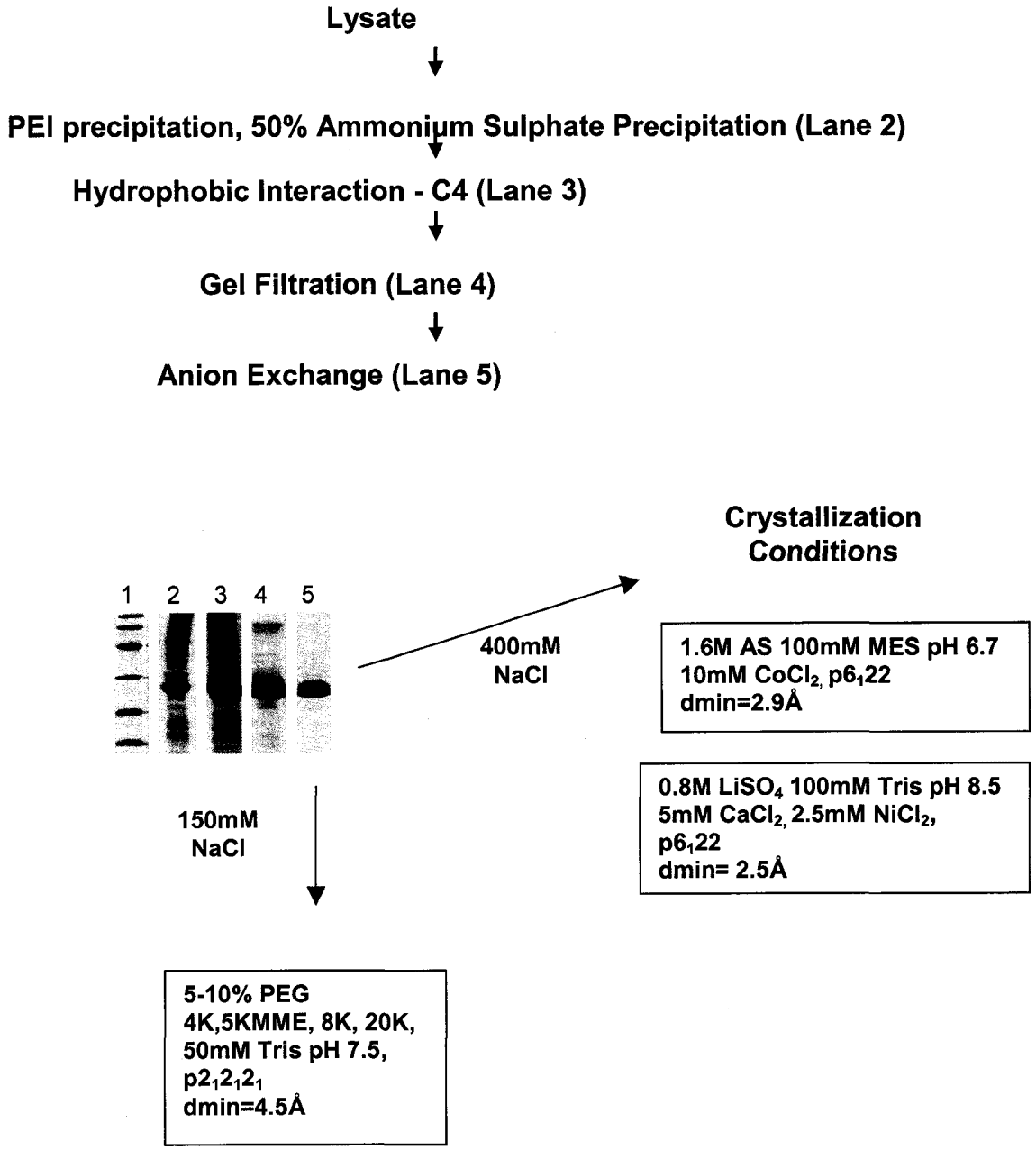

Figure 2.4 Expression, purification and crystallization scheme for BRCT trypsin fragment derivatives. BRCT-CD6 (aa 1646-1859) was purified by ammonium sulphate precipitation and a combination of three chromatographic steps. In low salt (150mM NaCl), poorly diffracting crystals are obtained with high molecular weight polyethylene glycols as the precipitant. Dialysis of the pure protein into higher salt conditions (400mM NaCl) helps yield two related crystal forms of the BRCT that were used for crystallographic phasing and refinement.

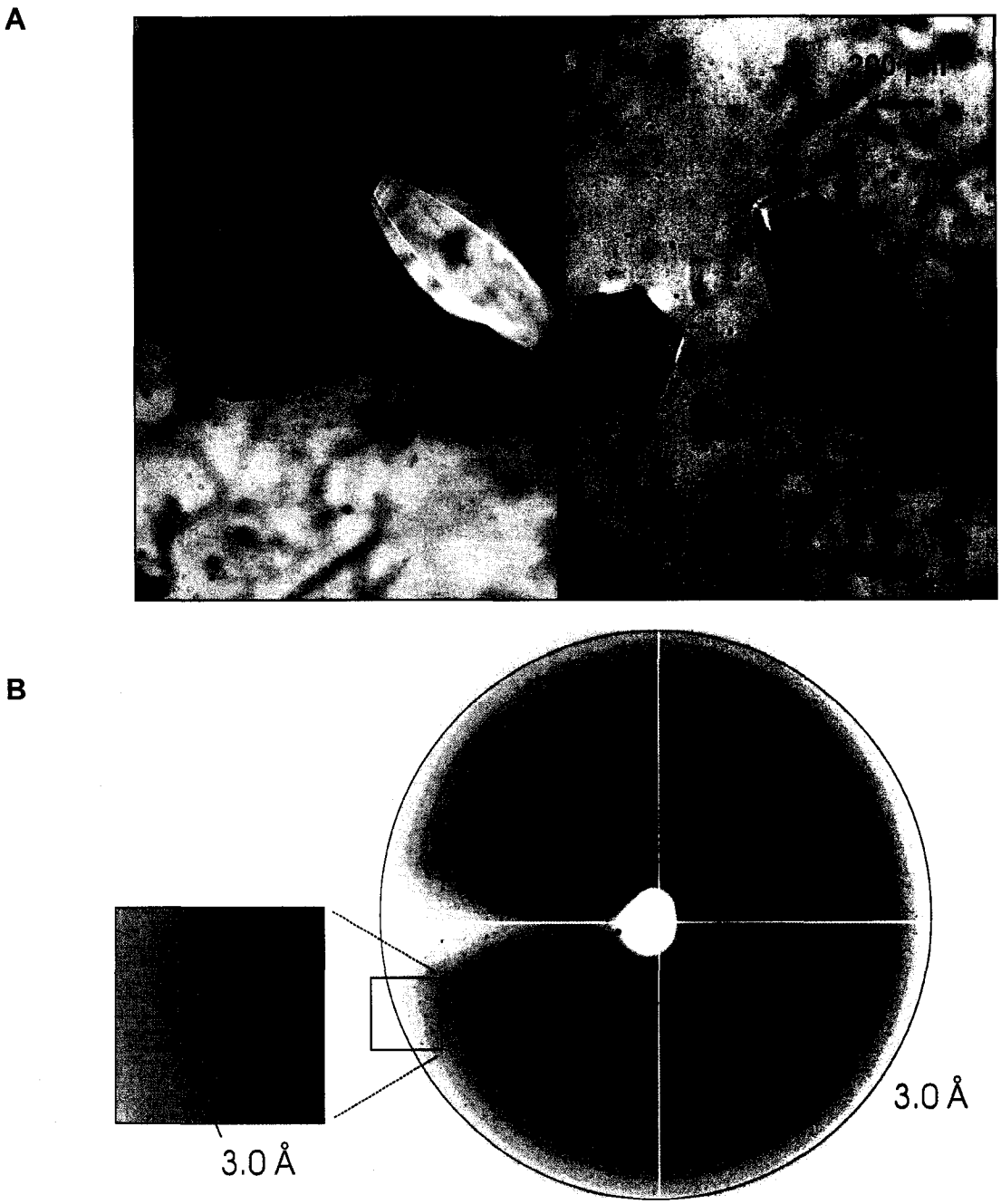

Figure 2.5 Ammonium sulphate / Cobalt hexagonal crystal form. A. BRCT-CD6 (aa 1646-1859) crystals grown with $(NH4)_2SO4$ as the precipitant and a $CoCl_2$ additive. **B.** Sample diffraction pattern from the seleno-methionine substituted protein crystals used for phasing.

A

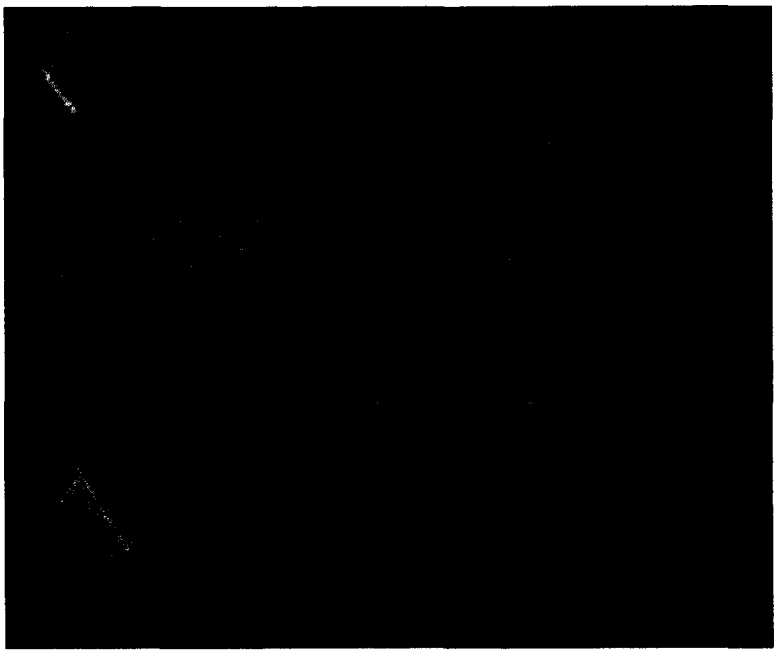

B

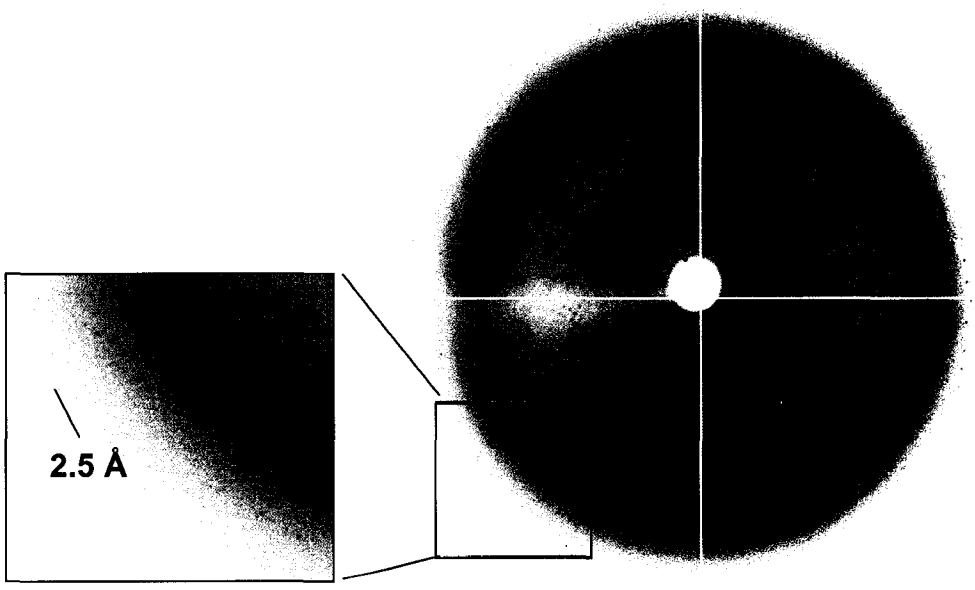

Figure 2.6 Lithium sulphate / Nickel-Calcium hexagonal crystal form. A. BRCT-CD6 (aa1646-1859) crystals grown with LiSO4 as the precipitant with $NiSO_4$ and $CaCl_2$ additives. **B.** Sample diffraction pattern from native protein crystals used in refinement.

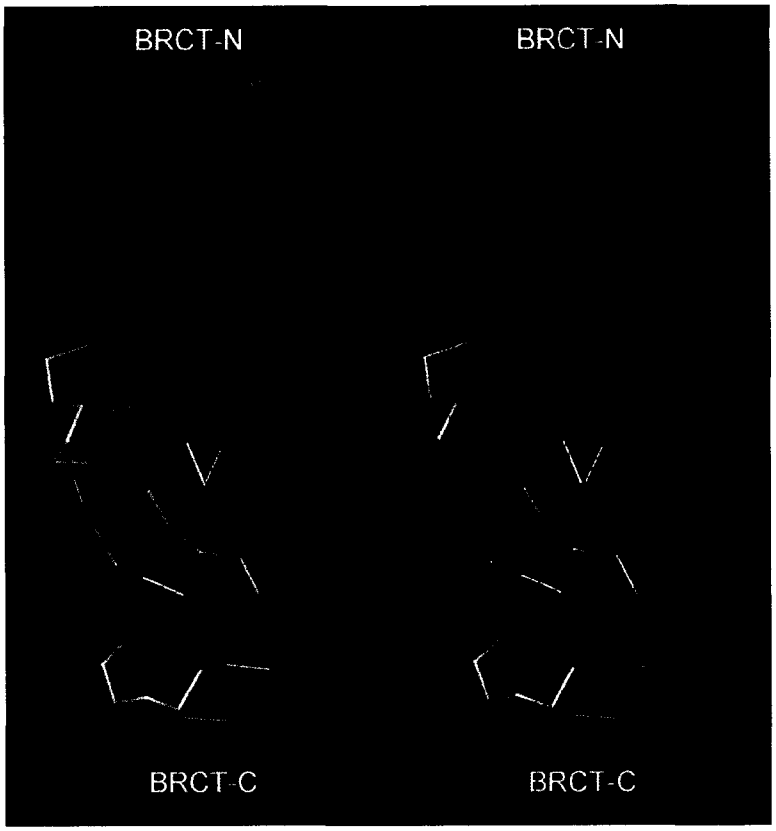

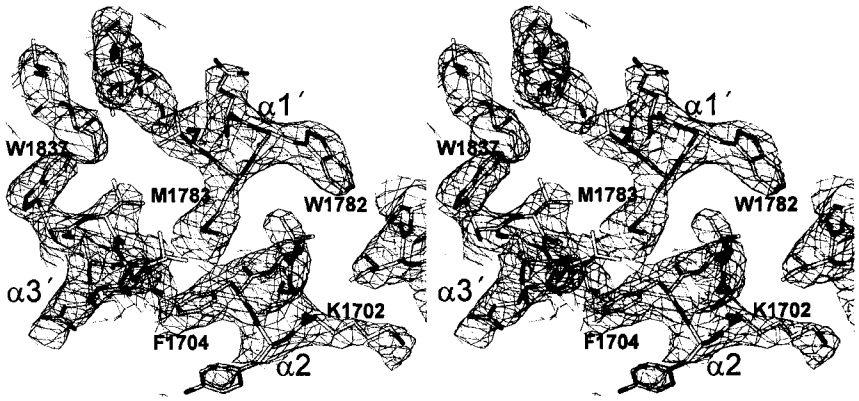

Figure 2.7. Experimental electron density maps from selenomethionine substituted BRCT hexagonal crystals. A. The MAD-phased, density modified, electron density at 2.9 Å resolution is contoured at 1.0 σ and displayed for the crystallographic asymmetric unit and contoured around an alpha carbon trace of the BRCT repeat. **B.** Electron density as in "A" is displayed for a portion of the three-helix pack that forms the inter-BRCT repeat interface (see Figure 2.10).

Table 2.2: X-ray data collection, phasing and refinement statistics

Data Collection

Data set		Native		MAD	
Space group		$P6_122$		$P6_122$	
Cell dimensions	a=b(Å)	114.44		114.39	
	c (Å)	122.11		121.38	
			$\lambda 1$	$\lambda 2$	$\lambda 3$
Wavelength (Å)		1.00	0.9793	0.9789	0.9563
Resolution range (Å)		40-2.5	20-2.9	20-2.9	20-2.9
Observations[1]		209,566	81,799	78,519	83,902
Unique reflections[1]		16,968	21,866	21,894	21,928
Data coverage total/final shell[2] (%)		99.8 /100	99.7/100	99.6/100	99.6/100
$\langle I/\sigma I \rangle$ total/final shell		43.2/9.1	22.3/4.3	21.7/4.0	22.2/4.0
R_{sym} total/final shell (%)[3]		4.8/29.2	4.7/26.5	4.7/27.0	4.9/30.1

Refinement Statistics			**Phasing Statistics**	
Resolution range(Å)		25-2.5	Resolution range(Å)	20.0-2.9
R_{work}/R_{free} (%)[4]		25.9/30.2	No. of Selenium Sites	8/9
No. of refined atoms	Protein	1545	FOM – Solve	0.64
	Water	115		
	Nickel	1		
R.m.s. deviations	Bonds (Å)	0.017		
	Angles (°)	1.81		
Average B-factors(Å^2)	Protein	37.8		
	Water	47.6		

[1] For MAD datasets, Bijvoets (I+ and I-) were kept separate during scaling and for calculation of statistics.

[2] Final shell: 2.57 – 2.50 Å (native); 3.02 – 2.90 Å (MAD)

[3] $R_{sym}=\Sigma |(I_{hkl}) - \langle I \rangle| / \Sigma(I_{hkl})$ where I_{hkl} is the integrated intensity of a given reflection.

[4] $R_{work} = \Sigma_h|F_o(h) - F_c(h)| / \Sigma_h | F_o(h)|$, where $F_o(h)$ and $F_c(h)$ are observed and calculated structure factors. R_{free} calculated with 5% of all reflections excluded from refinement stages using the native data set. No I/σI cutoff was used in the refinement.

face of the sheet (Fig. 2.8). A structural alignment of the two BRCA1 BRCT repeats with the XRCC1 repeat (Fig. 2.9) reveals that the relative arrangement of α1, α3 and the central β-sheet is conserved in all three repeats. However, the conformations of the β1-α1, β2-β3 and β3-α2 connecting loops, as well as the orientation of α2 relative to the central β-sheet, are much less conserved. The conservation of the α1-α3-β-sheet structure is maintained by the packing of a limited number of key conserved hydrophobic residues in the core of the BRCT fold (Zhang et al. 1998).

BRCT repeat interactions

The two BRCT repeats in BRCA1 interact in a head-to-tail fashion, burying ~1600 $Å^2$ of hydrophobic, solvent accessible surface area in the interface (Fig. 2.10 *a-c*). The core of this interface is formed by the interaction of three α helices: α2 of the N-terminal repeat and α1' and α3' from the C-terminal repeat. The residues in these helices that contribute to the inter-repeat interface are almost all hydrophobic, and pack tightly in a knobs-into-holes manner. The 23 amino acid linker connecting the two BRCT repeats is poorly defined in the electron density, possibly indicating flexibility. It is clear, however, that the central portion of the linker is helical (αL) and packs against the C-terminal base of the α2-α1'-α3' helical bundle. The only salt bridge across the interface occurs between Arg 1699, immediately N-terminal to α2, and a pair of acidic residues, Glu 1836 and Asp 1840, exposed on the surface of α3'.

Multiple, tandem BRCT repeats are common in many of the BRCT-containing proteins such as 53BP1, RAD9, RAD4, DNA ligase IV, XRCC1, and the topoisomerase II binding protein TOPBP1. An amino acid sequence alignment of the two BRCA1 BRCT repeats with those in 53BP1 and RAD9 reveals that the residues that occupy the interface between the two repeats in α2, α1' and α3' of BRCA1 are highly conserved in 53BP1 and RAD9 (Fig. 2.10d). This observation strongly suggests that the two BRCT repeats in 53BP1 and RAD9 also pack via a triple helical interface similar to that seen in BRCA1. Sequence alignments in the α2 regions of the other BRCT-containing proteins are less reliable, due to the low level of sequence similarity between these proteins in this region. Nevertheless, many of these proteins show significant conservation of interface residues in α1' and α3', suggesting that this mode of packing could be common within the BRCT family. In proteins with more than two BRCT repeats, such as RAD4, the DNA polymerase II subunit Dpb11, and TOPBP1, this kind of packing could result in long, rod-like protein structures, whose surfaces would consist of the BRCT repeat loops and the highly variable inter-repeat linker peptides. Such elongated structures could provide a scaffold for the regulated assembly of multi-protein complexes.

Individual BRCT repeats have also been found to interact in *trans* with the BRCT repeats of other proteins. For example, the C-terminal BRCT repeat in the DNA repair protein XRCC1 has been shown to interact with the DNA ligase III BRCT repeat (Nash et al. 1997). While it is tempting to speculate that such interactions may occur through interactions between α2 of one protein and the

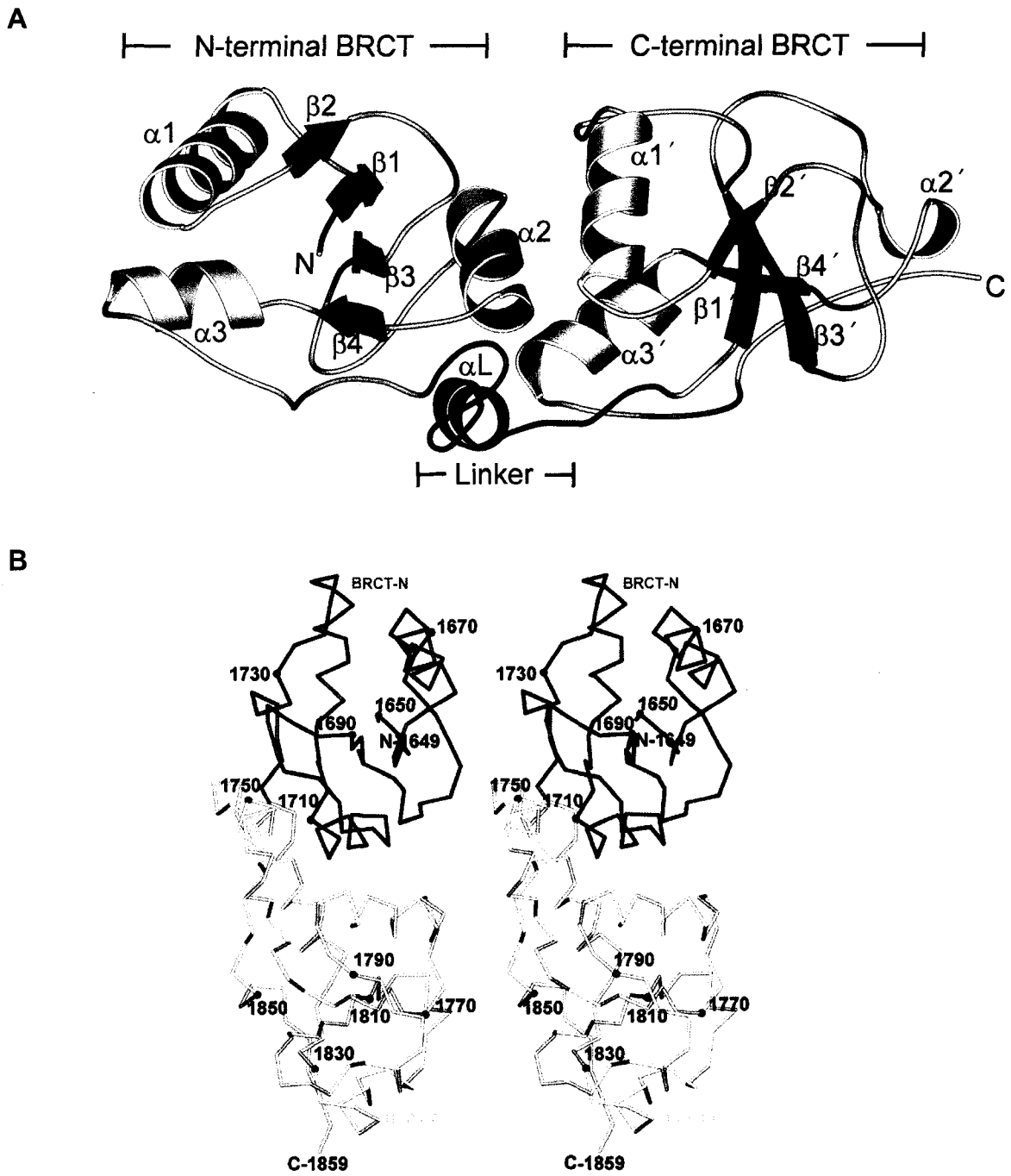

Figure 2.8. The structure of the dual-repeat BRCT domain of BRCA1. A. The secondary structure elements in the C-terminal BRCT repeat are labeled "prime" to distinguish them from the corresponding secondary structure elements in the N-terminal repeat. **B.** Stereoview of a Cα backbone trace of the BRCA1 BRCT domain. The N-terminal BRCT repeat is colored turquoise, the C-terminal repeat is gold and the inter-repeat linker is colored gray. The view is rotated 90° clockwise from the view shown in *"A"*.

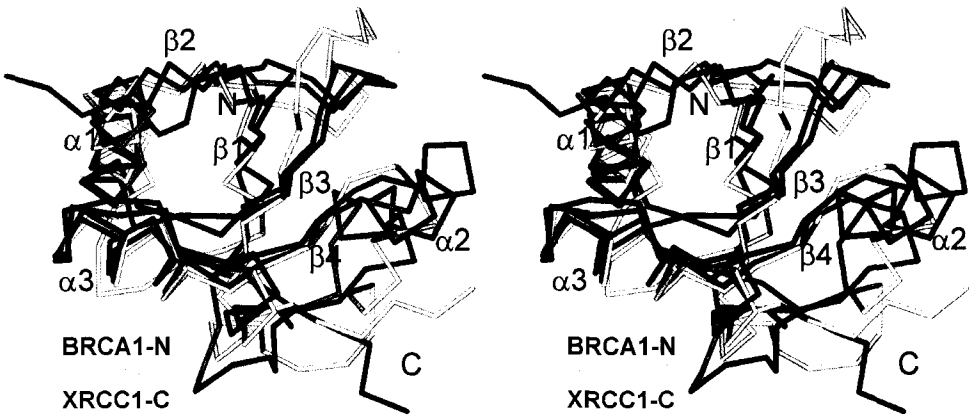

Figure 2.9. Stereoview of a structural alignment of the N- and C-terminal BRCA1 BRCT repeats and the C-terminal BRCT repeat from XRCC1. Least squares alignments were produced using O.

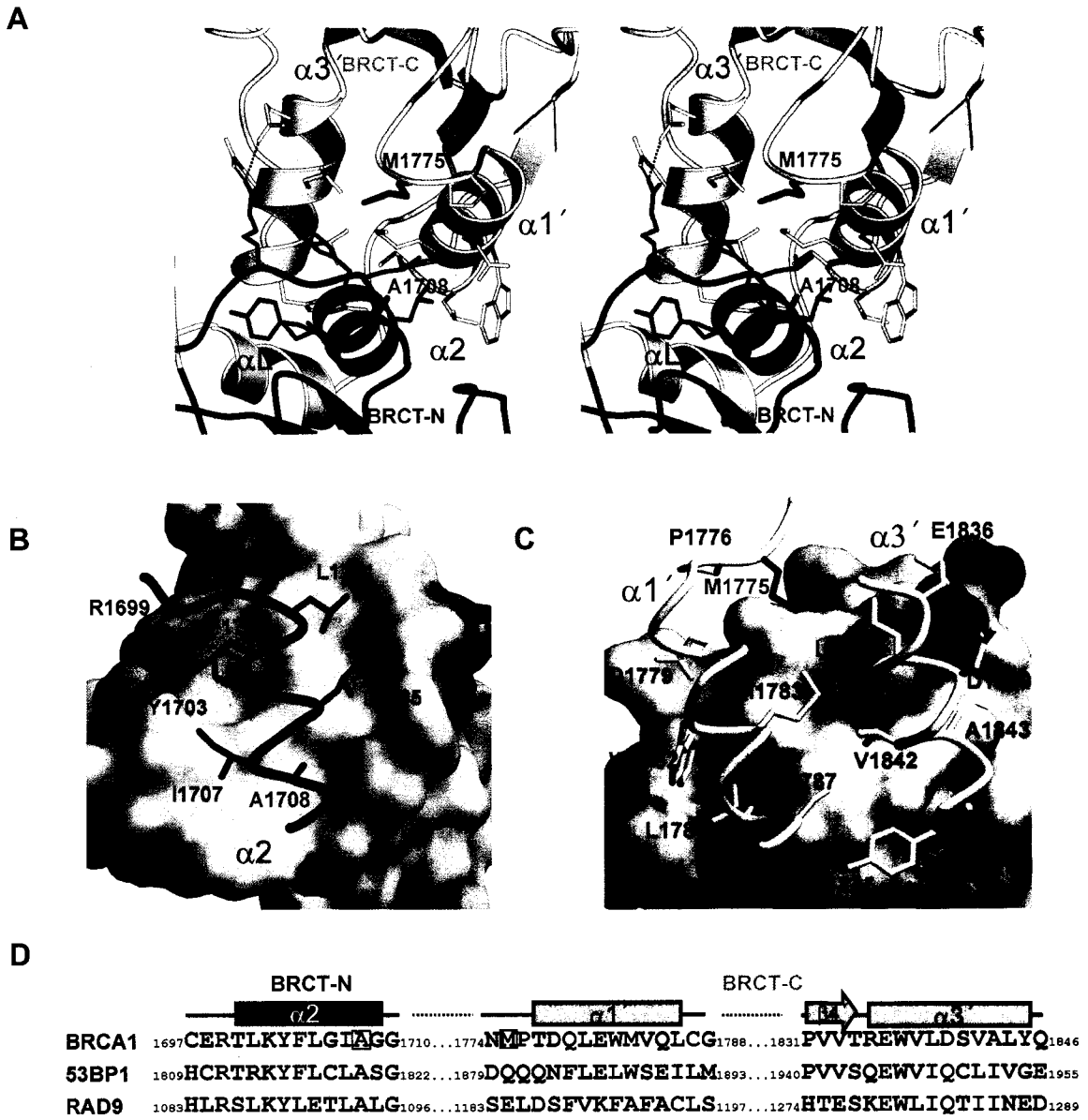

Figure 2.10. The packing of BRCT repeats. In *a-c*, the N-terminal repeat is colored turquoise, the C-terminal repeat gold, and residues that cause cancer when mutated are red. ***a,*** Three helices interact to form the core of the BRCT repeat interface (stereoview). ***b,*** An electrostatic surface representation of the C-terminal BRCT repeat is displayed with a worm representation of α2 from the N-terminal repeat. ***c,*** An electrostatic surface representation of the N-terminal repeat is shown with a worm representation of α1' and α3' from the C-terminal repeat. ***d,*** An amino acid sequence alignment of the regions of BRCA1, 53BP1 and RAD9 that are predicted to form BRCT-BRCT interfaces. Residues that constitute this interface in BRCA1, as well as conserved residues in h53BP1 and *S. cerevisiae* RAD9 are colored green. Residues where cancer-causing missense mutations have been identified are boxed in red.

α1/α3 face of the other, recent evidence suggests that XRCC1-DNA ligase III BRCT interactions involve residues exposed on the surface of α1 in both proteins (Zhang et al. 1998, Dulic et al. 2001). Structural studies of other BRCT-BRCT complexes, as well as an analysis of the effects of surface exposed mutations on the ability of BRCT proteins to associate and carry out their function *in vivo,* will be required to further test structural models of heteromeric BRCT-BRCT interactions.

BRCT mutations

The structure of the BRCT region of BRCA1 provides a powerful tool to interpret the large database of mutations that have been found in this domain in breast and ovarian cancer patients. For example, a nonsense mutation at Tyr-1853 deletes the last 11 amino acids of the second BRCA1 BRCT domain and is associated with early-onset breast cancer (Friedman et al. 1994). The peptide corresponding to the deleted residues normally adopts an extended conformation which packs against α2' and the β–sheet of the C-terminal BRCT repeat. Three hydrophobic residues within the deleted region, Tyr-1853, Leu-1854 and Ile-1855, are conserved in other BRCT repeats and are packed in the hydrophobic core of the C-terminal BRCT repeat. We predict that the deletion of these residues should destabilize the protein fold.

Two missense mutations within the BRCT region, Ala 1708 → Glu, and Met 1775 → Arg, are linked to breast and ovarian cancer (Futreal et al. 1994, Miki et al. 1994). These mutations cripple the DNA double-strand break repair function of BRCA1 in human cells (Scully et al. 1999). They also block the ability of the

BRCT domain to interact with CtIP (Yu et al. 1998, Li et al. 1999), histone deacetylases (Yarden & Brody 1999) and BACH1 (Cantor et al. 2001) and to activate transcription (Chapman & Verma 1996, Monteiro et al. 1996). Ala-1708 and Met-1775 are part of the hydrophobic contact surface between the two BRCT repeats (Fig. 2.10 *a-c*). Ala-1708 in α2 packs into a small hydrophobic pocket formed by α1' and α3' near the center of the interface, which would not be expected to accommodate the larger, negatively charged glutamate at position 1708. Met-1775 is packed within a predominantly hydrophobic pocket near the edge of the inter-repeat interface. Substitution of this residue with an arginine could be sterically accommodated but would position the positive charge near another basic residue, Arg-1835. We therefore predict that these mutations destabilize the hydrophobic inter-repeat interface and could lead to a repositioning of the repeats relative to one another, or, potentially, the complete unfolding of the structure.

To test further the structural consequences of these mutations, we assayed the sensitivity of dual-repeat BRCT domain proteins harboring these mutations to proteolytic degradation (Fig. 2.11, 2.12). Both wild type and mutant proteins were produced by *in vitro* transcription/translation because the Tyr 1853 → *stop* and Ala 1708 → Glu mutants were insoluble when expressed in *E. coli*. The wild type protein is highly resistant to digestion by trypsin, elastase, or chymotrypsin, indicating that the *in vitro* produced BRCT protein is stably folded.

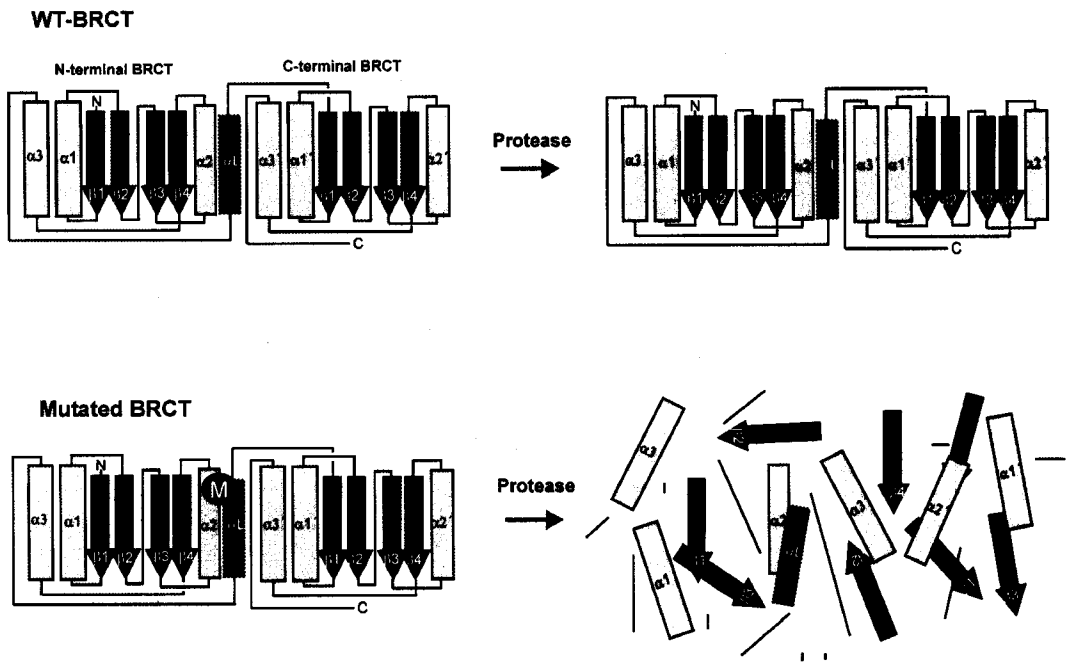

Figure 2.11. A protease based assay for assessing structural effects of BRCT missense mutations. A secondary structure topology diagram is shown for the BRCT dual repeat. The wild type protein is highly stable to digestion by trypsin, chymotrypsin, and elastase. Missense or truncation mutation induced destabilization or conformational change renders the BRCT repeats susceptible to proteolytic digestion.

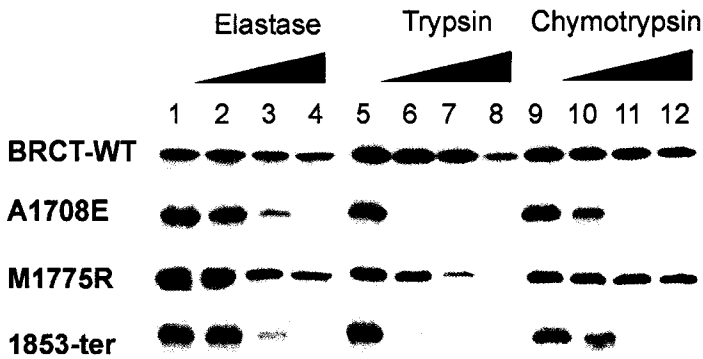

Figure 2.12. Analysis of the structural consequences of mutations in the BRCT domain. ^{35}S-methionine-labelled wild type BRCA1(1646-1859), as well as variants harboring the indicated mutations were digested with the indicated proteases and the reaction products were analysed by SDS-PAGE and autoradiography. Reactions were carried out at elastase concentrations of 0, 3, 30 and 300 μg mL^{-1} (lanes 1-4), trypsin concentrations of 0, 6, 60 and 600 μg mL^{-1} (lanes 5-8), and chymotrypsin concentrations of 0, 6, 60 and 600 μg mL^{-1} (lanes 9-12).

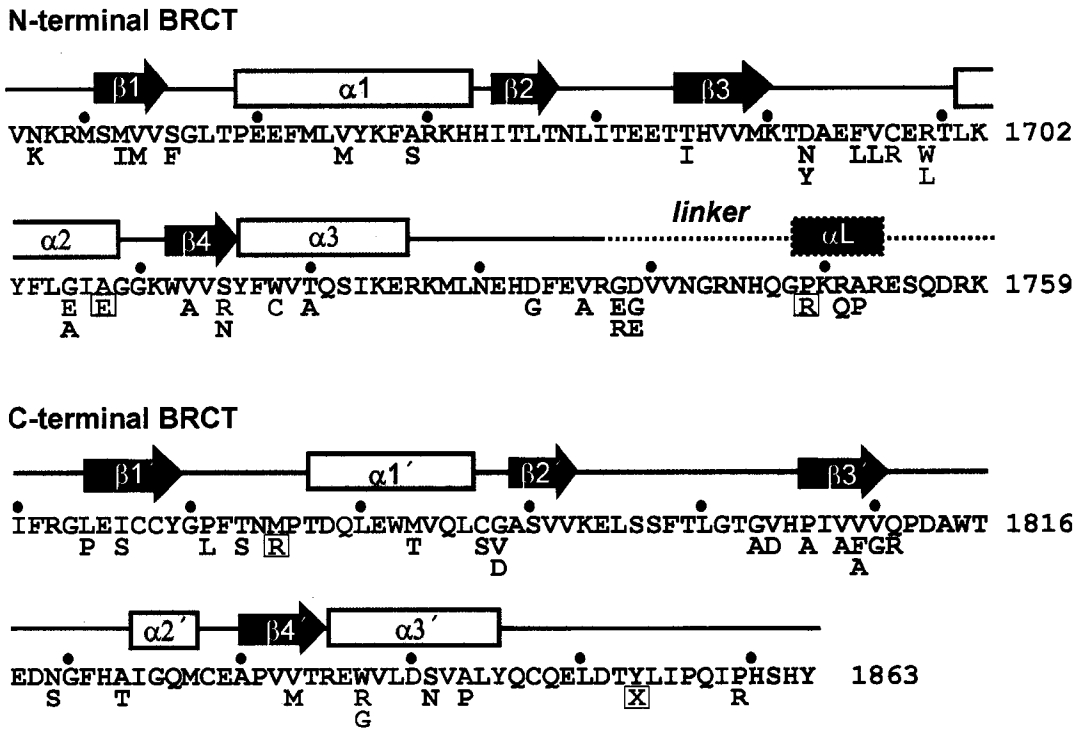

Figure 2.13. Missense mutations in the human BRCA1 BRCT domain. Missense mutations derived from the BIC are indicated below the BRCT amino acid sequence and the Tyr 1853→stop mutation is indicated with an X. Mutations with predicted deleterious effects on folding are colored red. Mutations known to cause cancer are boxed. Residues in green are involved in the inter-BRCT repeat interface.

In contrast, the Tyr 1853 → *stop* and Ala 1708 → Glu mutants are almost completely degraded by low concentrations of all enzymes, indicating that these proteins are not stably folded under the assay conditions. The Met 1775 → Arg mutant displays an intermediate sensitivity to proteolytic degradation, suggesting that the Met 1775 → Arg mutant exhibits a subtler structural defect.

The cancer risks associated with the vast majority of BRCA1 missense mutations deposited in the Breast cancer information core (BIC) database are unknown. Using our structure, we predict several of these mutations will seriously impair the folding of the BRCT domain, and will therefore lead to an elevated cancer risk (Fig. 2.13). Such mutations include non-conservative substitutions of key hydrophobic residues packed in the protein core or mutations that disrupt electrostatic interactions. Many mutations remain unclassified, such as mutations in the hydrophobic core that replace one hydrophobic residue with another of significantly smaller or larger size. While such mutations can be accommodated in highly stable proteins such as lysozyme through a subtle re-packing of the hydrophobic core (Eriksson et al. 1992), similar mutations may be more detrimental in the less stable BRCA1 BRCT domain. Finally, many mutations occur on the surface of the structure, and are not predicted to alter the fold of the BRCT domain, but may nevertheless perturb a binding site for an important BRCT partner. The analysis of the biochemical and *in vivo* effects of such surface mutations could provide strong evidence for the involvement of specific BRCT-interacting proteins in BRCA1 function and tumor suppression.

References:

Bork, P., Hofmann, K., Bucher, P., Neuwald, A. F., Altschul, S. F., and Koonin, E. V. A superfamily of conserved domains in DNA damage-responsive cell cycle checkpoint proteins. FASEB J, *11*: 68-76, 1997.

Brünger, A. T., Adams, P. D., Clore, G. M., DeLano, W. L., Gros, P., Grosse-Kunstleve, R. W., Jiang, J.-S., Kuszewski, J., Nilges, M., Pannu, N. S., Read, R. J., Rice, L. M., Simonson, T., and and Warren, G. L. Crystallography & NMR System: A New Software Suite for Macromolecular Structure Determination. Acta Cryst, *D54*: 905-921, 1998.

Callebaut, I. and Mornon, J. P. From BRCA1 to RAP1: a widespread BRCT module closely associated with DNA repair. FEBS Lett 400(1): 25-30. 1997.

Cantor, S. B., Bell, D. W., Ganesan, S., Kass, E. M., Drapkin, R., Grossman, S., Wahrer, D. C., Sgroi, D. C., Lane, W. S., Haber, D. A., and Livingston, D. M. Bach1, a novel helicase-like protein, interacts directly with brca1 and contributes to its dna repair function. Cell 105(1): 149-60. 2001.

Chapman, M. S. and Verma, I. M. Transcriptional activation by BRCA1. Nature, *382*: 678-9. 1996.

Collaborative Computational Project, Number 4. Acta Crystallogr D 50: 60-3. 1994.

Cowtan , K. Joint CCP4 and ESF-EACBM Newsletter on Protein Crystallography 31, 34-38. 1994.

Deng, C. X. and Brodie, S. G. Roles of BRCA1 and its interacting proteins.

Bioessays, *22*: 728-37. 2000.

Doublie, S. Preparation of selenomethionyl proteins for phase determination. Meth Enzymology, 276: 523-529. 1997.

Dulic, A., Bates, P. A., Zhang, X., Martin, S. R., Freemont, P. S., Lindahl, T., and Barnes, D. E. BRCT Domain Interactions in the Heterodimeric DNA Repair Protein XRCC1-DNA Ligase III. Biochemistry, 40(20): 5906-5211. 2001.

Eriksson, A. E., Baase, W. A., Zhang, X. J., Heinz, D. W., Blaber, M., Baldwin, E. P., and Matthews, B. W. Response of a protein structure to cavity-creating mutations and its relation to the hydrophobic effect. Science, 255(5041):178-83. 1992.

Esnouf, R. M. An extensively modified version of MolScript that includes greatly enhanced coloring capabilities. J Mol Graph Model, *15*: 132-4. 1997.

Esnouf, R. M. Further additions to MolScript version 1.4, including reading and contouring of electron-density maps. Acta Crystallogr D Biol Crystallogr, *55*: 938-40. 1999.

Friedman, L. S., Ostermeyer, E. A., Szabo, C. I., Dowd, P., Lynch, E. D., Rowell, S. E., and King, M. C. Confirmation of BRCA1 by analysis of germline mutations linked to breast and ovarian cancer in ten families. Nat Genet, 8(4): 399-404. 1994.

Futreal, P. A., Liu, Q., Shattuck-Eidens, D., Cochran, C., Harshman, K., Tavtigian, S., Bennett, L. M., Haugen-Strano, A., Swensen, J., Miki, Y. and others. BRCA1 mutations in primary breast and ovarian carcinomas. Science, 266(5182): 120-2. 1994.

Gayther, S. A., Harrington, P., Russell, P., Kharkevich, G., Garkavtseva, R. F., and Ponder, B. A. Rapid detection of regionally clustered germ-line BRCA1 mutations by multiplex heteroduplex analysis. UKCCCR Familial Ovarian Cancer Study Group. Am J Hum Genet, 58(3): 451-6. 1996.

Gayther, S. A., Warren, W., Mazoyer, S., Russell, P. A., Harrington, P. A., Chiano, M., Seal, S., Hamoudi, R., van Rensburg, E. J., Dunning, A. M. and others. Germline mutations of the BRCA1 gene in breast and ovarian cancer families provide evidence for a genotype-phenotype correlation. Nat Genet, 11: 428-33. 1995.

Jones, T. A., Zou, J. Y., Cowan, S. W., and Kjeldgaard Improved methods for binding protein models in electron density maps and the location of errors in these models. Acta Crystallogr A, *47*: 110-9. 1991.

Laskowski, R. A., MacArthur, M. W., and Thornton, J. M. Validation of protein models derived from experiment. Curr Opin Struct Biol, *8*: 631-9, 1998.

Lee, J. Y., Chang, C., Song, H. K., Moon, J., Yang, J. K., Kim, H. K., Kwon, S. T., and Suh, S. W. Crystal structure of NAD(+)-dependent DNA ligase: modular architecture and functional implications. EMBO J, 19(5): 1119-29. 2000.

Li, S., Chen, P. L., Subramanian, T., Chinnadurai, G., Tomlinson, G., Osborne, C. K., Sharp, Z. D., and Lee, W. H. Binding of CtIP to the BRCT repeats of BRCA1 involved in the transcription regulation of p21 is disrupted upon DNA damage. J Biol Chem, 274(16): 11334-8. 1999.

Merritt, E. A. and Bacon, D. J. Raster3D: Photorealistic Molecular Graphics. Meth

Enzymology 277: 505-524. 1997.

Miki, Y., Swensen, J., Shattuck-Eidens, D., Futreal, P. A., Harshman, K., Tavtigian, S., Liu, Q., Cochran, C., Bennett, L. M., Ding, W. and others. A strong candidate for the breast and ovarian cancer susceptibility gene BRCA1. Science, 266(5182): 66-71. 1994.

Monteiro, A. N., August, A., and Hanafusa, H. Evidence for a transcriptional activation function of BRCA1 C-terminal region. Proc Natl Acad Sci U S A, 93(24): 13595-9. 1996.

Nash, R. A., Caldecott, K. W., Barnes, D. E., and Lindahl, T. XRCC1 protein interacts with one of two distinct forms of DNA ligase III. Biochemistry, 36(17): 5207-11. 1997.

Otwinowski, Z. and Minor, W. Processing of X-ray diffraction data collected in oscillation mode. Meth Enzymology, 276: 307-325. 1997.

Scully, R., Chen, J., Ochs, R. L., Keegan, K., Hoekstra, M., Feunteun, J., and Livingston, D. M. Dynamic changes of BRCA1 subnuclear location and phosphorylation state are initiated by DNA damage. Cell, 90(3): 425-35. 1997.

Scully, R., Ganesan, S., Vlasakova, K., Chen, J., Socolovsky, M., and Livingston, D. M. Genetic analysis of BRCA1 function in a defined tumor cell line. Mol Cell, *4*: 1093-9. 1999.

Sodeoka, M. Larson C. J. Chen L. Leclair K. P. and Verdine G. L. A multifunctional plasmid for protein expression by ECPCR: overproduction of NF-kB p50 DNA-binding subunit. Bioorg. Med. Chem. Lett 3: 1089.

1993.

Terwilliger, T. C. and Berendzen, J. Automated MAD and MIR structure solution. Acta Crystallogr D Biol Crystallogr, 55: 849-861. 1999.

Williams, R. S., Green, R., and Glover, J. N. Crystal structure of the BRCT repeat region from the breast cancer- associated protein BRCA1. Nat Struct Biol, *8*: 838-42, 2001.

Winn, M. D., Isupov, M. N., and Murshudov, G. N. Use of TLS parameters to model anisotropic displacements in macromolecular refinement. Acta Crystallogr D Biol Crystallogr, *57*: 122-33, 2001.

Yarden, R. I. and Brody, L. C. BRCA1 interacts with components of the histone deacetylase complex. Proc Natl Acad Sci U S A, 96(9): 4983-8. 1999.

Yu, X., Wu, L. C., Bowcock, A. M., Aronheim, A., and Baer, R. The C-terminal (BRCT) domains of BRCA1 interact in vivo with CtIP, a protein implicated in the CtBP pathway of transcriptional repression. J Biol Chem, 273(39): 25388-92. 1998.

Zhang, X., Morera, S., Bates, P. A., Whitehead, P. C., Coffer, A. I., Hainbucher, K., Nash, R. A., Sternberg, M. J., Lindahl, T., and Freemont, P. S. Structure of an XRCC1 BRCT domain: a new protein-protein interaction module. EMBO J, 17(21): 6404-11. 1998.

Chapter 3:

Structural consequences of a cancer-causing BRCA1-BRCT missense mutation

SUMMARY:

The integrity of the C-terminal, BRCT repeat region is critical for BRCA1 tumour suppressor function, however the molecular details of how a number of clinically derived BRCT missense mutations affect BRCA1 function remain largely unknown. Here we assess the structural response of the BRCT tandem repeat domain to a well-characterized, cancer-associated single amino acid substitution, Met1775 → Arg1775. The structure of BRCT-M1775R reveals that the mutated side chain is extruded from the protein hydrophobic core, thereby altering the protein surface. Charge-charge repulsion, rearrangement of the hydrophobic core, and disruption of the native hydrogen bonding network at the interface between the two BRCT repeats contribute to the conformational instability of BRCT-M1775R. Destabilization and global unfolding of the mutated BRCT domain at physiological temperatures explains the pleiotropic molecular and genetic defects associated with the BRCA1- M1775R protein.

INTRODUCTION:

Germline mutations within the breast and ovarian cancer susceptibility gene *BRCA1* predispose carriers to early-onset breast and ovarian cancer and it is estimated that approximately 5-10 % of all breast cancers are caused by inheritance of dominant disease genes (Miki et al. 1994). Various lines of evidence suggest that the *BRCA1* protein product is involved in the regulation of multiple nuclear functions including transcription, recombination, DNA repair, and checkpoint control (for reviews, see Deng & Brodie 2000, Scully & Livingston 2000, Venkitaraman 2002). BRCA1 is an 1863 amino acid nuclear phosphoprotein that includes a N-terminal RING finger domain and two tandem carboxy-terminal repeats, termed the BRCT domain. The importance of the conserved RING and BRCT domains to the tumour suppressor function of BRCA1 is demonstrated by the fact that the majority of known cancer-causing BRCA1 mutations localize to these domains (Friedman et al. 1994, Futreal et al. 1994, Gayther et al. 1995, Couch & Weber 1996, Shen & Vadgama 1999, Brzovic et al. 2001).

The extreme C-terminal region of BRCA1 contains two ~90-100 amino acid sequence repeats called BRCT (**BR**CA1 **C**-terminal) repeats which are the prototypical members of a protein fold superfamily that includes many proteins associated with DNA repair (Koonin et al. 1996, Bork et al. 1997, Callebaut & Mornon 1997). The recently determined X-ray crystal structures of the human (Williams et al. 2001) and rat (Joo et al. 2002) BRCA1 BRCT repeats provide a framework for the interpretation of BRCT mutations identified in patients from

breast cancer screening programs. The two structurally similar BRCT repeats resemble the structures of the isolated BRCT domains from XRCC1 (Zhang et al. 1998) and DNA ligase III (Krishnan et al. 2001) and are composed of a central four stranded, parallel β-sheet flanked by a single α–helix on one side (α2), with a pair of α-helices (α1 and α3) and a short 3_{10}-helix on the opposite side. The two repeats are connected by a relatively flexible linker, and pack together in a specific, head-to-tail manner that is not only conserved between human and rat BRCA1, but also in the BRCT domain of the p53-interacting protein, 53BP1 (Williams et al. 2001, Joo et al. 2002).

Several cancer-associated BRCT missense mutations (Futreal et al. 1994, Miki et al. 1994) have been characterized in functional detail. Two extensively studied variants, A1708E and M1775R, ablate double-strand break repair and transcription function of BRCA1 (Chapman & Verma 1996, Monteiro et al. 1996, Scully et al. 1999) and inhibit BRCT interactions with histone deacetylases (Yarden & Brody 1999), the DNA helicase BACH1 (Cantor et al. 2001) and the transcriptional co-repressor CtIP (Yu et al. 1998, Li et al. 1999). Both of these mutations occur at the interface between the N- and C-terminal BRCT repeats and are predicted to affect the way in which the two repeats interact. The enhanced sensitivity of the A1708E mutant to proteolytic digestion indicates that this mutation has profound structural consequences (Williams et al. 2001). In contrast, the M1775R mutant displays a proteolytic sensitivity that is intermediate between that of the wild type protein and the A1708E mutant, suggesting that the M1775R mutation results in a milder structural defect.

In the present study we employ limited proteolysis, CD spectroscopy and X-ray structural analysis to probe the structural consequences of the M1775R mutation. Our results show that the methionine – arginine substitution leads to a rearrangement of the BRCT repeat interface, alterations in the surface of the protein, and global destabilization of the BRCT domain. This chapter was originally published in the *Journal of Biological Chemistry* (Williams and Glover 2003)

EXPERIMENTAL PROCEDURES

Proteolysis

For proteolytic assays, BRCT-WT and BRCT-M1775R were expressed from the T7 expression vector pLM1 and labelled with ^{35}S-methionine using the TNT-Quick *in vitro* transcription/translation system (Promega). Immediately before digestion, proteins were translated at 30 °C for 2 hr. The reticulocyte lysates were then centrifuged for 2 min. at 10000 x *g* to remove insoluble material and 3 μL of the lysate supernatants containing the labelled translation products were added to 12 μL digestion buffer (150 mM NaCl, 50 mM potassium phosphate, pH 7.5) containing increasing concentrations of TLCK treated chymotrypsin (Sigma). Following digestion at 20 °C or 37 °C for 12 minutes, the reactions were stopped with PMSF. Digestion products were electrophoresed on 15% SDS-PAGE gels and visualized with a phosphorimaging plate and a Molecular Dynamics Typhoon scanner. Quantification of the reaction products within ImageQuant (Molecular Dynamics) used a local average background correction.

Protein Expression and Purification.

Expression and purification of recombinant human BRCA1$_{(1646\text{-}1859)}$ (BRCT-WT) and BRCA1$_{(1646\text{-}1859)}$ -M1775R (BRCT-M1775R) was performed essentially as described (Williams et al. 2001), with some changes. When expressed at 30 °C and 37 °C, yields of BRCT-M1775R were greatly reduced relative to BRCT-WT, likely due to degradation. To obtain large quantities of BRCT-M1775R protein for crystallization studies, growth of cells and induction of

protein expression were carried out at 25 °C. Purification using a combination of ammonium sulphate precipitation, hydrophobic interaction, gel filtration, and anion exchange chromatography yielded 4-5 mg protein/L *E.coli* culture for both proteins. MALDI-TOF mass spectrometric analysis confirmed mutation of residue M1775 to arginine.

CD spectroscopy.

For circular dichroism measurements, proteins were dialyzed into 400 mM NaCl, 50 mM potassium phosphate (pH 7.5), 0.1 % β-mercaptoethanol, in a Millipore Ultrafree-10 concentration unit. Protein concentrations for molar ellipticity calculations were derived from amino acid analysis. Far-UV (195-255 nm) CD spectra were determined using 0.2 mg/mL solutions of protein and were acquired using a Jasco J-720 spectrapolarimeter that was interfaced with Jasco software and equipped with a 0.1 cm quartz cuvette cell. For denaturation experiments, temperature within the cell was regulated using a Peltier thermal control unit. Assuming a two state unfolding model, denaturation midpoints were determined by following the change in molar ellipticity at 222 nm as a function of temperature. Measurements were taken at 0.5 °C intervals and the temperature was increased at a rate of 30 °C/h. Ellipticity readings were normalized to the mole fraction of protein folded (f_f) or denatured (f_u) using the standard equations:

$$f_f = ([\theta] - [\theta]_u)/([\theta]_n - [\theta]_u)$$

$$f_u = (1 - f_f)$$

where $[\theta]_n$ and $[\theta]_u$ are the molar ellipticity for the fully folded and fully denatured protein species. $[\theta]$ is the observed ellipticity at each temperature.

The midpoint of the temperature dependant folding-unfolding transition for both proteins was reproducible, but this transition was irreversible and characterized by precipitation within the cell under the conditions used.

Crystallization of BRCT-M1775R.

Protein concentrations for crystallization were determined using the BCA protein assay (Pierce). Unlike the wild type protein, storage of the mutant at concentrations greater than 5 mg/mL resulted in irreversible aggregation within days. To attain high protein concentrations suitable for crystallization, BRCT-M1775R at 1 mg/mL was dialyzed into Protein buffer (400 mM NaCl, 5 mM Tris-HCl, pH 7.5), and concentrated to 20 mg/mL immediately prior to crystallization. Crystals were grown at room temperature (20-22 °C) using the hanging drop vapour diffusion technique. 2 μL of 20 mg/mL BRCT-M1775R in Protein buffer was mixed with 2 μL of well solution (1.4 M ammonium sulphate, 100 mM MES, pH 6.7, 10 mM $CoCl_2$) to produce hexagonal crystals within 1 to 2 days (see Table 3.1).

Data Collection, Structure Solution, and Refinement.

For data collection, crystals were gradually transferred to a cryoprotectant solution containing 1.2 M ammonium sulphate, 100 mM MES, pH 6.7, 10 mM $CoCl_2$, 26% glycerol, over the course of 45-60 minutes. Diffraction data to 2.8 Å resolution were collected from a single crystal at 100 K at the Structural Biology Centre (Argonne National Laboratory) – APS beamline 19-ID. Intensity data were processed using the HKL2000 package (Otwinowski & Minor 1997) (see Table 3.1). Crystallographic phase information for BRCT-M1775R was obtained

using molecular replacement with the native human BRCT model (RCSB:1JNX). All data between 20 and 2.8 Å was used in crystallographic refinement and 7 % of this data was allocated for cross-validation. Initial rigid body fitting of the model in CNS (Brünger et al. 1998) lowered the R_{factor}/R_{free} to 36.2/38.6 %. Side chains of regions of the protein that change with mutation of the BRCT were built using O (Jones et al. 1991) into SigmaA weighted model-phased F_o-F_c and $2F_o$-F_c electron density maps calculated with CNS. Maximum likelihood targets, bulk solvent correction and overall anisotropic B-factor scaling were applied throughout the refinement process. Further refinement involved iterative cycles of manual building and restrained refinement with TLS group anisotropic thermal parameter modeling as implemented in REFMAC (v5.0.32) (Collaborative Computational Project 1994, Winn et al. 2001). The quality of the model was assessed using PROCHECK (Laskowski et al. 1998) (Table 3.1). The final model has good stereochemistry, and a working R-factor of 27.3 % (R_{free}, 29.8 %) for all data in the resolution range 20-2.8 Å. Structural diagrams were created using BOBSCRIPT (Esnouf 1997, Esnouf 1999) and rendered with POVRAY (www.povray.org) (Fig. 1,4, 5-*A,B*) or RASTER3D (Merritt & Bacon 1997) (Fig. 5–*C,D,E*). Molecular surfaces were drawn with GRASP (Nicholls et al. 1991). The atomic coordinates and structure factors for BRCT-M1775R have been submitted to the RCSB protein data bank (www.rcsb.org/pdb) (RCSB ID code 1N5O).

RESULTS AND DISCUSSION:

Native packing environment of M1775

The tandem BRCT repeat structure is composed of two α/β fold BRCT domains which interact end-to-end, with helicies α1' and α3' from the C-terminal BRCT intimately contacting α2 from the N-terminal repeat in a three-helix bundle like packing arrangement (Fig. 3.1*a*) (Williams et al. 2001, Joo et al. 2002). Residue M1775 is largely buried within the interface between the two repeats, and lies in a pocket formed by L1701 and F1704 from the N-terminal repeat, and L1780, M1783, R1835 and L1839 from the C-terminal repeat. Sequence and structural conservation of M1775 and its contacting residues among mammalian, xenopus and avian BRCA1 homologues highlights the importance of M1775 in orienting the two BRCT repeats (Fig. 3.1*b*). With the exception of residue R1835, which is replaced by a tryptophan in the mouse and rat BRCT domains, the residues forming this pocket are highly conserved. This substitution within the pocket is significant, however, as proximity of the positively charged residue R1835 to M1775 in the human protein influences the response of the structure to the cancer-linked substitution, M1775R.

Proteolytic sensitivity of M1775R

Mutation M1775R conferred moderate sensitivity to digestion with trypsin at 20 °C (Williams et al. 2001). As R1775 immediately precedes a proline residue, this substitution is not expected to introduce a new trypsin cleavage site, thus the enhanced trypsin sensitivity is an indication of a subtle

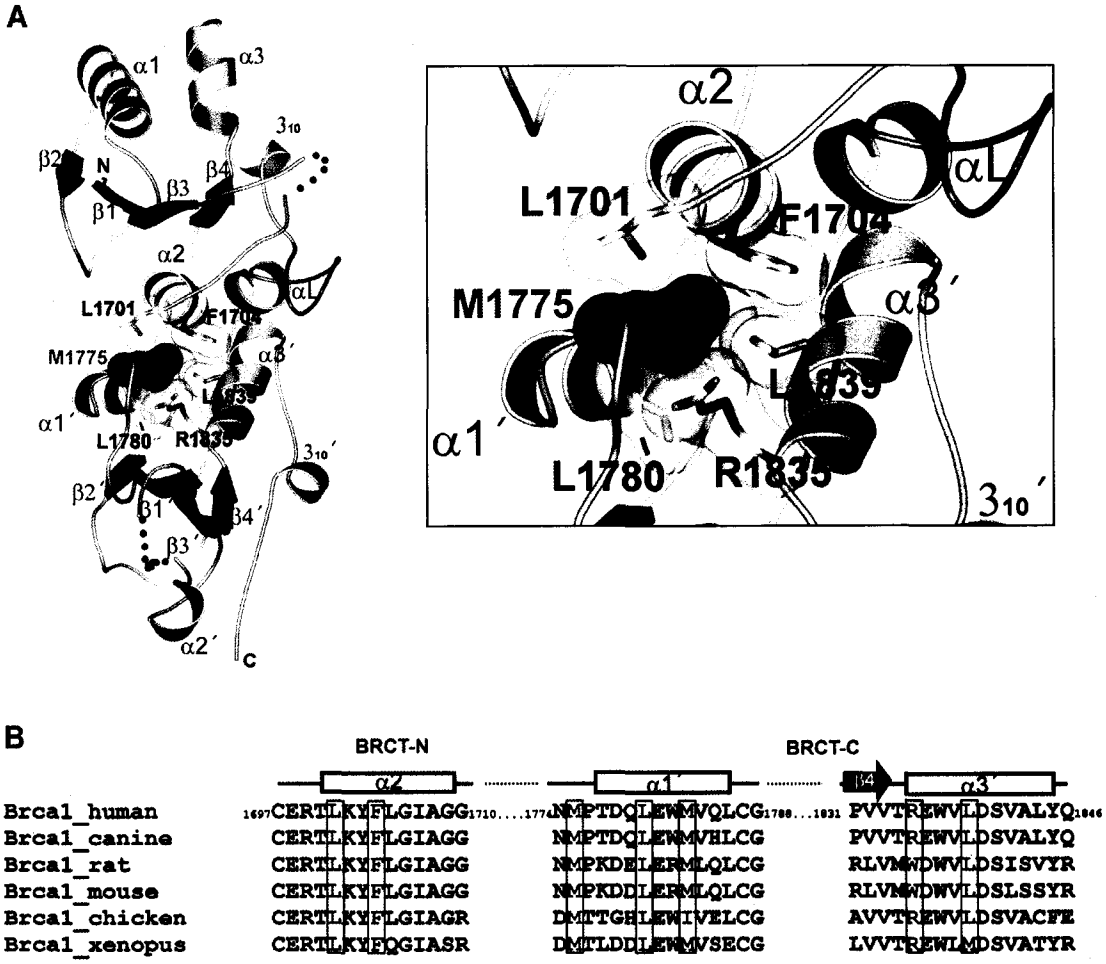

Figure 3.1. Evolutionary conservation of the M1775 packing environment A. Ribbons diagram of the BRCT repeat region of BRCA1. M1775 (red) in BRCT-WT is positioned between the two BRCT fold repeats. M1775 (red surface) lies in a hydrophobic pocket created by L1701, F1704, L1780, M1783 (behind M1775), R1835 and L1839 (grey surfaces). Inset: Enlarged view of the M1775 environment. **B.** Multiple sequence alignment of BRCA1 homologues for the BRCT regions surrounding M1775. M1775 is red, and contacting amino acids are blue. Numbering is for human BRCA1.

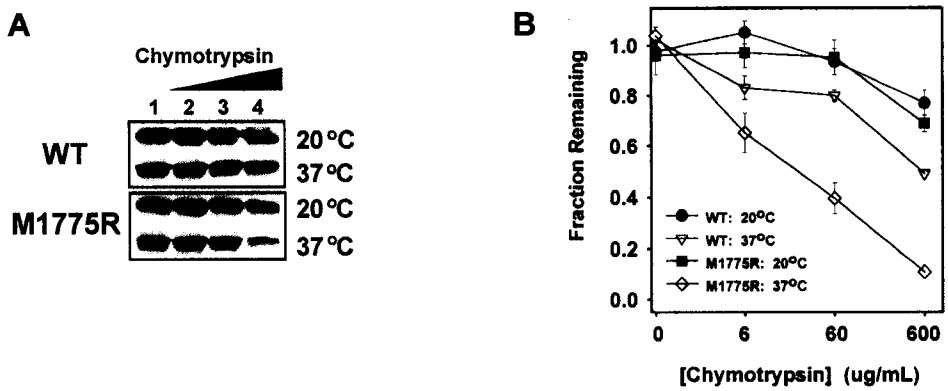

Figure 3.2. Protease sensitivity of BRCT-M1775R. A. Reticulocyte lysates containing ^{35}S-labelled, *in-vitro* translated BRCT-WT and BRCT-M1775R were digested at the indicated temperatures for 12 minutes using chymotrypsin at concentrations of 0, 6, 60, 600 μg/mL (lanes 1-4). Reaction products were analyzed by SDS-PAGE and autoradiography. **B.** Quantification of chymotryptic digestions. The fraction remaining is the percent of starting protein present following digestion with the indicated concentrations of chymotrypsin. Data points are the mean value of digestions performed in triplicate with error bars reflecting the standard deviations.

structural change in the M1775R mutant. To assess further the stability of the M1775R mutant, we compared its chymotrypsin sensitivity to that of the wild-type protein (Fig. 3.2-*a,b*). BRCT-WT and BRCT-M1775R both show resistance to digestion at 20 °C for all protease concentrations. Elevating the temperature to 37 °C enhanced cleavage of the mutant by chymotrypsin at all protease concentrations, where the wild type showed only a slight increase in cleavage efficiency at the highest concentration. The fact that the BRCT-M1775R exhibits modest but significant increases in sensitivity to digestion by two proteases with different cleavage specificities, especially at elevated temperatures, indicates that M1775R results in a folding defect in the BRCT domain.

CD analysis

To probe further the extent of protein destabilization induced by the M1775R substitution, we compared the secondary structure and thermal stability of BRCT-M1775R to the wild type protein using CD spectroscopy (Fig. 3.3). The mutant exhibits a far-UV CD absorbance spectrum that is characteristic of a mixed α/β protein, and is similar to the wild type, indicating that the overall fold of the M1775R domain is maintained in solution at 20 °C. BRCT-M1775R however is less stable, having a midpoint of thermal denaturation of approximately 41 °C, 11 °C less than the wild type protein (Fig. 3.3 - *Inset*, Experimental Procedures). Consistent with these findings, solvent denaturation measurements of the thermodynamic stability of the BRCT-tandem domain indicates that M1775R

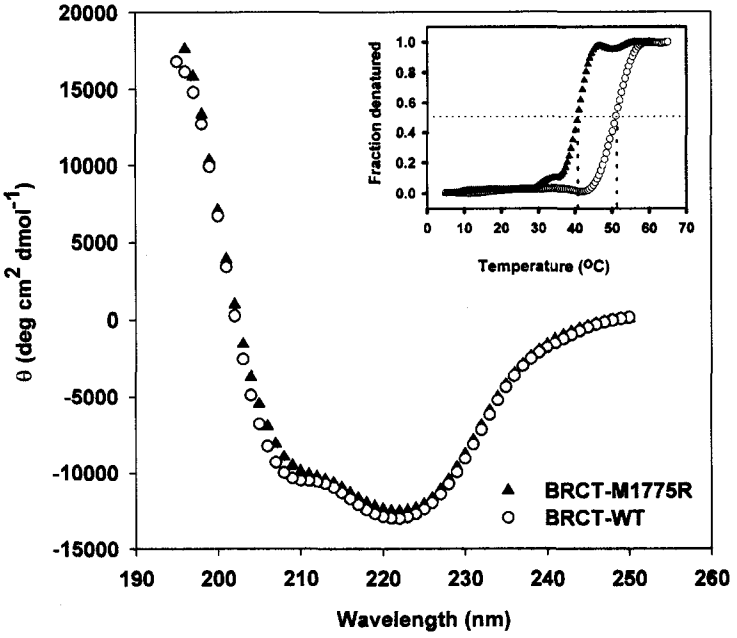

Figure 3.3. CD spectra of BRCT-WT and BRCT-M1775R. The far UV CD spectrum for the wild type (O) and mutant protein (▲) are similar at 20 °C. **Inset**: Thermal denaturation of BRCT-WT and BRCT-M1775R. Molar ellipticity at 222 nm was measured, and the values were used to calculate a mole fraction of denatured molecules for each temperature. Midpoints of the transitions (WT-52 °C, M1775R-41 °C) are marked by dotted lines.

destabilizes the BRCT fold by 5.0 kcal/mol at 20 °C (Ekblad et al. 2002). Taken together, these results suggest that functional defects associated with BRCA1-M1775R may be attributed to destabilization of the BRCT domain at physiological temperatures.

X-ray structure of missense variant M1775R

To gain structural insights into the destabilizing effect M1775R, we crystallized and determined the structure of BRCT- M1775R at 2.8 Å (Fig. 3.4*a*, Table 1, Experimental Procedures). $2F_o$-F_c and F_o-F_c difference electron density indicate that structural rearrangements in response to the mutation are confined to residues within a ~5 Å radius of R1775. Paired 4σ positive and negative electron density features in the F_o-F_c map near residue 1775 reveal that the substituted arginine is displaced from the hydrophobic core of the protein (Fig. 3.4*a-c*). The mutation is further accommodated by a ~1 Å shift of a neighbouring residue, P1776 in the β1'-α1' connecting loop, and a series of side chain rearrangements that perturb the native inter-BRCT hydrogen bonding and van der Waals contact networks (Fig. 3.5 *a-c*).

Introduction of an arginine at position 1775 creates a clustering of three positively charged residues; R1699, R1775 and R1835. In the native structure, R1699 from the N-terminal BRCT repeat participates in the sole conserved inter-BRCT repeat salt bridge with a pair of C-terminal BRCT acidic residues, D1840 and E1836 (Fig. 3.5*a*). R1835 in human BRCA1 normally participates in a hydrogen bonding network with Q1811, thereby helping to orient the β1'-α1' loop

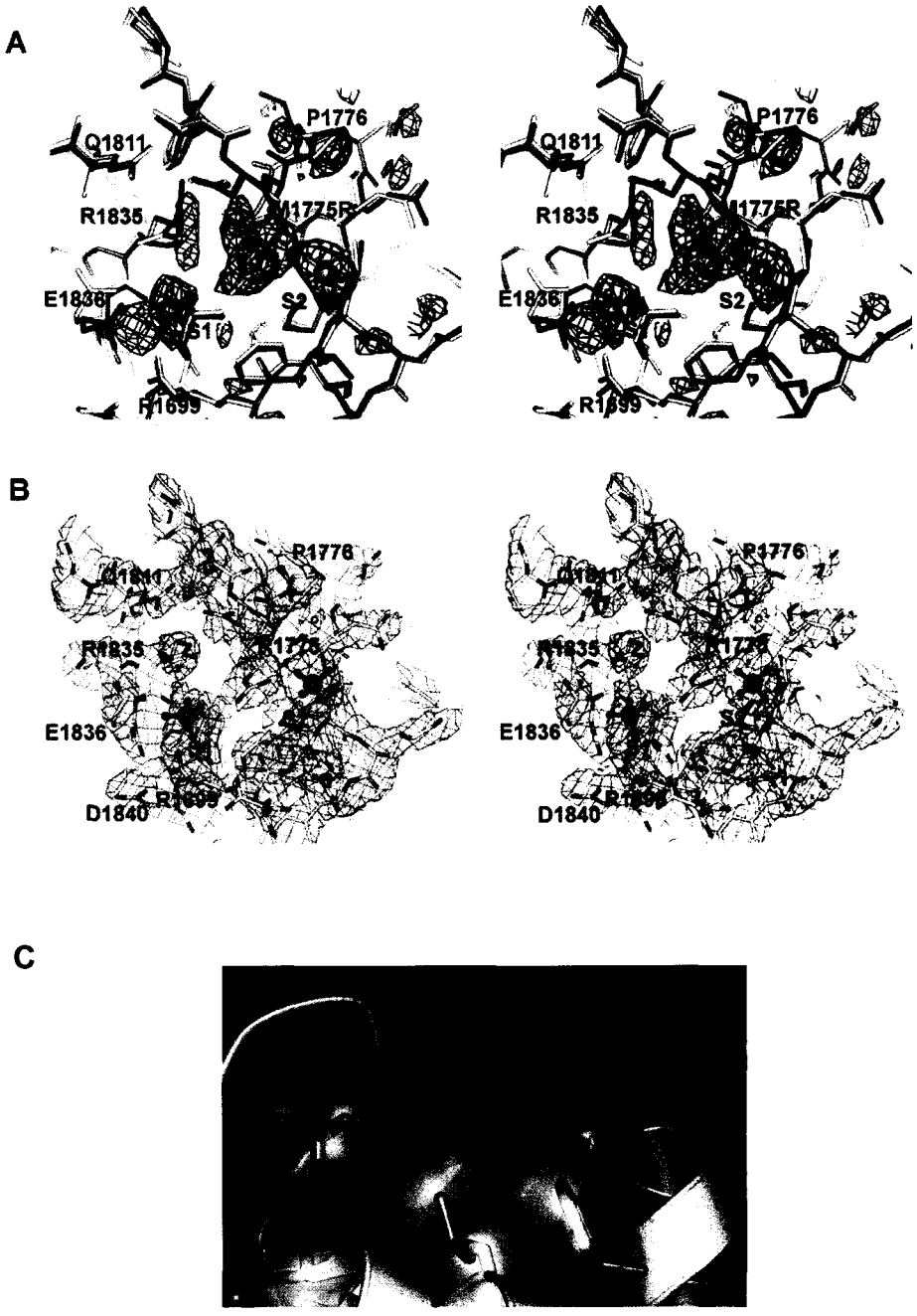

Figure. 3.4. M1775R Structure determination. A. Stereoview of an overlay of BRCT-WT (gray) and BRCT-M1775R (gold) for the region surrounding M1775R. The 2.8 Å positive (blue) and negative (red) sigma-A weighted F_o-F_c electron density (phased with the wild type model, RCSB:1JNX) is contoured at (+/-) 2.9 $\tilde{\sigma}$Two large positive peaks, modeled as sulphate molecules S1 and S2, are found coplanar to R1775. **B.** A stereoview of model phased sigma-A weighted $2F_o$-F_c map contoured at 1.0 σ is displayed for the final model of BRCT-M1775R. Electron density maps were calculated with CNS **(A)**, or REFMAC **(B)**. **C.** Arg-1775 (*red surface*) is flipped out of the hydrophobic pocket where the methionine (*green surface*) normally packs. This movement and additional rearrangements (see Fig 3.5) contribute to protein instability and an increased susceptibility to disease.

Table 3.1: Crystallographic Data and Refinement Statistics for M1775R

Unit cell (space group $p6_122$)	a = b (Å)	114.708
	c (Å)	121.676
Resolution Range (Å)		50 - 2.8
No. of observed reflections		100697
No. of unique reflections		12024
Completeness (%)		99.3 (100)[a]
R_{sym} (%)[b]		6.8 (40.4)
Overall I / σI		29.9 (3.3)
R_{cryst} / R_{free} (%)[c]		27.3 / 29.8
No. of residues / H_2O / SO_4^{2-} / Co^{2+}		213 / 59 / 2 / 1
Ramachandran plot (%):		
Most Favored / Allowed / Generous /Disallowed		87.2 / 11.7 / 1.1 / 0
RMSD Bonds (Å) / Angles (°)		0.013 / 1.857

[a] Values in parentheses are statistics for the highest resolution shell, (2.90 - 2.80 Å).
[b] $R_{sym} = 100 \sum_{hkl} | < I > - I | / \sum_n < I >$
[c] $R_{cryst} = \sum_n |F_o(h) - F_c(h)| / \sum_n | F_o(h) |$; Where $F_o(h)$ and $F_c(h)$ are observed and calculated structure factors for the resolution range 20 – 2.8 Å. R_{free} calculated with 7 % of all reflections excluded from refinement.

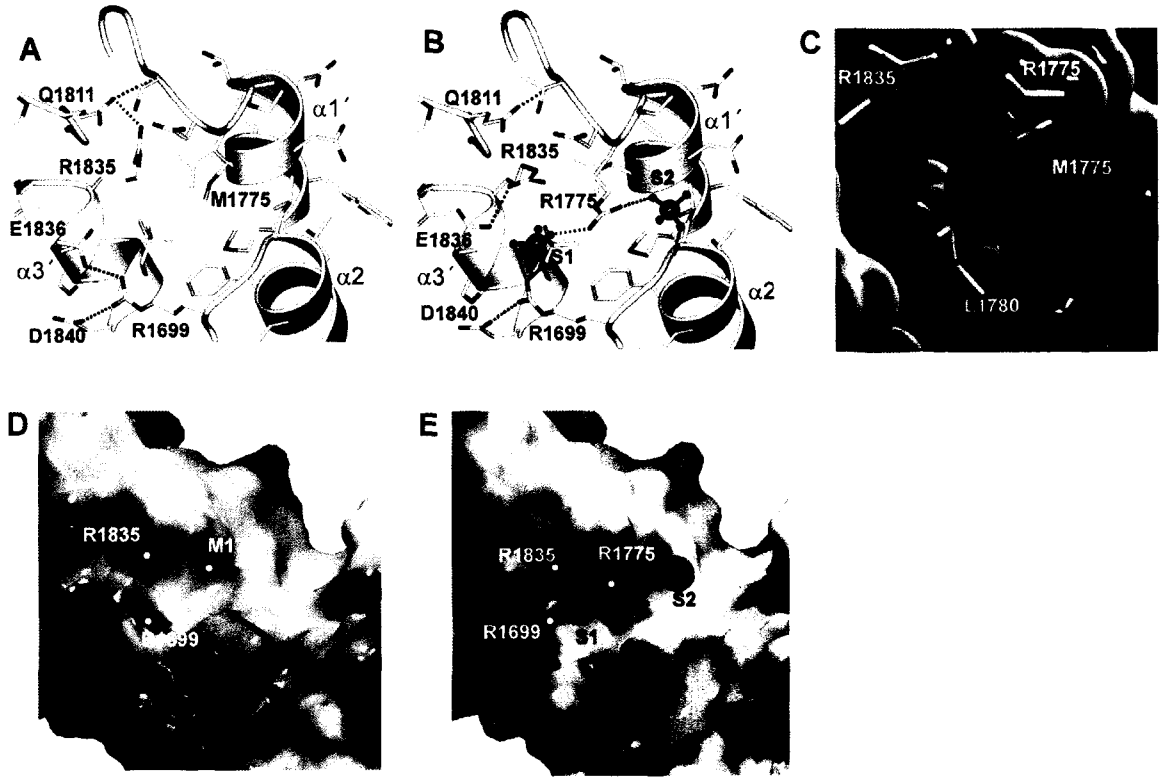

Figure 3.5. Structural rearrangements accommodate M1775R. A. Native hydrogen bonding interactions proximal to M1775. Hydrogen bonds are indicated by dashed lines. **B.** Hydrogen bonding, salt bridging for mutant M1775R. R1775 participates in the coordination of two solvent anions, S1 and S2 and has been flipped out from the hydrophobic pocket where M1775 normally packs. **C.** Cutaway view of the hydrophobic core of the BRCT. Structural overlay of WT (grey with red surface) and M1775R (gold with grey surface) hydrophobic core residues that move upon mutation. **D.** Charge-potential GRASP surface for BRCT -WT. Blue surface reflects positive charge potential and red is negative. The arrow indicates a hydrophobic groove near M1775. **E.** Charge-potential GRASP surface for BRCT-M1775R. Green spheres mark the positions of bound anions.

(Fig. 3.5*a*). The positively charged guanidinium group of variant R1775 is found positioned between two large positive peaks in our electron density maps which we have interpreted to be sulphate molecules, the highest concentration anion in the crystallization mother liquor (Fig. 3.4,3.5*b*). In the mutant, R1699 retains the salt bridge with D1840, but no longer contacts E1836 and instead coordinates an anion. R1835 rotates away from Q1811 and forms a new salt bridge with E1836. Thus, it appears that electrostatic stabilization of this positive charge cluster is achieved through ordering of solvent anions and a cascade of hydrogen bonding alterations.

The adjustments in the positions of R1775 and R1835 described above result in the displacement of the aliphatic portions of these side chains from the protein core (Fig. 3.5*C*). In response to these movements, L1780 shifts to maintain van der Waals contact with the arginine residues. These movements are accomplished without the creation of large, energetically costly cavities within the hydrophobic core (Liang et al. 1998, Matthews 1996). The repacking of the core however, in combination with instability created by hydrogen bonding changes and charge-charge repulsion of basic residues at the BRCT-BRCT interface, may collectively help account for the 5 kcal/mol destabilization reported for the BRCT-M1775R protein (Ekblad et al. 2002).

Few crystallographic examples documenting protein structural responses to the introduction of charged residues into the hydrophobic core are available. Structural investigation of a comparable, highly destabilizing mutation in T4 lysozyme, M102→ K102, reveals the position of the lysine side chain changes

little when compared to native M102 packing (Dao-pin et al. 1991). Instead, the mutation is accompanied by increased mobility of flanking residues including a helix that normally packs against the substituted methionine. This motion allows access of the buried, basic side chain to solvent via a folding-unfolding transition of neighbouring structured regions. The structural rearrangement that we observe in BRCT-M1775R is less dramatic, but nevertheless results in the expulsion of the charged side chain from the hydrophobic protein core.

Destabilization of the BRCT abrogates BRCA1-M1775R function

At the surface of the protein, a hydrophobic groove near M1775 is apparent in the wild type structure (Fig. 3.5*d*). With the movement of R1775 in the mutant, this cleft becomes occluded with charged atoms (Fig. 3.5*e*). This raises the possibility that, in addition to the destabilizing effect of the mutation, the substitution may disrupt association of BRCA1 with its interaction partners by directly modifying an exposed protein-binding site. However, this site does not overlap with a BACH1 binding site that maps to the $\beta3$–$\alpha2$ connecting loop (Fig. 3.1) of the N-terminal BRCT repeat (Joo et al. 2002), which is greater than 20 Å away from M1775. As BACH1 binding is impaired by the M1775R substitution, this would suggest that global structural defects resulting from the mutation, rather than localized structural and electrostatic perturbation, are responsible for the binding defect. Moreover, variant M1775R is defective in many biochemical assays that assess BRCA1 function and is unable to interact with several other proteins that associate with the wild type BRCT domain (Table 3.2). As it is unlikely that all of these proteins target a common surface near M1775 that is

changed by the mutation, we suggest that the wide spectrum of molecular defects reported for variant M1775R are explained by the destabilization of the domain.

Measurement of the steady state levels of BRCA1 missense variants M1775R, P1749R and A1708E reveals they are similar to the wild type, suggesting that these proteins are not destabilized to the degree that they are degraded significantly *in vivo* (Yu et al. 1998, Scully et al. 1999). Although it is difficult to predict individual energetic contributions of the M1775R rearrangements to BRCT destabilization, it is clear that the cumulative changes affecting the structure across the BRCT-BRCT interface result in a temperature sensitive tandem BRCT domain (Fig. 3.2, Fig. 3.3) which is defective in BRCA1 protein interaction, transcription, and DNA repair functions. In analogous studies, the quantitative measurement of the thermodynamic stability of the p53 tumour suppressor has shown that many of the common cancer-causing mutations are destabilizing. Consequently, p53 is inactivated by mutation, and cell cycle control is lost (Bullock & Fersht 2001). As many of the BRCT missense variants destabilize the BRCT to the same extent or more than M1775R (Ekblad et al. 2002), we might expect these variants to possess molecular and disease phenotypes similar to M1775R. Examination of the effects of other missense mutations on BRCA1 cellular function will be necessary to correlate BRCT loss of structure with BRCA1 loss of function and will further establish protein misfolding as a basic molecular mechanism of disease.

Table 3.2: Defects associated with BRCA1-M1775R

Deleterious Effect	References
Mutant BRCA1 allele encoding BRCA1-M1775R segregates with disease in families with breast and ovarian cancer	Miki et al. 1994 Futreal et al. 1994
Impaired kinetics of double strand DNA break repair	Scully et al. 1999
Transcription activation activity abolished	Monteiro et al. 1996 Chapman and Verma 1996
Impaired protein binding to CtIP	Yu et al. 1998
Impaired protein binding to histone deacetylase complexes	Yarden and Brodie 1999
Impaired protein binding to the BACH1 DNA helicase	Cantor et al. 2001

References:

Bork, P., Hofmann, K., Bucher, P., Neuwald, A. F., Altschul, S. F., and Koonin, E. V. A superfamily of conserved domains in DNA damage-responsive cell cycle checkpoint proteins. FASEB J, *11*: 68-76. 1997.

Brünger, A. T., Adams, P. D., Clore, G. M., DeLano, W. L., Gros, P., Grosse-Kunstleve, R. W., Jiang, J.-S., Kuszewski, J., Nilges, M., Pannu, N. S., Read, R. J., Rice, L. M., Simonson, T., and and Warren, G. L. Crystallography & NMR System: A New Software Suite for Macromolecular Structure Determination. Acta Cryst, *D54*: 905-921, 1998.

Brzovic, P. S., Rajagopal, P., Hoyt, D. W., King, M. C., and Klevit, R. E. Structure of a BRCA1-BARD1 heterodimeric RING-RING complex. Nat Struct Biol, *8*: 833-7, 2001.

Bullock, A. N. and Fersht, A. R. Rescuing the function of mutant p53. Nat Rev Cancer, *1*: 68-76, 2001.

Callebaut, I. and Mornon, J. P. From BRCA1 to RAP1: a widespread BRCT module closely associated with DNA repair. FEBS Lett, 400(1): 25-30. 1997.

Cantor, S. B., Bell, D. W., Ganesan, S., Kass, E. M., Drapkin, R., Grossman, S., Wahrer, D. C., Sgroi, D. C., Lane, W. S., Haber, D. A., and Livingston, D. M. Bach1, a novel helicase-like protein, interacts directly with brca1 and contributes to its dna repair function. Cell, 105(1): 149-60. 2001.

Chapman, M. S. and Verma, I. M. Transcriptional activation by BRCA1. Nature, *382*: 678-9. 1996.

Collaborative Computational Project, Number 4. Acta. Crystallogr. D 54: 905-921. 1994.

Couch, F. J. and Weber, B. L. Mutations and polymorphisms in the familial early-onset breast cancer (BRCA1) gene. Breast Cancer Information Core. Hum Mutat, 8: 8-18. 1996.

Dao-pin, S., Anderson, D. E., Baase, W. A., Dahlquist, F. W., and Matthews, B. W. Structural and thermodynamic consequences of burying a charged residue within the hydrophobic core of T4 lysozyme. Biochemistry, *30*: 11521-9. 1991.

Deng, C. X. and Brodie, S. G. Roles of BRCA1 and its interacting proteins. Bioessays, 22: 728-737. 2000.

Ekblad, C. M., Wilkinson, H. R., Schymkowitz, J. W., Rousseau, F., Freund, S. M., and Itzhaki, L. S. Characterisation of the BRCT domains of the breast cancer susceptibility gene product BRCA1. J Mol Biol, *320*: 431-42. 2002.

Esnouf, R. M. An extensively modified version of MolScript that includes greatly enhanced coloring capabilities. J Mol Graph Model, *15*: 132-4.1997.

Esnouf, R. M. Further additions to MolScript version 1.4, including reading and contouring of electron-density maps. Acta Crystallogr D Biol Crystallogr, *55*: 938-40. 1999.

Friedman, L. S., Ostermeyer, E. A., Szabo, C. I., Dowd, P., Lynch, E. D., Rowell, S. E., and King, M. C. Confirmation of BRCA1 by analysis of germline mutations linked to breast and ovarian cancer in ten families. Nat Genet, 8(4): 399-404. 1994.

Futreal, P. A., Liu, Q., Shattuck-Eidens, D., Cochran, C., Harshman, K., Tavtigian, S., Bennett, L. M., Haugen-Strano, A., Swensen, J., Miki, Y. and others. BRCA1 mutations in primary breast and ovarian carcinomas. Science, 266(5182): 120-2. 1994.

Gayther, S. A., Warren, W., Mazoyer, S., Russell, P. A., Harrington, P. A., Chiano, M., Seal, S., Hamoudi, R., van Rensburg, E. J., Dunning, A. M. and others. Germline mutations of the BRCA1 gene in breast and ovarian cancer families provide evidence for a genotype-phenotype correlation. Nat Genet, 11: 428-33. 1995.

Jones, T. A., Zou, J. Y., Cowan, S. W., and Kjeldgaard Improved methods for binding protein models in electron density maps and the location of errors in these models. Acta Crystallogr A, *47* : 110-9, 1991.

Joo, W. S., Jeffrey, P. D., Cantor, S. B., Finnin, M. S., Livingston, D. M., and Pavletich, N. P. Structure of the 53BP1 BRCT region bound to p53 and its comparison to the Brca1 BRCT structure. Genes Dev, *16*: 583-93. 2002.

Koonin, E. V., Altschul, S. F., and Bork, P. BRCA1 protein products ... Functional motifs... *Nat Genet.*, *13*: 266-8, 1996.

Krishnan, V. V., Thornton, K. H., Thelen, M. P., and Cosman, M. Solution structure and backbone dynamics of the human DNA ligase IIIalpha BRCT domain. Biochemistry, *40*: 13158-66. 2001.

Laskowski, R. A., MacArthur, M. W., and Thornton, J. M. Validation of protein models derived from experiment. Curr Opin Struct Biol, *8*: 631-9. 1998.

Li, S., Chen, P. L., Subramanian, T., Chinnadurai, G., Tomlinson, G., Osborne,

C. K., Sharp, Z. D., and Lee, W. H. Binding of CtIP to the BRCT repeats of BRCA1 involved in the transcription regulation of p21 is disrupted upon DNA damage. J Biol Chem, 274(16): 11334-8. 1999.

Liang, J., Edelsbrunner, H., and Woodward, C. Anatomy of protein pockets and cavities: measurement of binding site geometry and implications for ligand design. Protein Sci, *7*: 1884-97. 1998.

Matthews, B. W. Structural and genetic analysis of the folding and function of T4 lysozyme. FASEB J, *10*: 35-41. 1996.

Merritt, E. A. and Bacon, D. J. Raster3D: Photorealistic Molecular Graphics. Meth Enzymology 277: 505-524. 1997.

Miki, Y., Swensen, J., Shattuck-Eidens, D., Futreal, P. A., Harshman, K., Tavtigian, S., Liu, Q., Cochran, C., Bennett, L. M., Ding, W. and others. A strong candidate for the breast and ovarian cancer susceptibility gene BRCA1. Science, 266(5182): 66-71. 1994.

Monteiro, A. N., August, A., and Hanafusa, H. Evidence for a transcriptional activation function of BRCA1 C-terminal region. Proc Natl Acad Sci U S A, 93(24), 13595-9. 1996.

Nicholls, A., Sharp, K. A., and Honig, B. Protein folding and association: insights from the interfacial and thermodynamic properties of hydrocarbons. Proteins, *11*: 281-96. 1991.

Otwinowski, Z. and Minor, W. Processing of X-ray diffraction data collected in oscillation mode. Meth Enzymology 276: 307-325. 1997.

Scully, R., Ganesan, S., Vlasakova, K., Chen, J., Socolovsky, M., and Livingston,

D. M. Genetic analysis of BRCA1 function in a defined tumor cell line. Mol Cell, *4*: 1093-9. 1999.

Scully, R. and Livingston, D. M. In search of the tumour-suppressor functions of BRCA1 and BRCA2. Nature, *408*: 429-32. 2000.

Shen, D. and Vadgama, J. V. BRCA1 and BRCA2 gene mutation analysis: visit to the Breast Cancer Information Core (BIC). Oncol Res, *11*: 63-9. 1999.

Venkitaraman, A. R. Cancer susceptibility and the functions of BRCA1 and BRCA2. Cell, *108*: 171-82. 2002.

Williams, R. S., Green, R., and Glover, J. N. Crystal structure of the BRCT repeat region from the breast cancer- associated protein BRCA1. Nat Struct Biol, *8*: 838-42. 2001.

Williams, R. S. and Glover, J. N. Structural Consequences of a Cancer-causing BRCA1-BRCT Missense Mutation. J Biol Chem, *278*: 2630-5. 2003.

Winn, M. D., Isupov, M. N., and Murshudov, G. N. Use of TLS parameters to model anisotropic displacements in macromolecular refinement. Acta Crystallogr D Biol Crystallogr, *57*: 122-33. 2001.

Yarden, R. I. and Brody, L. C. BRCA1 interacts with components of the histone deacetylase complex. Proc Natl Acad Sci U S A, 96(9): 4983-8. 1999.

Yu, X., Wu, L. C., Bowcock, A. M., Aronheim, A., and Baer, R. The C-terminal (BRCT) domains of BRCA1 interact in vivo with CtIP, a protein implicated in the CtBP pathway of transcriptional repression. J Biol Chem, 273 :5388-92. 1998.

Zhang, X., Morera, S., Bates, P. A., Whitehead, P. C., Coffer, A. I., Hainbucher,

K., Nash, R. A., Sternberg, M. J., Lindahl, T., and Freemont, P. S. Structure of an XRCC1 BRCT domain: a new protein-protein interaction module. EMBO J, 17(21), 6404-11. 1998.

Chapter 4:

Detection of protein folding defects caused by BRCA1-BRCT truncation and missense mutations

SUMMARY:

Most cancer-associated BRCA1 mutations identified to date result in the premature translational termination of the protein, highlighting a crucial role for the C-terminal, BRCT repeat region in mediating BRCA1 tumour suppressor function. However, the molecular and genetic effects of missense mutations that map to the BRCT region remain largely unknown. Using a protease based assay, we directly assessed the sensitivity of the folding of the BRCT domain to an extensive set of truncation and single amino acid substitutions derived from breast cancer screening programs. The protein can tolerate truncations of up to 8 amino acids but further deletion resulted in drastic BRCT folding defects. This molecular phenotype can be correlated with an increased susceptibility to disease. 20/25 missense mutations tested showed enhanced sensitivity to proteolytic digestion, suggesting that the large majority of BRCT missense mutations contribute to BRCA1 loss of function and disease through protein destabilizing effects. The use of simple proteolytic methods to detect mutant BRCA1 conformations at the protein level will augment the efficacy of current BRCA1 screening protocols, especially in the absence of clinical data that can discriminate deleterious BRCT missense mutations from benign polymorphisms.

INTRODUCTION:

Germline mutations within the breast and ovarian cancer susceptibility gene *BRCA1* predispose carriers to early-onset breast and breast-ovarian cancers (Nathanson et al. 2001). Accumulating evidence points to a role for the *BRCA1* protein product in the regulation of multiple nuclear functions including transcription, recombination, DNA repair, and checkpoint control (Venkitaraman 2002, Monteiro 2000, Scully & Livingston 2000). Tumour associated mutations occur throughout the *BRCA1* coding sequence, but cluster to sequences encoding the N-terminal RING finger domain and the two carboxy-terminal repeat BRCT domains (Shattuck-Eidens et al. 1995, Couch & Weber 1996, Shen & Vadgama 1999).

The molecular details of how BRCA1 mutations contribute to the pathogenesis of cancer remain largely unknown. The functional significance of the BRCT region is highlighted by the high degree of sequence conservation within the BRCT regions among mammalian, Xenopus, and avian BRCA1 homologues (Sharan et al. 1995, Chen et al. 1996, Joukov et al. 2001). Several lines of evidence reveal the BRCT is required for tumour suppressor function. A nonsense mutation, which removes 11 C-terminal residues of the second, BRCT (Tyr1853 → stop), is associated with early-onset breast cancer (Friedman et al. 1994). Two cancer-linked BRCT missense mutations (Miki et al. 1994) that destabilize the BRCT fold (Williams et al. 2001, Ekblad et al. 2002), A1708E and M1775R, ablate the double-strand break repair and transcription function of BRCA1 (Scully et al. 1999) and inhibit BRCT interactions with histone

deacetylases (Yarden & Brody 1999), BACH1 (Cantor et al. 2001) and the transcriptional co-repressor CtIP (Yu et al. 1998, Li et al. 1999). Furthermore, mice with homozygous targeted mutations removing the C-terminal half of BRCA1 are viable but develop tumours, suggesting the missing BRCT and/or other domains are expendable for survival, but not for tumour suppression (Ludwig et al. 2001).

While all frameshift or nonsense mutations recorded in the Breast cancer Information Core (BIC) resulting in BRCA1 protein truncation are viewed as functionally deleterious (Couch & Weber 1996, Shen & Vadgama 1999), the physiological significance of the majority of missense variants has not been determined due to the absence of a distinctive functional assay for BRCA1. More than 50 missense substitutions have been recorded that alter the primary sequence of the tandem BRCT-repeats but pedigree analysis clarifying the disease linkage of these alleles is available for only eight of these variants (Futreal et al. 1994, Miki et al. 1994, Couch & Weber 1996, Shen & Vadgama 1999, Hayes et al. 2000, Vallon-Christersson et al. 2001, Carvalho et al. 2002, Worley et al. 2002). Many of these amino acid substitutions that may be linked with disease have been categorized as unclassified variants in the BIC because the presence of the allele has not been tested in the general population, or the segregation of the allele with disease within a family is unclear (Couch & Weber 1996, Shen & Vadgama 1999).

The recent determination of the x-ray crystal structures of the rat and human BRCA1 BRCT repeat domains were important first steps towards

understanding tumourigenic BRCT mutations and provide a novel platform for the interpretation of the effects of these alterations in the absence of clinical data (Williams et al. 2001, Joo et al. 2002). Previous subjective assessments of the structural effects of BRCT missense mutations have been made using inaccurate BRCA1 models derived from the structure of the XRCC1 BRCT domain (Zhang et al. 1998, Huyton et al. 2000). In the present study we directly evaluate the consequences missense mutation has on the structure of the human BRCA1 BRCT repeats. Using a proteolysis-based assay to probe the BRCT for non-native conformations, we show that the majority of the tested missense and truncations alter the folding state of the BRCT. Most of the unclassified BRCT missense mutations are likely to be disease predisposing and perturb BRCA1 structure/function through protein destabilizing effects.

EXPERIMENTAL PROCEDURES:

Mutagenesis and vector construction

Coding sequences for BRCT C-terminal truncations of human BRCA1 were amplified from the T7 promoter based expression vector for pLM1-BRCA1 (1646-1863) (Williams et al. 2001) using the following oligonucleotides: (fragment 1646-1859) FT7-5'-gga cga gaa ttc tta acc agg gag ctg att atg gtg aac aaa aga atg tcc atg-3', CD6-5'-gat ctg gga tcc tca ggg gat ctg ggg tat cag-3'; (fragment 1646-1858) FT7, CD7-5'-gat ctg gga tcc tca gat ctg ggg tat cag gta-3' ; (fragment 1646-1857) FT7, CD1-5'-gat ctg gga tcc tca ctg ggg tat cag gta ggt-3' ; (fragment 1646-1855) FT7, CD5-5'-gat ctg gga tcc tca tat cag gta ggt gtc cag-3' ; (fragment 1646-1853) FT7, CD4-5'- gat ctg gga tcc tca gta ggt gtc cag ctc ctg-3' ; (fragment 1646-1852) FT7, 1853Ystop-5'-gat ctg gga tcc tca ggt gtc cag ctc ctg gca-3' ; (fragment 1646-1851) FT7, CD3-5'-gat ctg gga tcc tca gtc cag ctc ctg gca ctg-3' ; (fragment 1646-1849) FT7, CD2-5'-gat ctg gga tcc tca ctc ctg gca ctg gta gag-3' ; (fragment 1646-1829) FT7, 1829stop -5'- gat ctg gga tcc tca aca cat ctg ccc aat tgc-3' ; (fragment 1646-1805) FT7, 1805stop-5'-gat ctg gga tcc tca gac acc tgt gcc aag ggt-3'. The 5' primer FT7 incorporates a ribosome binding site and an EcoRI site for cloning. 3' oligonucleotides include the relevant stop codons and a BamHI restriction site. Gel purified PCR products were digested with EcoRI and BamHI and cloned into BamHI-EcoRI digested pLM1 (Sodeoka, 1993).

All BRCT single amino acid substitutions were introduced into the BRCT fragment 1646-1859. For missense mutations A1708E, M1775R, and W1837R,

mutated BRCA1 coding sequences were used as template for PCR amplification with the FT7 and CD6 primers. Mutation M1652I was generated by direct PCR amplification using primers F-M1652I and CD6. Missense variant Y1853C was generated by direct PCR amplification using primer FT7 in combination with R-Y1853C . All other missense substitutions were engineered using PCR splicing methods (Horton et al. 1993). Primary PCR mutagenesis reactions used oligo FT7 with the appropriate reverse (R) mutagenesis oligonucleotide (see below) and CD6 with the appropriate foward (F) mutagenesis oligonucleotide. PCR products from the primary reactions were gel purfied from 1.5% agarose gels using a QIAEX2 kit (Qiagen) and mixed together with oligonucleotides FT7 and CD6 in the secondary PCR splicing reactions to generate mutated PCR products that were subsequently digested with EcoRI/BamHI and ligated to pLM1. The mutagenesis oligos used were: D1692Y, F - 5' - gtt atg aaa aca tat gct gag ttt gtg – 3', R - 5' - cac aaa ctc agc ata tgt ttt cat aac - 3'; F1695L, F - 5' - aca gat gct gag ctt gtg tgt gaa cgg – 3', R - 5' - ccg ttc aca cac aag ctc agc atc tgt - 3'; V1696L, F - 5' - gat gct gag ttt ttg tgt gaa cgg aca – 3', R - 5' - tgt ccg ttc aca caa aaa ctc agc atc - 3'; C1697R, F-5'-gct gag ttt gtg cgt gaa cgg aca ctg-3', R-5'-cag tgt ccg ttc acg cac aaa ctc agc - 3'; R1699W, F - 5' - ttt gtg tgt gaa tgg aca ctg aaa tat – 3', R - 5' - ata ttt cag tgt cca ttc aca cac aaa - 3'; R1699Q, F - 5' - ttt gtg tgt gaa cag aca ctg aaa tat – 3', R - 5' - ata ttt cag tgt ctg ttc aca cac aaa - 3'; S1715R, F-5'- aaa tgg gta gtt aga tat ttc tgg gtg - 3', R-5'-cac cca gaa ata tct aac tac cca ttt-3'; W1718C, F-5'- gtt agc tat ttc tgt gtg acc cag tct - 3', R-5'- aga ctg ggt cac aca gaa ata gct aac - 3'; T1720A, F - 5' - tat ttc tgg gtg gcc cag tct att

aaa – 3', R - 5' - ttt aat aga ctg ggc cac cca gaa ata - 3'; G1738E, F-5'- ttt gaa gtc aga gaa gat gtg gtc aat g – 3', R-5'- cat tga cca cat ctt ctc tga ctt caa a-3'; G1738R F-5'- ttt gaa gtc aga aga gat gtg gtc aat g – 3', R-5'- cat tga cca cat ctc ttc tga ctt caa a-3'; P1749R, F-5'- aac cac caa ggt cgt aag cga gca aga g – 3', R-5'- ctc ttg ctc gct tac gac ctt ggt ggt t –3'; R1751Q, F - 5' - caa ggt cca aag caa gca aga gaa tcc – 3', R - 5' - gga ttc tct tgc ttg ctt tgg acc ttg - 3'; A1752P, F - 5' - ggt cca aag cga cca aga gaa tcc cag – 3', R - 5' - ctg gga ttc tct tgg tcg ctt tgg acc - 3'; I1766S, F-5'- agg ggg cta gaa agc tgt tgc tat ggg – 3', R-5'- ccc ata gca aca gct ttc tag ccc cct-3'; M1783T F-5'- caa ctg gaa tgg acc gta cag ctg tgt g - 3', R-5'- cac aca gct gta cgg tcc att cca ggt t; G1788V, F - 5' - gta cag ctg tgt gtt gct tct gtg gtg – 3', R - 5' - cac cac aga agc aac aca cag ctg tac - 3'; V1804D, F - 5' - ctt ggc aca ggt gac cac cca att gtg – 3', R - 5' - cac aat tgg gtg gtc acc tgt gcc aag - 3'; V1809F, F - 5' - cac cca att gtg ttt gtg cag cca gat – 3', R - 5' - atc tgg ctg cac aaa cac aat tgg gtg - 3'; W1837G, F-5'- gtg acc cga gag ggg gtg ttg gac agt g – 3', R-5'- cac tgt cca aca ccc cct ctc ggg tca c –3 '. All vectors were sequenced to confirm the success of the mutagenesis reactions.

Proteolysis assays

0.2 to 0.5 μg of pLM1 plasmid encoding the BRCT variants were used directly as template for protein synthesis reactions with the TNT-Quick *in vitro* transcription/translation system (Promega). Immediately prior to proteolytic digestion, proteins were translated and labelled with ^{35}S-methionine at 30 °C for 2 hr. The reticulocyte lysates were then centrifuged for 2 min. at 10000 x *g* to remove insoluble material and 3 μL of the lysate supernatants containing the

labelled translation products were added to 12 μL digestion buffer (150 mM NaCl, 50 mM potassium phosphate, pH 7.5) containing increasing concentrations of trypsin (Sigma) or TIck-treated chymotrypsin (Sigma). After digestion at 20 °C for 12 minutes, the reactions were stopped with PMSF. Digestion products were electrophoresed on 15% SDS-PAGE gels and visualized with a phosphorimaging plate and a Molecular Dynamics Typhoon scanner. A local average background correction was used during quantification of the reaction products with ImageQuant (Amersham-Molecular Dynamics).

Molecular graphics

Structural diagrams were created with Bobscript (Esnouf 1997, Esnouf 1999) and rendered using Povray (www.povray.org).

RESULTS:

Structural effects of BRCT truncation mutations

We previously demonstrated that the tandem BRCT repeat region of human BRCA1 forms a proteolytically resistant globular domain and that a cancer-linked mutation, Y1853ter, which removes the 11 C-terminal residues of the protein, reduces this proteolytic stability (Williams et al. 2001). To determine to what extent the BRCT fold could tolerate truncation mutations, we subjected a series of BRCT deletion mutants to a proteolytic sensitivity assay (Fig. 4.1, Experimental procedures). The oncogenic mutation Y1853ter and all larger C-terminal deletions of the protein were degraded by the lowest concentrations of trypsin whereas the full length BRCT (aa 1646-1863) is highly resistant to cleavage (Fig 4.2). Included with these mutations are the truncation protein products of two of the most common BIC frameshift mutants, 5382insC and IVS21-36del510, that result in stop codons at positions 1829 and 1805 of the BRCA1 coding sequence (Shen & Vadgama 1999) (Fig. 4.2, Fig. 4.3 *a-c*). Thus, BRCT folding defects resulting from cancer predisposing BRCA1 truncation mutations can be assayed for and detected at the protein level using a simple protease sensitivity assay.

The deletion experiment also demonstrates the protein can tolerate removal of up to 8 residues, but further deletion from the C-terminus greatly impairs the native folding of the domain, rendering it highly sensitive to proteolysis (Fig. 4.2, Fig 4.3 *d*). Consistent with this finding, the transcriptional

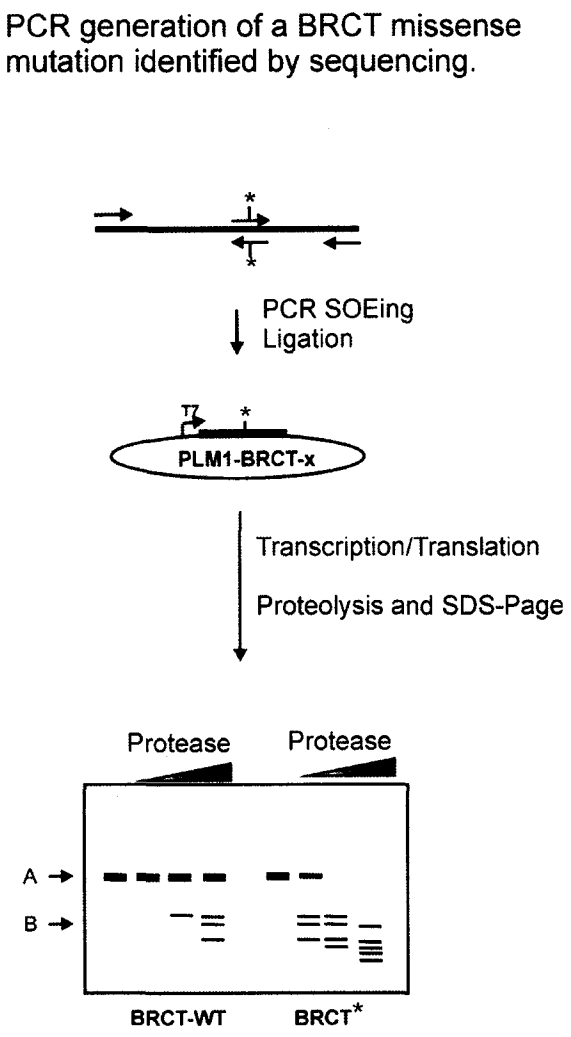

Figure 4.1. Assessing the structural effects of mutation on the BRCT. Missense mutations recorded in the Breast cancer Information Core or truncation causing mutations were generated by PCR methods and cloned into the T7 vector pLM1. Translation products were digested with protease and the disappearance of species "A" was monitored by autoradiography. The wild type protein is highly stable to digestion by trypsin, chymotrypsin, and elastase (Williams et al. 2001). Missense or truncation mutation induced destabilization or conformational change renders the BRCT repeats susceptible to proteolytic digestion.

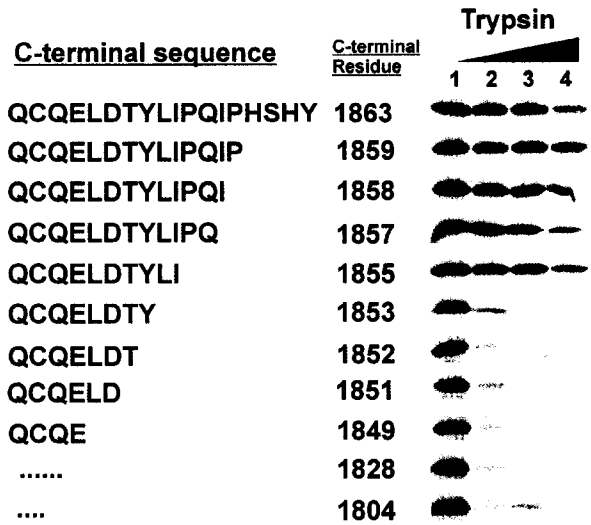

Figure 4.2. Destabilization of the BRCT domains by truncation mutation. The indicated BRCT truncation mutations were *in vitro* transcribed and translated, and then digested with increasing amounts of trypsin. Lanes 1-4: 0 μg/mL, 6 μg/mL, 60 μg/mL and 600 μg/mL trypsin. Translated protein products with C-termini at positions 1804, 1828, and 1852, correspond to the deletion products of the cancer-predisposing mutations whose truncation effects are depicted in Figure 4.3.

activation activity of the BRCT domains was abolished by C-terminal deletions that truncate beyond a hydrophobic pair of residues, L-1854 and I-1855 (Hayes et al. 2000). These hydrophobes mark the C-terminal boundary for conservation of mammalian, avian and xenopus BRCA1 homologues, and make critical aliphatic contacts to the β-sheet of the C-terminal BRCT in the structures of the rat and human BRCA1-BRCT repeats (Fig. 4.4) (Williams et al. 2001, Joo et al. 2002). Hence, the transcriptional activation defects observed for BRCT deletion mutants likely result from destabilization of the protein.

Missense substitutions destabilize the BRCT

Similar to the truncation mutants, two cancer predisposing missense mutations, A1708E and M1775R, are destabilizing and exhibit altered BRCT protease susceptibility (Williams & Glover 2003, Ekblad et al. 2002). To gain insights into the effects of other patient derived mutations recorded in the BIC, we generated 23 additional missense variants and tested these proteins for proteolytic sensitivity (see Experimental Procedures, Fig. 4.4). 20/25 of the missense mutations tested showed varying degrees of enhanced sensitivity to tryptic digestion at 20 °C (Fig 4.5 *a*). Five of six of the mutations that substitute an arginine into the protein (C1697R, S1715R, G1738R, P1749R and W1837R) also show increased sensitivity to chymotryptic cleavage at 20 °C (Fig. 4.5 *b*) suggesting that destabilizing effects, rather than the introduction of a trypsin cleavage site, are responsible for the protease sensitivity. Mutant M1775R is

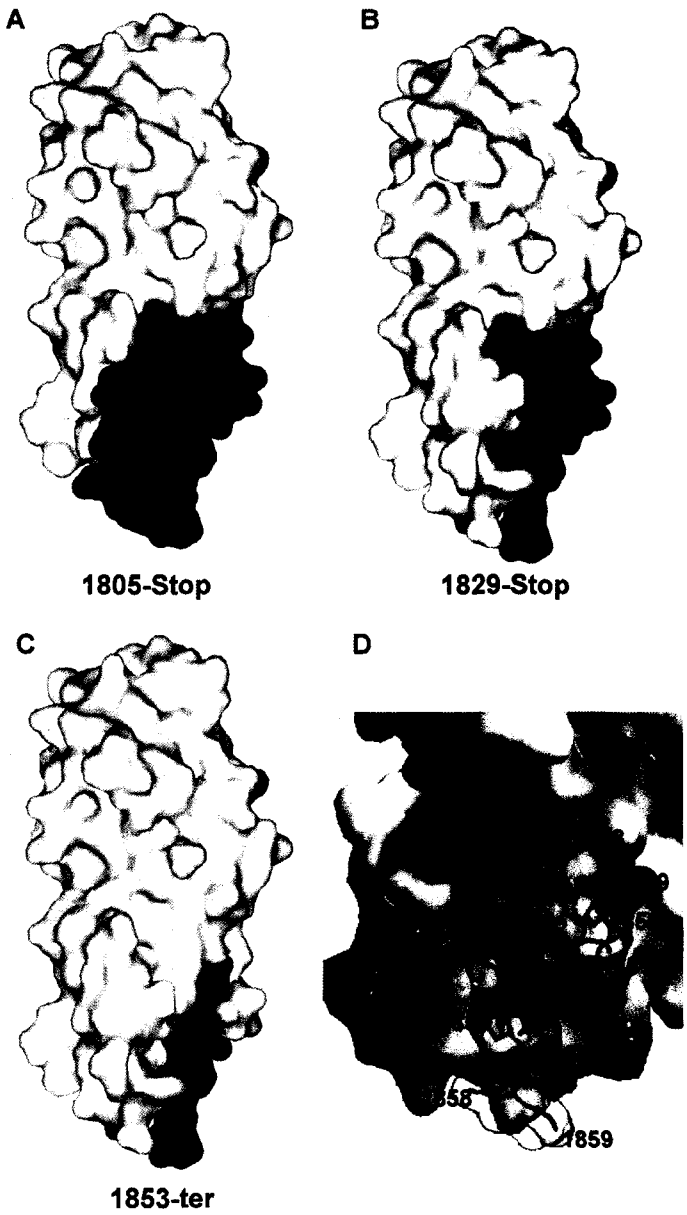

Figure 4.3. Structural effects of cancer-associated BRCA1 BRCT truncation causing mutations. A. A stop codon at position 1805 results from frameshift IVS21-36del510, removing much of the C-terminal BRCT domain. **B.** Frameshift 5382insC creates a stop codon at position 1829 in BRCA1 and is one of the most commonly recorded BIC mutations. **C.** A nonsense mutation 1853-ter results in the removal of the 11 C-terminal residues of the protein, and is linked to disease. **D.** Interaction of the C-terminal tail of BRCA1 with BRCT-C. Negative electrostatic potential is red and positive is blue. The C-terminus of BRCA1 forms a 3_{10} helix and an extended peptide that packs against α2' and the β–sheet. C-terminal deletions beyond the hydrophobic residues Leu-1854 and Ile-1855 are destabilizing.

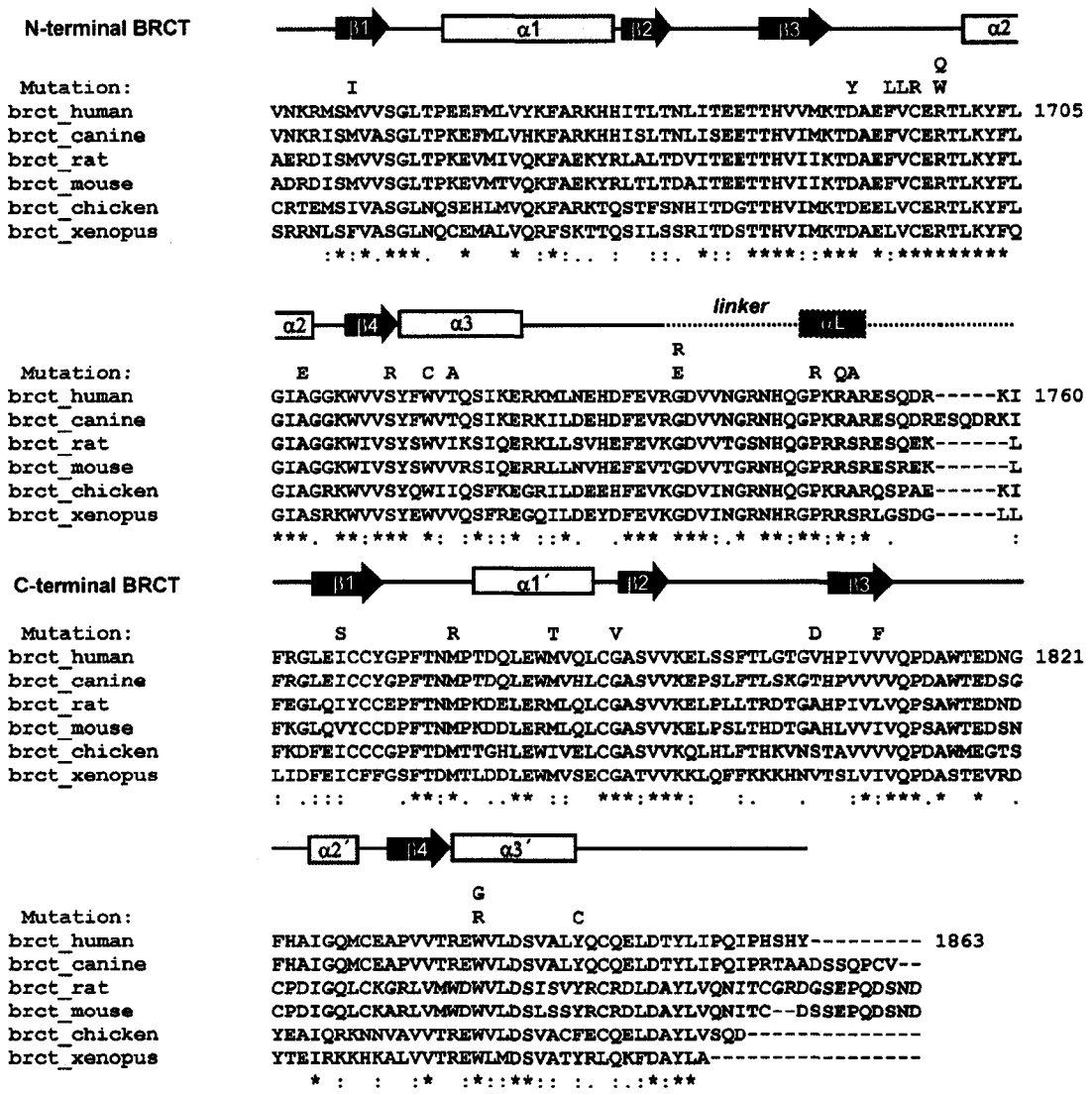

Figure 4.4. Amino acid sequence alignment of the BRCT repeat region of cloned BRCA1 homologues. Secondary structure elements are from the human BRCT repeat structure, RCSB: 1JNX. The positions of the 25 missense mutations studied here are indicated. Alignments were created with Clustal-X. Numbering is for Human BRCA1.

also clearly destabilizing and shows sensitivity to chymotrypsin at elevated temperatures (Williams & Glover 2003).

The expression levels of the BRCT variants in the reticulocyte lysates typically range between 0.3-1.2 fold of wild type levels. Since the expressed variants constitute less than 5% of the total protein digested in the lysates and we are using logarithmic increases in trypsin concentrations, we can quantify the percent protein remaining following digestion at each level of protease, and directly compare these values to establish a protease based hierarchy for the severity of the destabilizing effects (Fig. 4.6). Here we define highly destabilizing mutations as those mutants for which >60% of the protein is degraded at the lowest concentration (6 μg/mL) of trypsin. Intermediately destabilizing variants are >60% degraded at the intermediate trypsin concentration (60 μg/mL). Finally, the mutants showing wild type digestion profiles, with limited degradation until exposure to the highest trypsin concentration, are classified as having no destabilizing effect. Based on these criteria, the majority of the variants (13/25) are highly destabilizing, 7/25 are intermediately destabilizing and 5/25 have no apparent effect.

We further classified the BRCT missense mutants into four categories based on their distribution in the BRCT structure (Fig. 4.6 *a-d*, Table 4.1):

i. Surface mutations: This class of mutations includes amino acid residues found on the surface of the BRCT that appear to make little contribution to the structure of the domain. Three of five of the tested surface mutants (F1695L, T1720A, and V1804D) have no destabilizing effect. Two exposed mutations

localized to the β3-α2 connecting loop (D1692Y and V1696L) (Fig. 4.6a) confer moderate protease susceptibility to the domain. As highlighted by Joo et al. (2002), this loop forms an extended β-hairpin structure, participates in the formation of one of the two conserved BRCT surfaces targeted by missense mutations, and may be the primary site of interaction with the BRCA1 associated helicase BACH1. Hence, the BACH1 binding defect reported for mutation F1695L likely results from disruption of a contact site, whereas reduced BACH1 binding for the V1696L mutation may be due to a destabilizing effect, disruption of the contact site, or both.

ii. BRCT-interface mutations: The BRCA1 C-terminal domain consists of two BRCT repeats that stack together head-to-tail via a conserved triple-helical interface and several of the key residues mediating these BRCT-BRCT contacts are targeted by mutation (Fig. 4.6 *b*, Table 4.1) (Williams et al. 2001). Four of five of the tested BRCT-interface mutants are destabilizing. Three destabilizing mutants, A1708E, M1775R and M1783T, likely disrupt the hydrophobic packing between the repeats. The crystal structure of the M1775R variant revealed that mutation-induced structural rearrangements, including flipping of the mutated arginine out of the hydrophobic core of the protein, contribute to fold destabilization (Williams & Glover 2003). The intermediate protease sensitivity of mutation M1783T likely results from combined deleterious effects of protein core cavitation and the burial of a polar hydroxyl group at the BRCT interface. Residue R1699 normally participates in a salt bridge between the BRCT repeats. The loss of salt-bridging interactions and steric strain associated with

accommodating the tryptophan may contribute to conformational instability of the R1699W mutant. The intermediate stability of R1699W explains the temperature sensitive transcription phenotype ascribed to this mutation (Worley et al. 2002) Conversely, R1699Q has little to no effect on BRCT structure and appears to have little effect on transcription activation.

***iii. BRCA1-fold mutations*:** We have designated a third class of mutations as BRCA1-fold mutants. These substitutions include residues that participate in folding of the BRCT linker region, and residues that do not fall at BRCT-fold special positions, but are buried and conserved amongst BRCA1 homologues (Fig. 4.6 *c*). All of the tested BRCA1-fold class mutants tested alter the folding of the domain. The majority of these mutants (C1697R, S1715R, G1738R, G1738E, and P1749R) introduce charged residues into the protein core and are highly destabilizing. The A1752P mutant likely disrupts the linker helix and is highly destabilizing. The position of R1751 in the crystal structure of human BRCA1 is unclear, but the equivalent residue in the rat structure indicates this residue is involved in salt bridging interactions and the packing of BRCT linker helix (Joo et al. 2002). This arginine is conserved amongst all known BRCA1 homologues and the R1751Q mutation may disrupt similar electrostatic stabilization in the human protein.

iv. BRCT-fold mutations: A conserved hydrophobic clustering signature for the BRCT fold superfamily of proteins was originally identified using sequence based methods (Callebaut & Mornon 1997, Bork et al. 1997). Residues at these positions dictate the fold of an individual BRCT and participate in formation of the

BRCT hydrophobic core or are found in turns. As shown in Fig 4.6-*d*, 7/8 of the mutations tested (W1718C, I1766S, G1788V, V1809F, W1837G, W1837R, and Y1853C) at BRCT-fold positions are intermediately or highly destabilizing. The highly destabilizing mutations W1718C, W1837G and W1837R mutate the invariant BRCT-fold tryptophan of both the amino- and carboxyl-terminal BRCT domains. This critical core residue appears intolerant to both cavitating (W1718C and W1837G) or charge substitution mutations (W1837R) and mediates van der Waals contacts from helix α3 to other secondary structure elements of the BRCT fold including β-sheet, helix α1 and the 3_{10} helix. Mutation G1788V disrupts the conserved tight turn between α1' and β2' of the C-terminal BRCT. Figures 4.2-*d* and 4.6-*d* highlight the role of Y1853 in positioning the C-terminal BRCT 3_{10} helix that packs against the β-sheet, and substitution of this residue with a cysteine is highly destabilizing. Two of the three tested BRCT-fold class mutants that target residues that contribute to intra β-sheet packing, I1766S and V1809F, are destabilizing. The third β-sheet mutant, M1652I, has been classified as a benign polymorphism (Deffenbaugh et al. 2002, Monteiro et al. 1997) and does not increase the protease sensitivity of the domain.

Mutations that destabilize the BRCT predispose carriers to disease

Pedigree analysis clarifying the disease predisposition of *BRCA1* alleles is currently available for 8 of the 79 reported BRCA1-BRCT single amino acid substitution variants (Table 4.1). Seven of the mutations, D1692Y, C1697R, R1699W, A1708E, S1715R, P1749R and M1775R, are destabilizing (Fig. 4.5) and are linked to cancer (Table 4.1). In contrast, the frequently recorded BIC

polymorphism M1652I exhibits no structural defect, indicating the protease stability assay can successfully discriminate benign mutations from disease causing variants. The cancer-associated truncation mutants are also protease sensitive (Fig. 4.2). Taken together, these results indicate that protease based detection of altered BRCT stability provides a novel and powerful predictive tool that can be used to assess disease linkage of BRCT mutations in instances where pedigree data is not available. Thus, we suggest that the 20 destabilizing missense mutants and truncations greater than eight amino acids are cancer-predisposing.

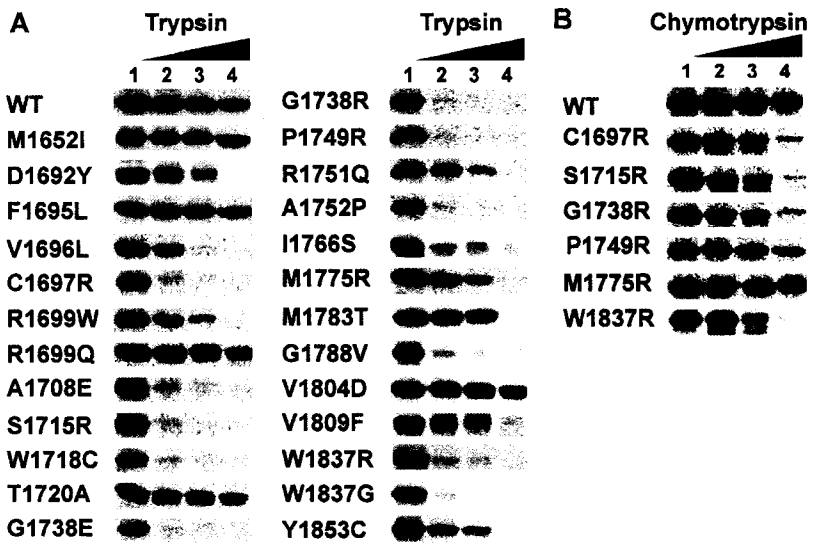

Figure 4.5. Destabilization of the BRCT domains by missense mutations. A. The indicated missense mutations were digested with increasing concentration amounts of trypsin. Lanes 1-4: 0 μg/mL, 6 μg/mL, 60 μg/mL and 600 μg/mL trypsin. **B.** Mutations harbouring a trypsin cleavage site were digested with chymotrypsin. Lanes 1-4: 0 μg/mL, 6 μg/mL, 60 μg/mL and 600 μg/mL chymotrypsin.

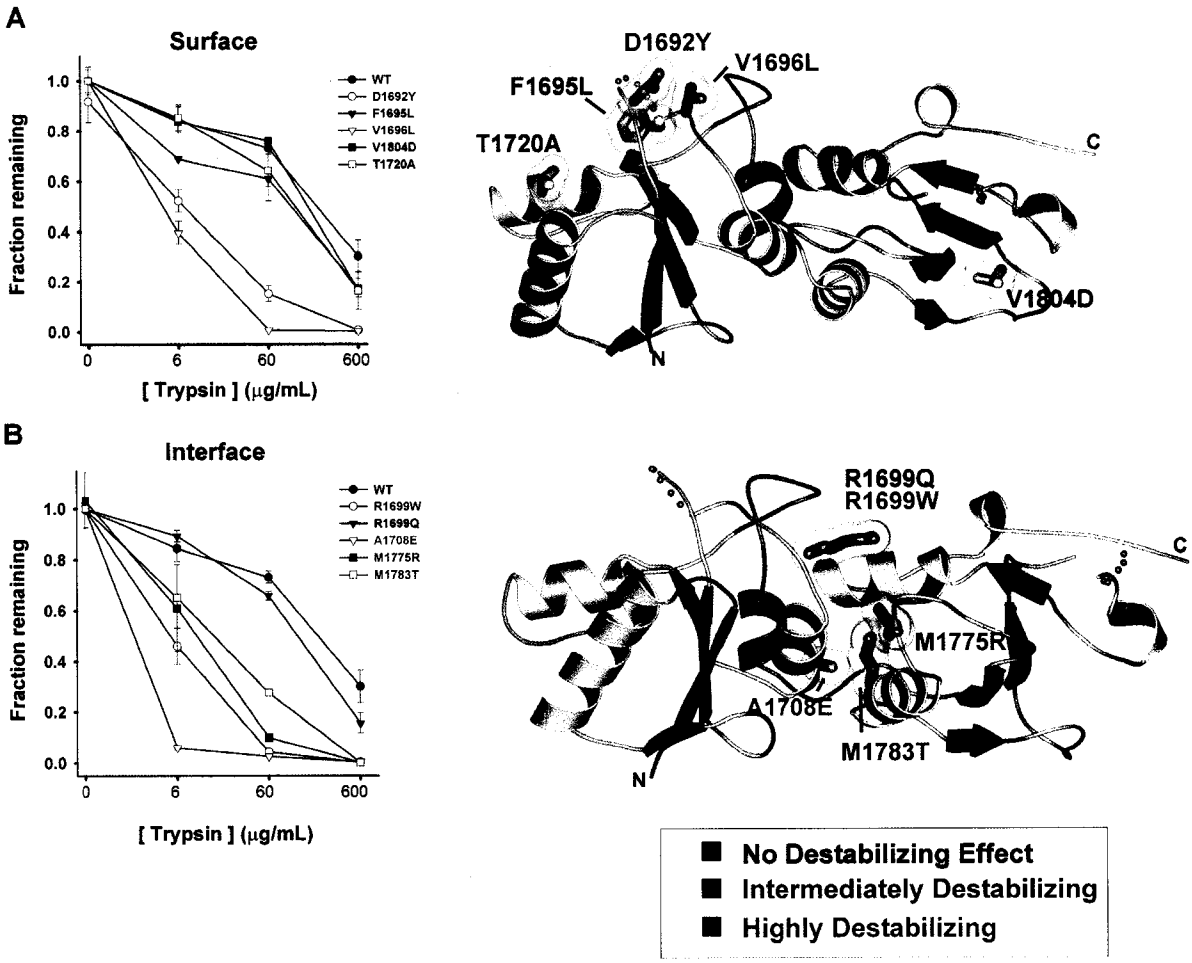

Figure 4.6-AB. Classification and Quantification of the structural effects of BRCT missense mutations. A-D: The tested BRCT missense mutations have been divided into 4 classes based on their distribution in the BRCT structure (see text). The fraction remaining is the percent of starting protein present following digestion with the indicated concentrations of trypsin. Data points are the mean value of digestions performed in triplicate with error bars reflecting the standard deviations. Red - highly destabilizing mutation (BRCT variant is >60% degraded at 6 μg/mL trypsin, Blue - Intermediately destabilizing mutation (BRCT variant is >60% degraded at 60 μg/mL trypsin), Black/grey - no destabilizing effect (similiar to wild type tryptic sensitivity). **A.** Surface mutations. **B.** Interface mutations **C.** BRCA1-fold mutations. **D.** BRCT-fold mutations.

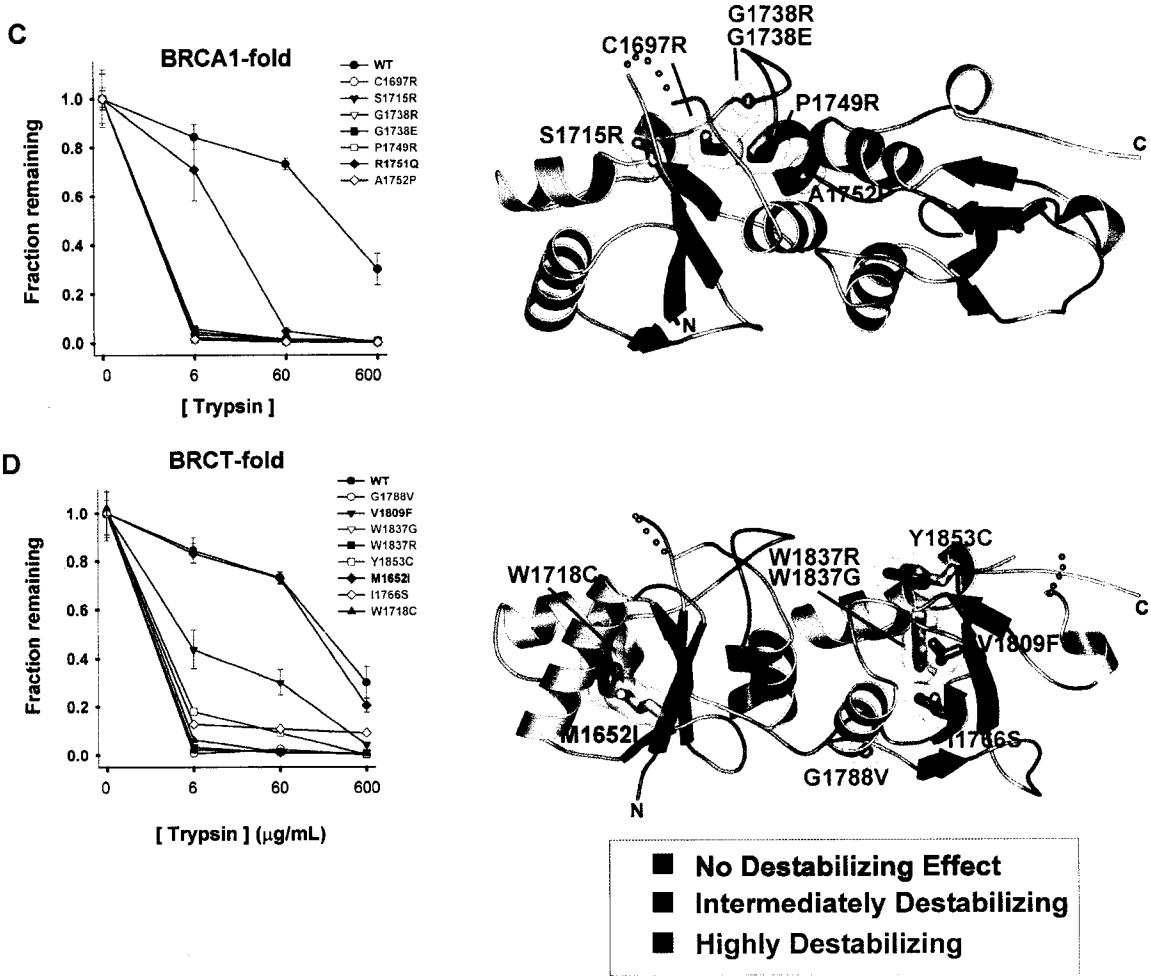

Figure 4.6-CD

Discussion:

The Protease based assay for ranking BRCT destabilizing effects

Proteolytic degradation proceeds via an unfolded state for small globular proteins (Imoto et al. 1986, Wang & Kallenbach 1998) indicating a correlation between proteolytic resistance and the thermodynamic stability of a protein may exist. This principle forms the basis for phage based proteolytic selection methods where the evolution of proteins with increased thermodynamic stability closely follows the selection of polypeptides with enhanced resistance to degradation by increasing concentration of protease (Sieber et al. 1998, Pedersen et al. 2002). Thus, the application of a protease-based assay to assess the structural consequences of missense mutation on the BRCT provides a quick, effective, complimentary method to categorize and rank the extent of destabilization of the mutant BRCT proteins.

A recent biophysical assessment of the effects of 8 missense substitutions and the truncation Y1853ter on the thermodynamic stability of the BRCT revealed that four of these missense mutations and the truncation were highly destabilizing and could not be produced as soluble protein in *E. coli* (Ekblad et al. 2002). All four of these missense mutants, A1708E, G1738E, G1788V and W1837R and the truncation show extreme sensitivity to tryptic digestion (Table 4.1). The remaining four (M1775R, M1783T, V1808A, and V1833M) can be produced recombinantly, but destabilize the protein by 3.5–5.5 kcal/mol. Two of these, M1775R and M1783T, show an intermediate sensitivity

to proteolysis. At least three other BRCT mutant proteins (D1692Y, R1699W and V1809F) with intermediate protease sensitivity are soluble in *E. coli* (data not shown). Altogether, these data indicate a three-tiered hierarchy of destabilizing effects inferred from the proteolytic data is consistent with results obtained from solubility analysis and direct thermodynamic measurements of BRCT protein stability. Highly destabilizing mutations show sensitivity to low levels of trypsin and tend to be degraded or insoluble when expressed in *E. coli.* Intermediate thermodynamically destabilizing mutations are sensitive to moderate levels of protease and can be produced in soluble form in *E. coli.* The small set of mutations that do not affect folding represent bona-fide benign polymorphisms or may directly affect surface regions of the protein involved in BRCT protein-protein, or possibly protein-DNA interactions.

Protein destabilization ablates BRCT mediated transcriptional activation

When tethered to a GAL4 DNA binding domain, the BRCT domains can activate transcription in yeast and mammalian systems (Chapman & Verma 1996, Monteiro et al. 1996, Haile & Parvin 1999). Significantly, potential targets of BRCA1 transcriptional regulation include the p53 responsive genes encoding p21 as well as GADD45 (Somasundaram et al. 1997, Harkin et al. 1999) suggesting that BRCA1 has a role in regulating DNA repair and checkpoint controls. The BRCT may modulate these functions through direct recruitment of the RNA polymerase holoenzyme (Scully et al. 1997, Anderson et al. 1998), however, the physiological significance of these effects and the precise

Table 4.1 Structure, function and disease effects of BRCT missense mutations

Mutant	Secondary Structure[a]	Mutant Class	Protease Sensitivity	Transcription[b] t/c (-) : no effect on transcription t/c (+): affects t/c	Disease effects[c] (+) linked to disease (-) not linked (?) unknown	Solubility and stability[d]
M1652I	β	Brct-fold	wt	t/c(-)	(-)	
D1692Y	c	Surface	T		(+)	Soluble
F1695L	c	Surface	wt		?	
V1696L	c	Surface	T		?	
C1697R	c	BRCA1-fold	TT	t/c (+)	(+)	
R1699W	c	Interface	T	t/c (-)	(+)	Soluble
R1699Q	c	Interface	wt	t/c (-)	?	
A1708E	α	Interface	TT	t/c (+)	(+)	Insoluble
S1715R	β	BRCA1-fold	TT	t/c (+)	(+)	
W1718C	α	Brct-fold	TT		?	
T1720A	α	Surface	wt		?	
G1738E	c	BRCA1-fold	TT	t/c (+)	(+)	Insoluble
G1738R	c	BRCA1-fold	TT		?	
P1749R	α	BRCA1-fold	TT		?	
R1751Q	α	BRCA1-fold	T		?	
A1752P	α	BRCA1-fold	TT		?	
I1766S	β	Brct-fold	TT		?	Insoluble
M1775R	c	Interface	T	t/c (+)	(+)	ΔΔG= 5.0 kcal/mol
M1783T	α	Interface	T		?	ΔΔG= 4.28kcal/mol
G1788V	c	Brct-fold	TT		?	Insoluble
V1804D	c	Surface	wt		?	
V1809F	β	Brct-fold	T		?	Soluble
W1837R	α	Brct-fold	TT		?	Insoluble
W1837G	α	Brct-fold	TT		?	Insoluble
Y1853C	α	Brct-fold	TT		?	

[a] Secondary structure is from the human BRCT domain structure (Williams et al. 2001)
[b] Transcription effects are those reported by Vallon-Christersson et al. 2001, Hayes et al. 2000, Worley et al. 2002, and Monteiro 1996.
[c] Disease linkage data is from recorded entries in the BIC, Vallon-Christersson et al. 2001, Hayes et al. 2000, and T.S. Frank, personal communication.
[d] Stabilities reported from Ekblad et. al 2002. The reported solubility in E. coli is from the study or Ekblad et. al 2002.

biochemical mechanism by which the BRCT activates transcription remain unclear (reviewed in Monteiro 2000). Nevertheless, this intrinsic activity forms the basis for a BRCA1 functional assay that has been used to probe for defects caused by several BRCT missense mutations (Vallon-Christersson et al. 2001, Hayes et al. 2000, Worley et al. 2002).

Comparison of the transcription and protease based assay data reveal a striking correlation between destabilizing phenotypes and transcriptional defects (Table 4.1). That is, less stable BRCT variants including the truncation mutants, C1697R, R1699W, A1708E, S1715R, G1738E, and M1775R disrupt transactivation function, whereas mutations with no effect on structure (M1652I and R1699Q) are fully active in these assays. Whether BRCT protein misfolding causes BRCA1 tumour suppressor inactivation via BRCA1 transcription function, DNA repair function, or both, has yet to be determined.

Conclusions

Greater than 60% of clinically relevant mutations delete a portion of or all of the BRCT domains, and the majority of BRCT missense alterations which target the 3 key classes of BRCT folding determinants (BRCT-fold, BRCA1-fold and Interface mutations) are destabilizing. It is apparent that BRCT destabilization or loss of function through truncation or missense substitution is sufficient to confer disease predisposition in carriers for these alleles. Such mutations are comparable to the subset of β-sandwich and zinc binding mutations that unfold the core DNA binding domain of the p53 tumour suppressor (reviewed in Bullock & Fersht 2001). Conversely, the p53 core domain mutation

database is largely populated by mutations that have little effect on stability, but directly target residues involved in sequence specific DNA binding. The identification of analogous cancer-associated mutations that are not destabilizing, but disrupt specific BRCT protein-protein or protein-DNA binding would provide strong support for the role of these interactions in mediating BRCA1 tumour suppressor function. To this end, two patient derived mutations (F1695L and V1696L) on the surface of the BRCT that affect BACH1 binding have recently been identified (Joo et. al. 2002). Further biochemical and structural characterization of these interactions will be necessary to confirm the nature of these defects.

We have established a set of protease-based criteria on which we can define the structural effects of mutation on the BRCT at the protein level. The early identification of carriers of potentially deleterious *BRCA1* alleles is an essential component of breast and ovarian cancer screening programs that facilitates detection, surveillance, and prevention of tumour growth. Further development of complementary methods that test the destabilizing and biological repercussions of missense variants will provide clinicians and researchers with important tools to unravel BRCA1 function and misfunction.

References:

Anderson, S. F., Schlegel, B. P., Nakajima, T., Wolpin, E. S., and Parvin, J. D. BRCA1 protein is linked to the RNA polymerase II holoenzyme complex via RNA helicase A. Nat Genet, 19: 254-6. 1998.

Bork, P., Hofmann, K., Bucher, P., Neuwald, A. F., Altschul, S. F., and Koonin, E. V. A superfamily of conserved domains in DNA damage-responsive cell cycle checkpoint proteins. FASEB J, 11(1): 68-76. 1997.

Bullock, A. N. and Fersht, A. R. Rescuing the function of mutant p53. Nat Rev Cancer, 1: 68-76, 2001.

Callebaut, I. and Mornon, J. P. From BRCA1 to RAP1: a widespread BRCT module closely associated with DNA repair. FEBS Lett, 400(1): 25-30. 1997.

Cantor, S. B., Bell, D. W., Ganesan, S., Kass, E. M., Drapkin, R., Grossman, S., Wahrer, D. C., Sgroi, D. C., Lane, W. S., Haber, D. A., and Livingston, D. M. Bach1, a novel helicase-like protein, interacts directly with brca1 and contributes to its dna repair function. Cell, 105(1): 149-60. 2001.

Carvalho, M. A., Billack, B., Chan, E., Worley, T., Cayanan, C., and Monteiro, A. N. Mutations in the BRCT Domain Confer Temperature Sensitivity to BRCA1 in Transcription Activation. Cancer Biol Ther, 1: 502-8. 2002.

Chapman, M. S. and Verma, I. M. Transcriptional activation by BRCA1. Nature, 382: 678-9. 1996.

Chen, K. S., Shepel, L. A., Haag, J. D., Heil, G. M., and Gould, M. N. Cloning, genetic mapping and expression studies of the rat Brca1 gene. Carcinogenesis, 17: 1561-6. 1996.

Couch, F. J. and Weber, B. L. Mutations and polymorphisms in the familial early-onset breast cancer (BRCA1) gene. Breast Cancer Information Core. Hum Mutat, 8: 8-18. 1996.

Deffenbaugh, A. M., Frank, T. S., Hoffman, M., Cannon-Albright, L., and Neuhausen, S. L. Characterization of common BRCA1 and BRCA2 variants. Genet Test, 6: 119-21. 2002.

Deng, C. X. and Brodie, S. G. Roles of BRCA1 and its interacting proteins. Bioessays, 22: 728-737. 2000.

Ekblad, C. M., Wilkinson, H. R., Schymkowitz, J. W., Rousseau, F., Freund, S. M., and Itzhaki, L. S. Characterisation of the BRCT domains of the breast cancer susceptibility gene product BRCA1. J Mol Biol, 320: 431-42. 2002.

Esnouf, R. M. An extensively modified version of MolScript that includes greatly enhanced coloring capabilities. J Mol Graph Model, 15: 132-4. 1997.

Esnouf, R. M. Further additions to MolScript version 1.4, including reading and contouring of electron-density maps. Acta Crystallogr D Biol Crystallogr, 55 : 938-40, 1999.

Friedman, L. S., Ostermeyer, E. A., Szabo, C. I., Dowd, P., Lynch, E. D., Rowell, S. E., and King, M. C. Confirmation of BRCA1 by analysis of germline mutations linked to breast and ovarian cancer in ten families. Nat Genet 8(4): 399-404. 1994.

Futreal, P. A., Liu, Q., Shattuck-Eidens, D., Cochran, C., Harshman, K., Tavtigian, S., Bennett, L. M., Haugen-Strano, A., Swensen, J., Miki, Y. and others. BRCA1 mutations in primary breast and ovarian carcinomas. Science, 266(5182): 120-2. 1994.

Haile, D. T. and Parvin, J. D. Activation of transcription in vitro by the BRCA1 carboxyl-terminal domain. J Biol Chem, 274(4): 2113-7. 1999.

Harkin, D. P., Bean, J. M., Miklos, D., Song, Y. H., Truong, V. B., Englert, C., Christians, F. C., Ellisen, L. W., Maheswaran, S., Oliner, J. D., and Haber, D. A. Induction of GADD45 and JNK/SAPK-dependent apoptosis following inducible expression of BRCA1. Cell, 97(5): 575-86. 1999.

Hayes, F., Cayanan, C., Barilla, D., and Monteiro, A. N. Functional assay for BRCA1: mutagenesis of the COOH-terminal region reveals critical residues for transcription activation. Cancer Res, 60: 2411-8. 2000.

Horton, R. M., Ho, S. N., Pullen, J. K., Hunt, H. D., Cai, Z., and Pease, L. R. Gene splicing by overlap extension. Methods Enzymol, 217: 270-9. 1993.

Huyton, T., Bates, P. A., Zhang, X., Sternberg, M. J., and Freemont, P. S. The BRCA1 C-terminal domain: structure and function. Mutat Res, 460: 319-332. 2000.

Imoto, T., Yamada, H., and Ueda, T. Unfolding rates of globular proteins determined by kinetics of proteolysis. J Mol Biol, 190: 647-9.1986.

Joo, W. S., Jeffrey, P. D., Cantor, S. B., Finnin, M. S., Livingston, D. M., and Pavletich, N. P. Structure of the 53BP1 BRCT region bound to p53 and its comparison to the Brca1 BRCT structure. Genes Dev, 16: 583-93. 2002.

Joukov, V., Chen, J., Fox, E. A., Green, J. B., and Livingston, D. M. Functional communication between endogenous BRCA1 and its partner, BARD1, during Xenopus laevis development. Proc Natl Acad Sci U S A, 98: 12078-83. 2001.

Li, S., Chen, P. L., Subramanian, T., Chinnadurai, G., Tomlinson, G., Osborne, C. K., Sharp, Z. D., and Lee, W. H. Binding of CtIP to the BRCT repeats of BRCA1 involved in the transcription regulation of p21 is disrupted upon DNA damage. J Biol Chem, 274(16): 11334-8. 1999.

Ludwig, T., Fisher, P., Ganesan, S., and Efstratiadis, A. Tumorigenesis in mice carrying a truncating Brca1 mutation. Genes Dev, 15: 1188-93. 2001.

Miki, Y., Swensen, J., Shattuck-Eidens, D., Futreal, P. A., Harshman, K., Tavtigian, S., Liu, Q., Cochran, C., Bennett, L. M., Ding, W. and others. A strong candidate for the breast and ovarian cancer susceptibility gene BRCA1. Science, 266(5182): 66-71. 1994.

Monteiro, A. N. BRCA1: exploring the links to transcription. Trends Biochem Sci, 25: 469-74. 2000.

Monteiro, A. N., August, A., and Hanafusa, H. Evidence for a transcriptional activation function of BRCA1 C-terminal region. Proc Natl Acad Sci U S A, 93(24): 13595-9. 1996.

Monteiro, A. N., August, A., and Hanafusa, H. Common BRCA1 variants and transcriptional activation. Am J Hum Genet, 61: 761-2. 1997.

Nathanson, K. L., Wooster, R., Weber, B. L., and Nathanson, K. N. Breast cancer genetics: what we know and what we need. Nat Med, 7: 552-6. 2001.

Pedersen, J. S., Otzen, D. E., and Kristensen, P. Directed evolution of barnase stability using proteolytic selection. J Mol Biol, 323: 115-23. 2002.

Scully, R., Anderson, S. F., Chao, D. M., Wei, W., Ye, L., Young, R. A., Livingston, D. M., and Parvin, J. D. BRCA1 is a component of the RNA polymerase II holoenzyme. Proc Natl Acad Sci U S A, 94: 5605-10. 1997.

Scully, R., Ganesan, S., Vlasakova, K., Chen, J., Socolovsky, M., and Livingston, D. M. Genetic analysis of BRCA1 function in a defined tumor cell line. Mol Cell, 4: 1093-9. 1999.

Scully, R. and Livingston, D. M. In search of the tumour-suppressor functions of BRCA1 and BRCA2. Nature, 408: 429-32. 2000.

Sharan, S. K., Wims, M., and Bradley, A. Murine Brca1: sequence and significance for human missense mutations. Hum Mol Genet, 4: 2275-8, 1995.

Shattuck-Eidens, D., McClure, M., Simard, J., Labrie, F., Narod, S., Couch, F., Hoskins, K., Weber, B., Castilla, L., Erdos, M. and others. A collaborative survey of 80 mutations in the BRCA1 breast and ovarian cancer susceptibility gene. Implications for presymptomatic testing and screening. JAMA, 273: 535-41. 1995.

Shen, D. and Vadgama, J. V. BRCA1 and BRCA2 gene mutation analysis: visit to the Breast Cancer Information Core (BIC). Oncol Res, 11(2): 63-9. 1999.

Sieber, V., Pluckthun, A., and Schmid, F. X. Selecting proteins with improved stability by a phage-based method. Nat Biotechnol, 16: 955-60. 1998.

Sodeoka, M. Larson C. J. Chen L. Leclair K. P. and Verdine G. L. A multifunctional plasmid for protein expression by ECPCR: overproduction of NF-kB p50 DNA-binding subunit. Bioorg. Med. Chem. Lett 3: 1089. 1993.

Somasundaram, K., Zhang, H., Zeng, Y. X., Houvras, Y., Peng, Y., Zhang, H., Wu, G. S., Licht, J. D., Weber, B. L., and El-Deiry, W. S. Arrest of the cell cycle by the tumour-suppressor BRCA1 requires the CDK-inhibitor p21WAF1/CiP1. Nature, 389 (6647): 187-190. 1997.

Vallon-Christersson, J., Cayanan, C., Haraldsson, K., Loman, N., Bergthorsson, J. T., Brondum-Nielsen, K., Gerdes, A. M., Moller, P., Kristoffersson, U., Olsson, H., Borg, A., and Monteiro, A. N. Functional analysis of BRCA1 C-terminal missense mutations identified in breast and ovarian cancer families. Hum Mol Genet, 10: 353-60. 2001.

Venkitaraman, A. R. Cancer susceptibility and the functions of BRCA1 and BRCA2. Cell, 108: 171-82, 2002.

Wang, L. and Kallenbach, N. R. Proteolysis as a measure of the free energy difference between cytochrome c and its derivatives. Protein Sci, 7: 2460-4. 1998.

Williams, R. S. and Glover, J. N. Structural Consequences of a Cancer-causing BRCA1-BRCT Missense Mutation. J Biol Chem, 278: 2630-5. 2003.

Williams, R. S., Green, R., and Glover, J. N. Crystal structure of the BRCT repeat region from the breast cancer- associated protein BRCA1. Nat Struct Biol, 8: 838-842. 2001.

Worley, T., Vallon-Christersson, J., Billack, B., Borg, A., and Monteiro, A. N. A Naturally Occurring Allele of BRCA1 Coding for a Temperature- Sensitive Mutant Protein. Cancer Biol Ther, 1: 497-501. 2002.

Yarden, R. I. and Brody, L. C. BRCA1 interacts with components of the histone deacetylase complex. Proc Natl Acad Sci U S A 96(9), 4983-8. 1999.

Yu, X., Wu, L. C., Bowcock, A. M., Aronheim, A., and Baer, R. The C-terminal (BRCT) domains of BRCA1 interact in vivo with CtIP, a protein implicated in the CtBP pathway of transcriptional repression. J Biol Chem, 273: 25388-92. 1998.

Zhang, X., Morera, S., Bates, P. A., Whitehead, P. C., Coffer, A. I., Hainbucher, K., Nash, R. A., Sternberg, M. J., Lindahl, T., and Freemont, P. S. Structure of an XRCC1 BRCT domain: a new protein-protein interaction module. EMBO J, 17(21):6404-11. 1998.

Chapter 5:

General Discussion and Conclusions

BRCT mediated protein-protein interactions

The family of BRCT containing protein structures has recently grown to include the crystal structures of the XRCC1 C-terminal BRCT repeat (Zhang et al. 1998), the dual repeat BRCT domains of the human (Williams et al. 2001) and rat (Joo et al. 2002) BRCA1 proteins, a complex of p53 with the BRCT repeats of 53BP1 (Joo et al. 2002), and the NMR structure of the DNA Ligase 3 BRCT (Krishnan et al. 2001) (Fig. 5.1). In addition, a structure of a BRCT linker of DNA Ligase 4, bound to XRCC4 has been solved (Sibanda et al. 2001). These advances have unveiled the molecular determinants of BRCT folding. Structural examples of intramolecular BRCT-BRCT, intermolecular BRCT-BRCT and intermolecular BRCT-nonBRCT modes of interaction illustrate the molecular versatility of these highly adaptable protein-ligand binding modules.

Structural conservation of the BRCT fold

Identified through sequence-based methods, the BRCT protein fold superfamily is defined by a conserved BRCT hydrophobic clustering signature (Bork et al. 1997, Callebaut & Mornon 1997). These studies hypothesized a central β-sheet structure with an amino and a carboxyl-terminal α-helix (Bork et al. 1997). Superposition of the structures of individual BRCT domains that have been solved to date confirm these early predictions and show that high structural conservation amongst the BRCTs is found for the β-sheet, helix α3, and the C-terminal base of α1 (Fig. 5.2). Strikingly, the regions of structural conservation closely follow the hydrophobic conservation in the primary structure for the

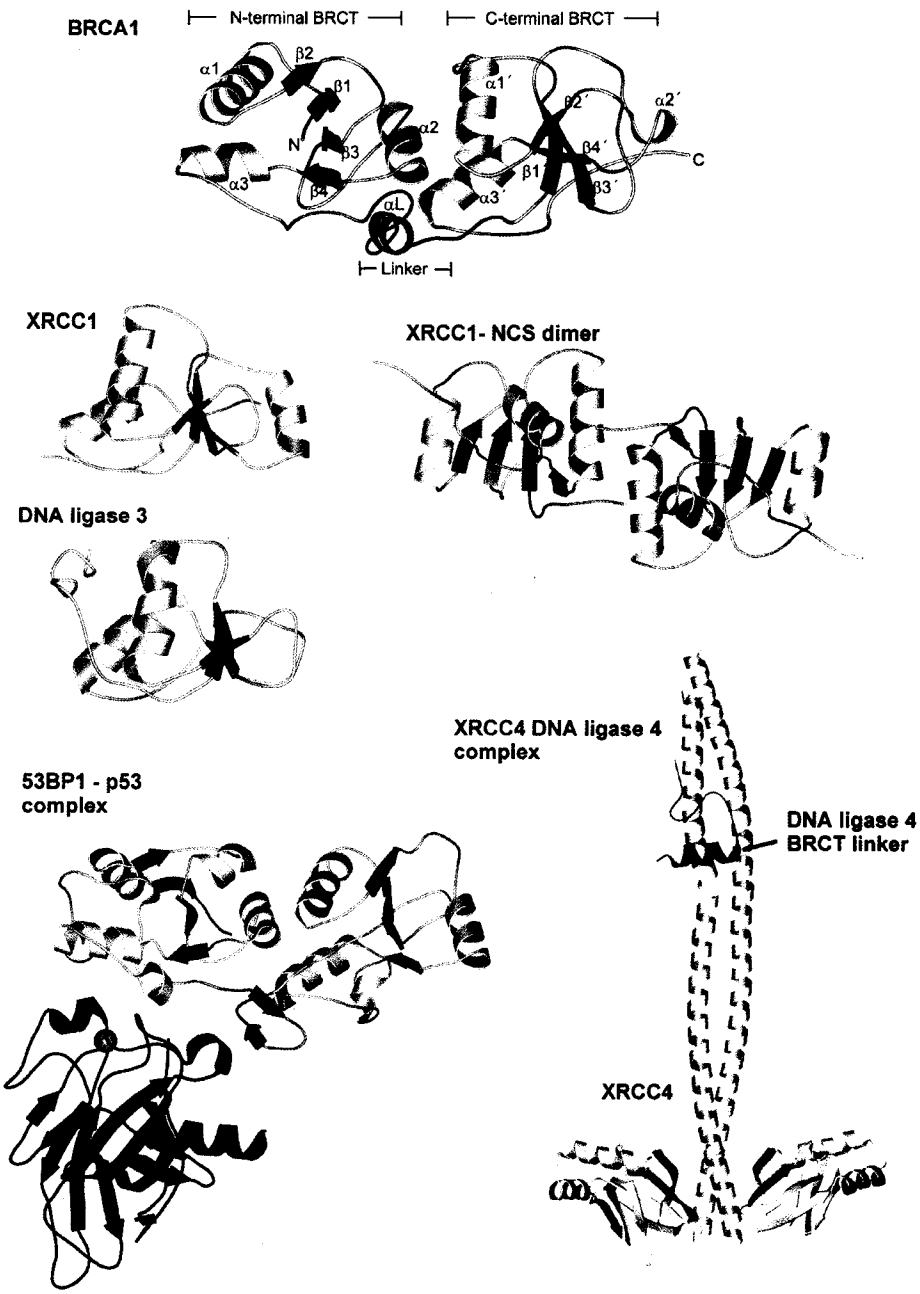

Figure 5.1. Structures of BRCT and BRCT-linker containing proteins and protein complexes.

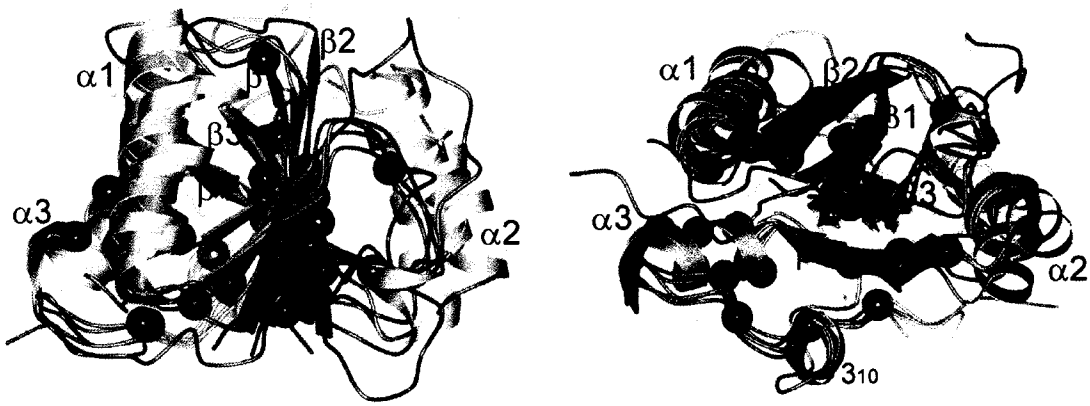

Figure 5.2. Least squares overlay of individual BRCT domains. The individual BRCT domain structures were overlayed using O. Red spheres mark the positions of conserved BRCT hydrophobes within the N-terminal BRCT domain of BRCA1.

protein family. This observation highlights the importance of the conserved BRCT hydrophobes in dictating the fold of an individual BRCT. Indeed, several patient isolated BRCA1 variants mutate these positions and are highly destabilizing (Fig. 4.5).

Intramolecular BRCT-BRCT interactions

The determination of the structure of the BRCT-repeat from 53BP1 confirmed our hypothesis that the intramolecular mode of BRCT-BRCT contact in this protein is similar to the BRCA1-BRCT repeat interactions (Joo et al. 2002). A structural overlay of the rat and human BRCA1-BRCT domains with the 53BP1-BRCT highlights the conservation of this pack (Williams et al. 2001, Joo et al. 2002) (Fig. 5.3a). The core of this interaction is formed by extensive hydrophobic packing of α2 (from the N-terminal repeat) with the α1' and α3' from the C-terminal repeat. Other contacts across the BRCT interface come from variable structures formed by BRCT linker domains at the base of the helical bundle.

In many respects these three helix bundles resemble a slice through a heterotrimeric coiled-coil. The tilt angles between helices deviate from those observed in trimeric coiled-coil structures (Harbury et al. 1994, Nautiyal & Alber 1999), but the helicies do pack via a knobs-in-holes arrangement. Specificity of the α2-α1'/α3' pack by salt bridging interactions between side chains found on the outside of the helical bundle, at positions analagous to trimeric coiled-coil "e-g" residues (Fig. 5.3 b) can occur. For instance, in 53BP1, R1813 (on α2) salt bridges to E1890 on helix α1'. Additional specificity likely comes from these

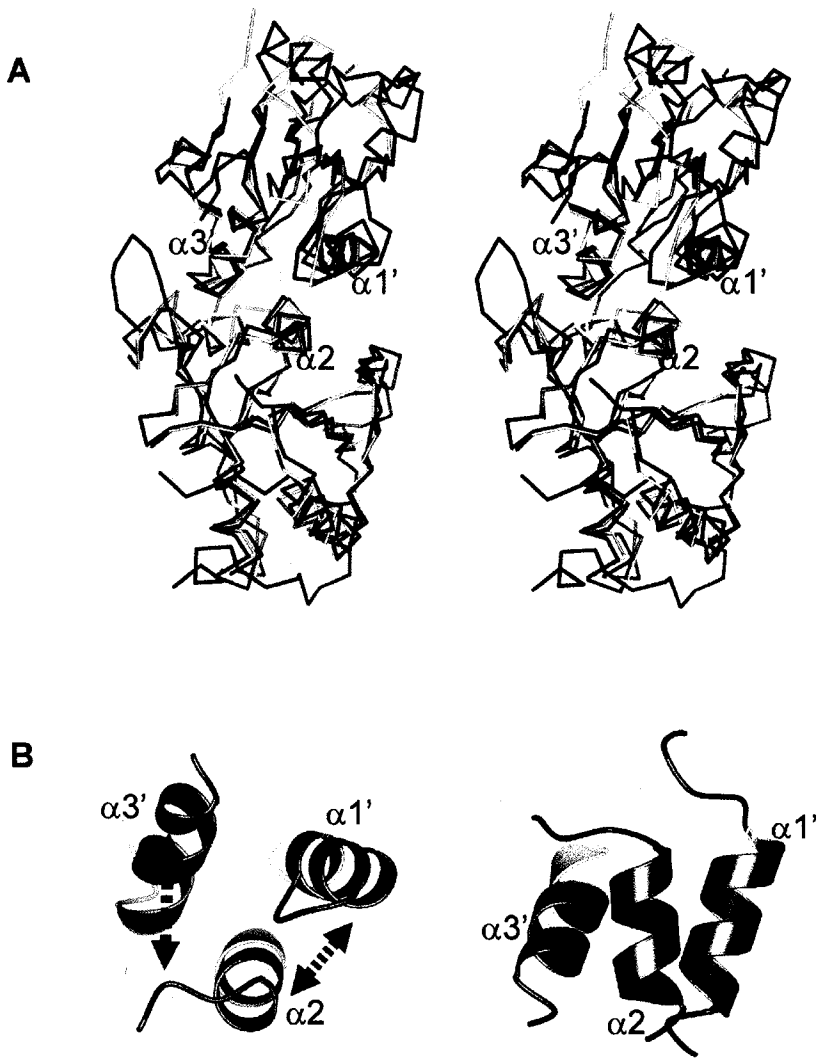

Figure 5.3. Conservation of the BRCT dual repeat structure. A. Stereoview of a least squares overlay of the dual BRCT repeats from human BRCA1 (gold), rat BRCA1 (green) and human 53BP1 (red). Highly conserved regions of the structures are found at the inter-BRCT repeat interface. **B.** A three helix bundle pack forms the conserved core of the dual repeat interface interactions. Orthogonal views are shown. The core of these interactions is formed by hydrophobic packing, but complementary electrostatic pairing (indicated by arrows) may help define specificities of BRCT-BRCT packing.

interactions is in part achieved through complementary van der Waals or paired ionic interactions between exposed side chains on the α3' helix, and residues on a surface exposed loop which precedes α2. For example, R1699 in human BRCA1 salt bridges to E1836 and D1840, and R1811 in 53BP1 salt bridges with E1945. For proteins with multiple BRCT domains, one might envisage long rod-like structures composed of chains of BRCT domains with repeated α2-α1'/α3' packing between the individual BRCTs.

The role of BRCT linkers in intermolecular BRCT-non BRCT interactions

The BRCT linker regions of tandem repeat BRCT domains are highly variable in size, but lengths of 0 to 5, or 18 to 24 residues appear to be favored (Huyton et al. 2000). The sequences and structures of the linkers are also variable and have been shown to adopt α-helical (BRCA1 linker), β-sheet (53BP1 linker), or mixed α–β structures (DNA ligase 4 linker). For the 53BP1-p53 (Joo et al. 2002) and XRCC4-DNL4 (Sibanda et al. 2001) complexes, these motifs directly participate in protein-protein contacts (Fig. 5.1). The BRCT repeat scaffold appears to provide a surface for the evolution and formation of unique structures in the BRCT linkers that are involved in protein-ligand binding. These hypervariable linker structures and the divergent surfaces of the BRCTs are thus key determinants of the functional diversity of members of the BRCT superfamily.

A modeled BRCT-BRCT intermolecular interaction

XRCC1 acts as a protein scaffold in the mammalian base excision repair (BER) pathway. The carboxyl terminal BRCT of XRCC1 partners with the BRCT of DNA Ligase 3. X-ray (XRCC1) and NMR (DNL3) methods have been used to

determine the structures of these domains in isolation (Zhang et al. 1998, Krishnan et al 2002) (Fig. 5.1). Both of these proteins homo and heterodimerize in solution (Krishnan et al. 2001), and two alternative forms of intramolecular homodimerization have been observed in as many crystal forms of XRCC1 (Zhang et al. 1998, Huyton et al. 2000). In one form, shown in Fig. 5.1, the XRCC1 non-crystallographic dimer makes end on end contacts via helix α1, and it has been suggested that this is how XRCC1 and DNL3 also interact (Zhang et al. 1998). Mutagenesis and modeling studies support this model for the heterodimer (Dulic et al. 2001), but this conclusion has been disputed (Krishnan et al. 2001) since in solution the XRCC1 and DNL3 BRCTs apparently can form heterotetramers, and this is inconsistent with the notion that the homo and heterodimer surfaces are the same. Notably, it is unlikely that this BRCT-BRCT contact could be achieved through an α2 – α1'α3' arrangement as the exposed faces of these helices on XRCC1 and DNL3 are largely populated with charged residues. An X-ray or high resolution NMR structure of this complex should resolve these issues, and provide another interesting example of BRCT directed protein interaction.

BRCA1 Ligand Interactions

The plethora of nuclear functions ascribed to BRCA1 has made it difficult to pinpoint a precise, relevant biochemical function for the full-length protein and for the isolated BRCT domains. Evidence suggests the BRCT repeats interact with DNA structure and/or proteins involved in transcriptional activation. What clues can BRCT structural data give us about the nature of these interactions?

BRCA1 interacts with RNA polymerase II

The co-purification of BRCA1 with the RNA polymerase holoenzyme pointed to BRCA1 as having a possible role in transcriptional regulation (Scully et al. 1997). When fused with a GAL4 DNA binding domain, the BRCTs can activate transcription of a reporter gene in yeast and mammalian cells (Fig.1.10) (reviewed in Monteiro 2000). The minimal transactivation domain of the BRCT was mapped to include the highly acidic C-terminal BRCA1-BRCT (aa 1760-1863) (Monteiro et al. 1996) (Fig. 5.1). Direct evidence showing gene specific targeting of this BRCA1 mediated transcriptional activation function has yet to be demonstrated, and the relevance of this activity remains a subject of debate. The interaction with the polymerase may be indirect, through binding to the RNA-Polymerase II associated helicase, RHA (RNA helicase A) (Anderson et al. 1998). However, biochemical studies with a purified mammalian transcription *in vitro* system that lacks a helicase component, have provided support for a more direct interaction of the BRCTs with conserved components of the multi-subunit eukaryotic RNA polymerase II (Schlegel et al. 2000). The BRCTs can directly interact with polymerase in fusion protein pull-down experiments, and BRCT mediated transactivation in this system could be attenuated by titration of the transcription reactions with purified GST-fusions of two of the RNA polymerase II subunits, Rpb10α, and a portion of large polymerase subunit Rpb2. The ~7 KDa Rpb10 protein, in combination with Rpb3/Rpb11/Rpb12, helps form a sub-complex of the core polymerase that is thought to regulate assembly of the structure (Cramer et al. 2001). Since a portion of Rpb10 is exposed on the

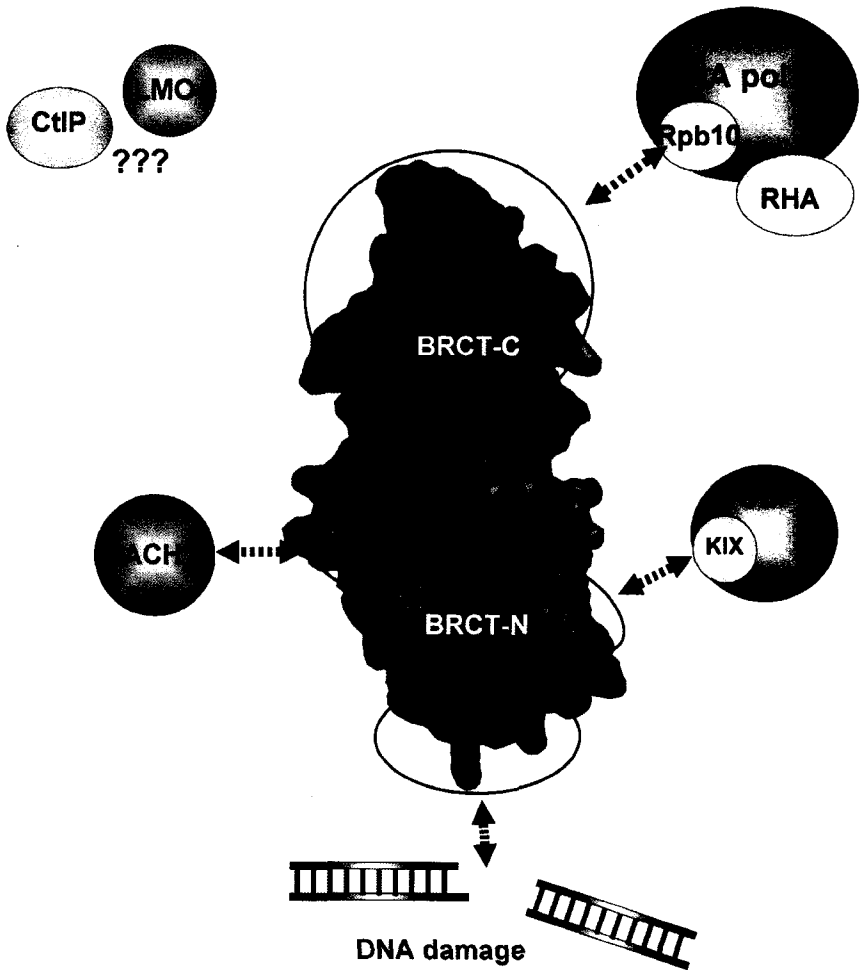

Figure 5.4. BRCA1-BRCT protein-protein interactions. An electrostatic surface representation is for the human BRCA1-BRCT repeat is shown. Proposed protein-protein and protein-DNA interaction surfaces are indicated.

surface of the polymerase, it is conceivable that this site represents a primary BRCT contact region (Fig. 5.4).

Binding to the transcriptional coactivator CBP

The CBP/p300 (CREB binding protein) transcriptional coactivator is a ~300 kDa multi-domain protein that harbors a histone acetyl-transferase domain (HAT) and a battery of protein-protein interaction modules (reviewed in Chan & La Thangue 2001, McManus & Hendzel 2001). Recruitment of the CBP HAT activity to promoters via interactions with sequence specific binding proteins has been shown to augment transcriptional activation. Transient transfection assays in mammalian cells show that CBP binding to the BRCT domain increases the transactivation activity of a GAL4-BRCT fusion (Pao et al. 2000). A direct interaction between the BRCT domains and a fragment of CBP that contains the structurally characterized CREB interaction domain (KIX) has been reported (Cui et al. 1998, Pao et al. 2000). The KIX domain itself is capable of binding a variety of peptide motifs, the best characterized of which is the phosphorlyation dependant interaction with the CREB KID transcriptional activation domain (Chrivia et al. 1993, Parker et al. 1996, Radhakrishnan et al. 1997). Recent structural data have helped define a new class of KIX interacting sequences that are conserved in MLL (Mixed lineage leukemia)-related proteins (Ernst et al. 2001, Goto et al. 2002). The BRCT contains this motif and the functionally relevant hydrophobes of this sequence are solvent accessible and form a continuous surface of helix α1 of the N-terminal BRCT domain (Fig. 5.4). Thus, this site may contribute to KIX domain binding.

Association of the BRCT with damaged DNA structures

An electrostatic surface potential of the BRCA1-BRCT repeat shows the charge distribution on the molecule is reminiscent of a bar magnet, with marked positive and negative dipoles at the amino and carboxyl terminal ends (Fig. 5.4). DNA end binding interactions reported for the BRCT (Yamane & Tsuruo 1999) are likely directed by the N-terminal positively charged end of the protein.

BACH1 binding

BRCA1 interacts *in vivo* and *in vitro* with the BACH1 (BRCA1 associated helicase) helicase and patient isolated BACH1 mutations are linked with breast cancer (Cantor, Bell, et al. 2001). Since BRCA1 and BACH1 mutant cell lines display similar delayed kinetics of double strand break repair, it is thought these proteins act together in a common DNA repair pathway, but little is known of the mechanism of this process. Mutagenesis and GST-pulldown experiments have mapped a putative BACH1 binding site on the BRCT and patient derived BRCA1 mutations disrupt this binding (Joo, Jeffrey, et al. 2002) (Fig. 5.4).

Other BRCT interactions

Other proteins including the CtBP associated transcriptional corepressor CtIP (Yu et al. 1998, Li et al. 1999) and the LIM-only protein LMO4 (Sum et al. 2002) appear to regulate BRCT transactivation. Possibly, these proteins may block the direct recruitment of RNA polymerase II by BRCA1. In one proposed model, which has been disputed (Wu-Baer and Baer, 2001), a BRCA1-CtIP complex is found to persist in cells under benign conditions. Ionizing radiation causes the ATM dependant hyper-phosphorylation of CtIP and this event

liberates BRCA1 from a physical association with CtIP (Li et al. 2000). It is thought that BRCA1 can then act in a transcriptional or repair capacity.

The proposed interaction sites for DNA, CBP, BACH1 and the core RNA polymerase are not mutually exclusive, consistent with a role for the BRCT as a multi-ligand scaffold. A full understanding of how these interactions mediate BRCA1 cellular functions awaits the biochemical and structural dissection of BRCT containing protein-protein or protein-DNA complexes. Structure based design of mutations that disrupt specific BRCA1 protein-ligand interactions, but do not destabilize the protein would provide researchers with useful tools to prove or disprove the relevance of these interactions to BRCA1-mediated tumor-suppressor function.

Understanding and detecting BRCA1 mutations

Direct sequencing of *BRCA1* intronic and exonic sequences by Myriad Genetics Inc. (Salt Lake City - USA) has become the *de facto* industry standard for the identification of *BRCA1* mutant alleles (Frank, 1999). Although these automated sequencing methods are highly sensitive and detect the majority of known BRCA1 mutation classes, they are incapable of sensing many large genetic deletions and rearrangements that may represent a significant fraction of familial *BRCA1* mutations (Petrij-Boschet al. 1997, Gad et al. 2001). The Breast Cancer Information Core database is therefore biased to include mutations detected by sequencing methods, and the frequency of occurrence of large-scale genetic alterations within the population is thus unknown. These technical

deficiencies and the relatively high cost of Myriad Genetics' services have spurred worldwide opposition to the companies controversial patent protected monopoly of the development and application of *BRCA1* genetic screening technologies (Lecrubier 2002, Benowitz 2003). However, the screening service provided by Myriad, and the corporation's open dissemination of mutation data, have made significant contributions to the growth of the BIC database and our understanding of *BRCA1* population genetics.

All BRCA1 protein truncating mutations caused by frameshift and nonsense mutations are clearly disease predisposing (Futreal et al. 1994, Couch & Weber 1996, Shen & Vadgama 1999). Conversely, knowledge of the cancer causing potential of single amino acid *BRCA1* substitutions has been limited to a small set of mutations for which pedigree data is available that clearly links the variant to disease. The subtle nature of missense mutations and the absence of a tractable, high throughput, measure of BRCA1 function has precluded analysis of the genetic and biochemical affects of these alterations. However, recent structural and biochemical approaches have provided important insights into the possible effects of missense substitutions that represent more than 1/4 of all recorded BIC *BRCA1* mutations. Studies have focused on the conserved N-terminal RING and C-terminal BRCT repeat domains.

N-terminal RING domain mutations BRCA1 binds to BARD1 (BRCA1 associated ring domain protein) and this interaction enhances a ubiquitin ligase activity of the heterodimer (Wu et al. 1996, reviewed in Baer & Ludwig 2002). The NMR structure of a complex of the BRCA1/BARD1 RING domains has been

solved, providing structural insight into nature of these interactions (Brzovic et al. 2001). A large number of missense mutations map to the interface between the BARD1 and BRCA1, and these alterations may thus disrupt heterodimer formation. Frequently recorded cancer-associated mutants target zinc-coordinating residues that help form the core scaffold of the RING domain fold. For two of these mutants (C61A and C61G), localized structural destabilization of a loop close to the zinc-binding site in the protein may hinder binding to the ubiquitin-conjugating enzyme UbcH7 (Brzovic et al. 2001). Other mutations affect surface regions and may inhibit additional protein-protein interactions the RING domain participates in. At least one cancer-associated missense substitution (C61G) inhibits the BARD1/BRCA1 ubiquitin lyase activity (Hashizume et al. 2001). The development of methods to quantitatively measure this activity will help to classify the effects of other RING domain missense mutations.

C-terminal BRCT mutations

Mutations that target the fold determinants of BRCT domains or residues that mediate BRCT-BRCT interactions in the BRCA1 tumour suppressor disrupt protein folding (Williams et al. 2001). The observation that the BRCA1 BRCT domains form a proteolytically resistant domain, and that cancer predisposing BRCT variants (but not benign single amino acid substitutions) have compromised stability, indicates that a protease-based screen for mutant BRCT conformations could be incorporated into routine BRCA1 screening protocols.

The protease-based assay we have used tests the stability of BRCT domains expressed in commercially available reticulocyte lysates. These lysates

are employed in Protein Truncation Test (PTT) genetic screens which have been used for detecting BRCA1 mutations (Shattuck-Eidens et al. 1995, Petrij-Bosch et al. 1997, Vossen 1999). In this method, patient isolated RNA is reverse transcribed to generate a cDNA that is then amplified using oligonucleotides that target a coding region of the protein that is to be tested for protein truncating effects. The cDNA message is then transcribed/translated and radiolabelled within the lysate, and the presence of truncated protein product is visualized by SDS-PAGE. Though effective at detecting frameshifts, nonsense and deletion mutations that lead to truncation of the expressed protein message, this technique is incapable of identifying missense substitutions.

An adaptation of the PTT, where a protease digestion step is added could, in principle, be appropriate for the detection of the large majority of cancer-associated BRCT mutations (Fig. 5.5, Table 5.1). Here, oligonucleotides would be specifically designed to amplify BRCT coding sequence (aa 1646-1863) from patient samples, and the translation step would be followed by a trypsinolysis series (Fig. 5.5a). This test would have the distinct advantage of sensing the protein destabilizing effects of both missense and truncation mutations. Conservative estimates indicate it could detect as much as 80% of the cancer-associated BRCT mutations (Table 5.1). The general application of this PTST (Protein Truncation and Stability Test) assay does not seem practical since it would only detect approximately 15% of all BRCA1 mutations recorded in the BIC (Table 5.1). Alternatively, a more pragmatic use of the protease screen that would be exclusively for missense mutations would involve PCR generation

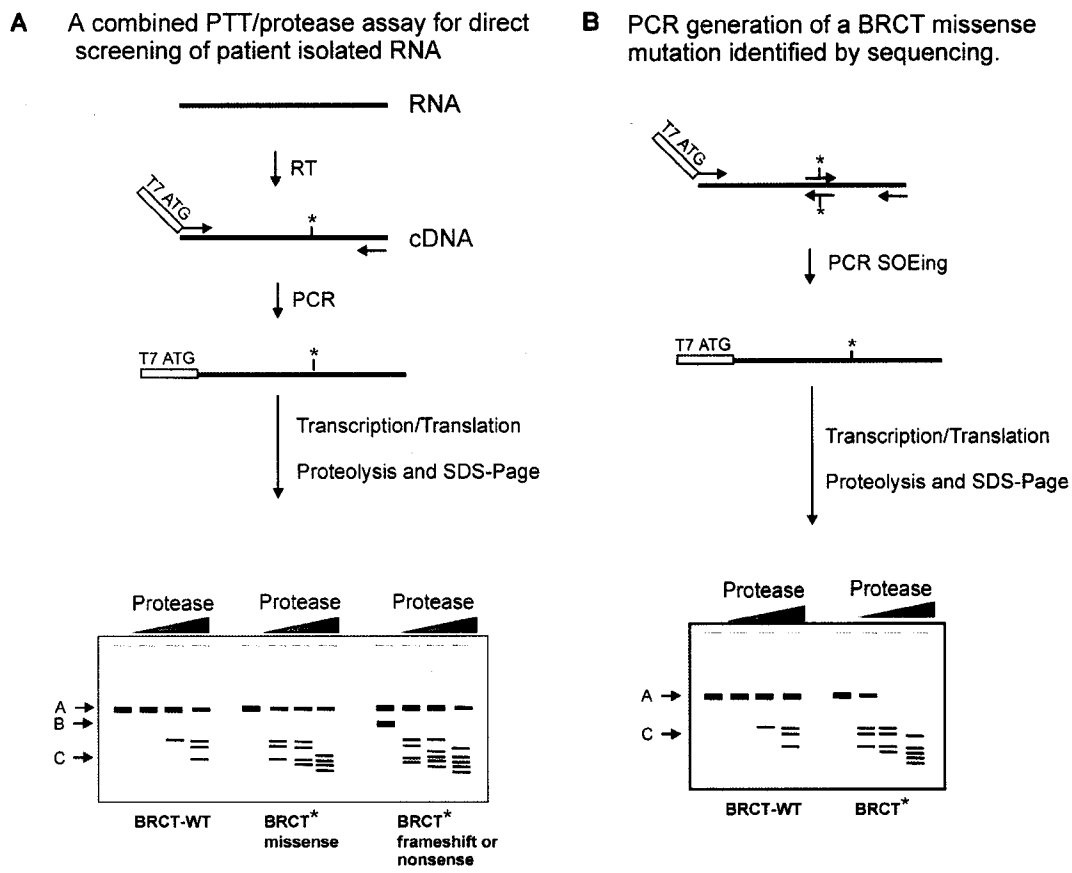

Figure 5.5. Proposed application of BRCT protease susceptibility assays in BRCA1 screening protocols. A. The commonly used protein truncation test could be modified to include a protease digestion step. This method typically generates coding sequence (and protein) from both alleles in an individual. In the case of a heterozygote carrier for missense mutation, highly destabilizing mutants would result in a 50% reduction in protein amounts of the BRCT. The quantitative nature of the protease susceptibility assay would allow one to monitor the disappearance of protein species "A". Proteolytic fragments (species "C") are also generated in a predictable manner for the wild type protein. Greater sensitivity for the assay could thus be achieved by monitoring the ratio of protein species C/A. For truncating mutations, truncated protein products ("B") are produced that would be rapidly degraded by protease. **B.** BRCT missense mutations identified by sequencing could be generated by PCR and transcribed directly from PCR products, eliminating the need for a cloning step (as in Fig. 4.1).

Table 5.1 Mutations in Exons encoding the BRCT domains of BRCA1

Exon † → / Mutation Type	17	18	19	20	21	22	23	24	Total	% of Total (BRCT)	% Total (BRCA1)
Framshift	21	13	25	545	6	49	2	19	680	56.0*	10.2*
In Frame Deletion	6	2	1	2	0	0	1	0	12	1.0	0.2
Missense	19	59	11	31	24	24	21	16	195	16.0*	2.9*
Nonsense	1	20	7	16	0	8	5	45	102	8.4*	1.5*
Polymorphism	7	13	0	5	0	7	0	6	38	3.1	0.6
Splice variant	14	13	16	43	6	6	8	13	119	9.8	1.7
Unclassified	8	5	4	35	3	8	0	6	69	5.7	1.0

† Exon 16 mutations were excluded as this region includes coding sequence for residues N-terminal to residue 1646.
* Cancer causing BRCT mutations that would be detected using a protease-based assay.

of the coding sequence for variants previously identified by sequencing (Fig 5.5b). Direct transcription/translation from the PCR product, followed by protein digestion, would provide a quick, relatively inexpensive test for mutant BRCT conformations.

Conclusions

Significant advances in the understanding of BRCA1 structure/function have been made in the nine years since the initial discovery of this highly penetrant breast cancer susceptibility gene. The biological function of BRCA1 remains somewhat enigmatic, and future work should be directed towards elucidation of the molecular details of BRCA1 mediated protein-protein interaction networks, and how mutations disrupt these interactions. The development of automated methods that increase the speed at which protein structures can be solved will facilitate the use of multidisciplinary approaches to tackle this interesting and complicated biological system. Certainly, basic biochemical and X-ray crystallographic studies of the BRCT domain of the protein have provided seminal insights into the molecular mechanism of inactivation of this tumour suppressor gene. The translation of such observations into tools that can be used to predict and detect the effects of familial mutations should help clinicians assess the risks associated with BRCA1 variants found in the general population.

References

Anderson, S. F., Schlegel, B. P., Nakajima, T., Wolpin, E. S., and Parvin, J. D. BRCA1 protein is linked to the RNA polymerase II holoenzyme complex via RNA helicase A. Nat Genet, 19: 254-6. 1998.

Baer, R. and Ludwig, T. The BRCA1/BARD1 heterodimer, a tumor suppressor complex with ubiquitin E3 ligase activity. Curr Opin Genet Dev, 12: 86-91, 2002.

Benowitz, S. European groups oppose Myriad's latest patent on BRCA1. J Natl Cancer Inst, 95: 8-9, 2003.

Bork, P., Hofmann, K., Bucher, P., Neuwald, A. F., Altschul, S. F., and Koonin, E. V. A superfamily of conserved domains in DNA damage-responsive cell cycle checkpoint proteins. FASEB J, 11(1): 68-76. 1997.

Brzovic, P. S., Meza, J. E., King, M. C., and Klevit, R. E. BRCA1 RING domain cancer-predisposing mutations. Structural consequences and effects on protein-protein interactions. J Biol Chem, 276: 41399-406, 2001.

Brzovic, P. S., Rajagopal, P., Hoyt, D. W., King, M. C., and Klevit, R. E. Structure of a BRCA1-BARD1 heterodimeric RING-RING complex. Nat Struct Biol, 8: 833-7, 2001.

Callebaut, I. and Mornon, J. P. From BRCA1 to RAP1: a widespread BRCT module closely associated with DNA repair. FEBS Lett, 400(1): 25-30. 1997.

Cantor, S. B., Bell, D. W., Ganesan, S., Kass, E. M., Drapkin, R., Grossman, S., Wahrer, D. C., Sgroi, D. C., Lane, W. S., Haber, D. A., and Livingston, D.

M. Bach1, a novel helicase-like protein, interacts directly with brca1 and contributes to its dna repair function. Cell, 105(1): 149-60. 2001.

Chan, H. M. and La Thangue, N. B. p300/CBP proteins: HATs for transcriptional bridges and scaffolds. J Cell Sci, 114: 2363-73. 2001.

Chrivia, J. C., Kwok, R. P., Lamb, N., Hagiwara, M., Montminy, M. R., and Goodman, R. H. Phosphorylated CREB binds specifically to the nuclear protein CBP. Nature, 365: 855-9. 1993.

Couch, F. J. and Weber, B. L. Mutations and polymorphisms in the familial early-onset breast cancer (BRCA1) gene. Breast Cancer Information Core. Hum Mutat, 8: 8-18. 1996.

Cramer, P., Bushnell, D. A., and Kornberg, R. D. Structural basis of transcription: RNA polymerase II at 2.8 angstrom resolution. Science, 292: 1863-76. 2001.

Cui, J. Q., Shao, N., Chai, Y., Wang, H., Reddy, E. S., and Rao, V. N. BRCA1 splice variants BRCA1a and BRCA1b associate with CBP co-activator. Oncol Rep, 5: 591-5. 1998.

Dulic, A., Bates, P. A., Zhang, X., Martin, S. R., Freemont, P. S., Lindahl, T., and Barnes, D. E. BRCT Domain Interactions in the Heterodimeric DNA Repair Protein XRCC1-DNA Ligase III. Biochemistry, 40(20): 5906-5211. 2001.

Ernst, P., Wang, J., Huang, M., Goodman, R. H., and Korsmeyer, S. J. MLL and CREB bind cooperatively to the nuclear coactivator CREB-binding protein. Mol Cell Biol, 21: 2249-58. 2001.

Frank, T. S. Laboratory determination of hereditary susceptibility to breast and

ovarian cancer. Arch Pathol Lab Med, 123: 1023-6. 1999.

Futreal, P. A., Liu, Q., Shattuck-Eidens, D., Cochran, C., Harshman, K., Tavtigian, S., Bennett, L. M., Haugen-Strano, A., Swensen, J., Miki, Y. and others. BRCA1 mutations in primary breast and ovarian carcinomas. Science, 266(5182): 120-2. 1994.

Gad, S., Scheuner, M. T., Pages-Berhouet, S., Caux-Moncoutier, V., Bensimon, A., Aurias, A., Pinto, M., and Stoppa-Lyonnet, D. Identification of a large rearrangement of the BRCA1 gene using colour bar code on combed DNA in an American breast/ovarian cancer family previously studied by direct sequencing. J Med Genet, 38: 388-92. 2001.

Goto, N. K., Zor, T., Martinez-Yamout, M., Dyson, H. J., and Wright, P. E. Cooperativity in transcription factor binding to the coactivator CREB-binding protein (CBP). The mixed lineage leukemia protein (MLL) activation domain binds to an allosteric site on the KIX domain. J Biol Chem, 277: 43168-74, 2002.

Harbury, P. B., Kim, P. S., and Alber, T. Crystal structure of an isoleucine-zipper trimer. Nature, 371: 80-3. 1994.

Hashizume, R., Fukuda, M., Maeda, I., Nishikawa, H., Oyake, D., Yabuki, Y., Ogata, H., and Ohta, T. The RING heterodimer BRCA1-BARD1 is a ubiquitin ligase inactivated by a breast cancer-derived mutation. J Biol Chem, 276: 14537-40. 2001.

Huyton, T., Bates, P. A., Zhang, X., Sternberg, M. J., and Freemont, P. S. The BRCA1 C-terminal domain: structure and function. Mutat Res, 460: 319-

332. 2000.

Joo, W. S., Jeffrey, P. D., Cantor, S. B., Finnin, M. S., Livingston, D. M., and Pavletich, N. P. Structure of the 53BP1 BRCT region bound to p53 and its comparison to the Brca1 BRCT structure. Genes Dev, 16: 583-93. 2002.

Krishnan, V. V., Thornton, K. H., Thelen, M. P., and Cosman, M. Solution structure and backbone dynamics of the human DNA ligase IIIalpha BRCT domain. Biochemistry, 40: 13158-66. 2001.

Lecrubier, A. Patents and public health: European institutions are challenging Myriad Genetics's patent monopoly on the brca1 gene. EMBO Rep, 3: 1120-2, 2002.

Li, S., Chen, P. L., Subramanian, T., Chinnadurai, G., Tomlinson, G., Osborne, C. K., Sharp, Z. D., and Lee, W. H. Binding of CtIP to the BRCT repeats of BRCA1 involved in the transcription regulation of p21 is disrupted upon DNA damage. J Biol Chem, 274:11334-8. 1999.

Li, S., Ting, N. S., Zheng, L., Chen, P. L., Ziv, Y., Shiloh, Y., Lee, E. Y., and Lee, W. H. Functional link of BRCA1 and ataxia telangiectasia gene product in DNA damage response. Nature, 406: 210-5. 2000.

McManus, K. J. and Hendzel, M. J. CBP, a transcriptional coactivator and acetyltransferase. Biochem Cell Biol, 79: 253-66. 2001.

Monteiro, A. N. BRCA1: exploring the links to transcription. Trends Biochem Sci, 25: 469-74, 2000.

Monteiro, A. N., August, A., and Hanafusa, H. Evidence for a transcriptional activation function of BRCA1 C-terminal region. Proc Natl Acad Sci U S A,

93: 13595-9. 1996.

Nautiyal, S. and Alber, T. Crystal structure of a designed, thermostable, heterotrimeric coiled coil. Protein Sci, 8: 84-90, 1999.

Pao, G. M., Janknecht, R., Ruffner, H., Hunter, T., and Verma, I. M. CBP/p300 interact with and function as transcriptional coactivators of BRCA1. Proc Natl Acad Sci U S A, 97: 1020-5. 2000.

Parker, D., Ferreri, K., Nakajima, T., LaMorte, V. J., Evans, R., Koerber, S. C., Hoeger, C., and Montminy, M. R. Phosphorylation of CREB at Ser-133 induces complex formation with CREB- binding protein via a direct mechanism. Mol Cell Biol, 16: 694-703. 1996.

Petrij-Bosch, A., Peelen, T., van Vliet, M., van Eijk, R., Olmer, R., Drusedau, M., Hogervorst, F. B., Hageman, S., Arts, P. J., Ligtenberg, M. J., Meijers-Heijboer, H., Klijn, J. G., Vasen, H. F., Cornelisse, C. J., van't Veer, L. J., Bakker, E., van Ommen, G. J., and Devilee, P. BRCA1 genomic deletions are major founder mutations in Dutch breast cancer patients. Nat Genet, 17: 341-5. 1997.

Radhakrishnan, I., Perez-Alvarado, G. C., Parker, D., Dyson, H. J., Montminy, M. R., and Wright, P. E. Solution structure of the KIX domain of CBP bound to the transactivation domain of CREB: a model for activator:coactivator interactions. Cell, 91: 741-52. 1997.

Schlegel, B. P., Green, V. J., Ladias, J. A., and Parvin, J. D. BRCA1 interaction with RNA polymerase II reveals a role for hRPB2 and hRPB10alpha in activated transcription. Proc Natl Acad Sci U S A, 97: 3148-53. 2000.

Scully, R., Anderson, S. F., Chao, D. M., Wei, W., Ye, L., Young, R. A., Livingston, D. M., and Parvin, J. D. BRCA1 is a component of the RNA polymerase II holoenzyme. Proc Natl Acad Sci U S A, 94: 5605-10. 1997.

Shattuck-Eidens, D., McClure, M., Simard, J., Labrie, F., Narod, S., Couch, F., Hoskins, K., Weber, B., Castilla, L., Erdos, M. and others. A collaborative survey of 80 mutations in the BRCA1 breast and ovarian cancer susceptibility gene. Implications for presymptomatic testing and screening. JAMA, 273, 535-41. 1995.

Shen, D. and Vadgama, J. V. BRCA1 and BRCA2 gene mutation analysis: visit to the Breast Cancer Information Core (BIC). Oncol Res, 11: 63-9. 1999.

Sibanda, B. L., Critchlow, S. E., Begun, J., Pei, X. Y., Jackson, S. P., Blundell, T. L., and Pellegrini, L. Crystal structure of an Xrcc4-DNA ligase IV complex. Nat Struct Biol, 8: 1015-9. 2001.

Sum, E. Y., Peng, B., Yu, X., Chen, J., Byrne, J., Lindeman, G. J., and Visvader, J. E. The LIM domain protein LMO4 interacts with the cofactor CtIP and the tumor suppressor BRCA1 and inhibits BRCA1 activity. J Biol Chem, 277: 7849-56. 2002.

Vossen, R and den-Dunnen J. T. Protein Truncation Test. Current Protocols in Human Genetics. John Wiley &Sons, Inc, pages: 9.11.1-9.11.21. 1999.

Williams, R. S., Green, R., and Glover, J. N. Crystal structure of the BRCT repeat region from the breast cancer- associated protein BRCA1. Nat Struct Biol, 8: 838-42. 2001.

Wu, L. C., Wang, Z. W., Tsan, J. T., Spillman, M. A., Phung, A., Xu, X. L., Yang,

M. C., Hwang, L. Y., Bowcock, A. M., and Baer, R. Identification of a RING protein that can interact in vivo with the BRCA1 gene product. Nat Genet, 14(4): 430-40. 1996.

Wu-baer, F. and Baer, R. Effect of DNA damage on a BRCA1 complex. Nature, 414: 36. 2001.

Yamane, K. and Tsuruo, T. Conserved BRCT regions of TopBP1 and of the tumor suppressor BRCA1 bind strand breaks and termini of DNA. Oncogene, 18(37): 5194-203. 1999.

Yu, X., Wu, L. C., Bowcock, A. M., Aronheim, A., and Baer, R. The C-terminal (BRCT) domains of BRCA1 interact in vivo with CtIP, a protein implicated in the CtBP pathway of transcriptional repression. J Biol Chem, 273: 25388-92. 1998.

Zhang, X., Morera, S., Bates, P. A., Whitehead, P. C., Coffer, A. I., Hainbucher, K., Nash, R. A., Sternberg, M. J., Lindahl, T., and Freemont, P. S. Structure of an XRCC1 BRCT domain: a new protein-protein interaction module. EMBO J, 17(21): 6404-11. 1998.